

NITINOL CHARACTERIZATION STUDY

By William B. Cross, Anthony H. Kariotis,
and Frederick J. Stimler

Distribution of this report is provided in the interest of information exchange. Responsibility for the contents resides in the author or organization that prepared it.

Issued by Originator as Report No. GER 14188

Prepared under Contract No. NAS 1-7522 by
GOODYEAR AEROSPACE CORPORATION
Akron, Ohio

for Langley Research Center

NATIONAL AERONAUTICS AND SPACE ADMINISTRATION

For sale by the Clearinghouse for Federal Scientific and Technical Information
Springfield, Virginia 22151 - CFSTI price \$3.00

FOREWORD

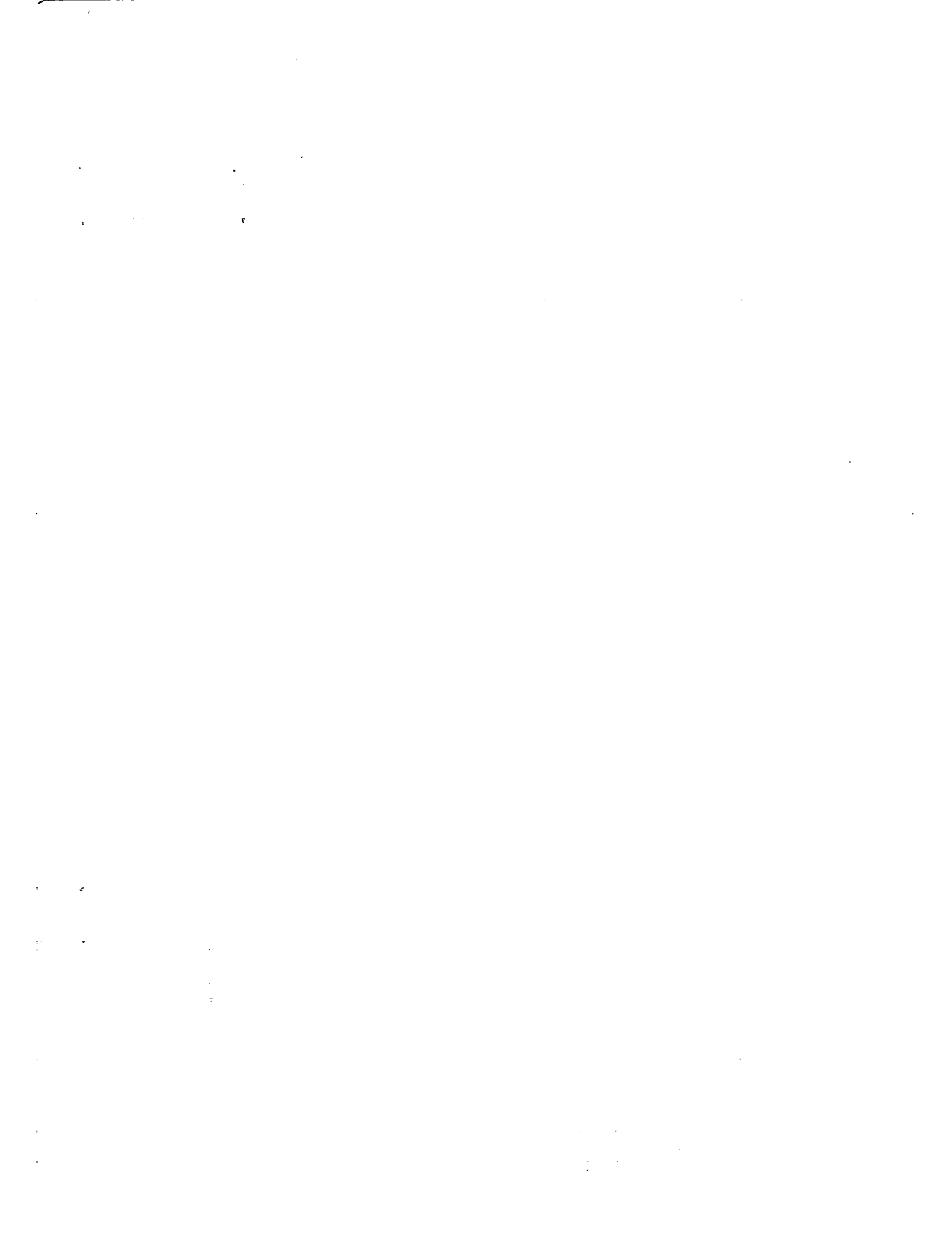
Goodyear Aerospace Corporation (GAC) of Akron, Ohio, conducted the Nitinol Characterization Study for NASA-Langley Research Center under Contract NAS 1-7522 to define the structural and recovery properties of several Nitinol compositions possessing different transition temperatures. Mr. Frederick J. Stimler of the Space Systems and Analytics Division was the GAC project engineer, Mr. William B. Cross the material specialist, and Mr. Anthony H. Kariotis the test engineer. The study was essentially a 19-month program conducted from July 1967 through January 1969.

The work was administered by the Applied Materials and Physics Division of Langley Research Center (LRC), with Mr. John E. Cooper of the Spacecraft Applications Section/Space Environment Branch acting as project engineer. Dr. David E. Bowker and Mr. Howard L. Price of AMPD also served as valuable technical monitors on the program. Mr. Kenneth D. Albert of the LRC Procurement Division was the contract administrator.

Nitinol rod and all foil materials were supplied by Mr. William J. Buehler of the Magnetism and Metallurgy Division of the U.S. Naval Ordnance Laboratory (NOL), Silver Spring, Maryland. Mr. Buehler's enthusiastic support and constructive suggestions did much to provide understanding of the behavior of this unique material and guidance during the test and data analysis phases of the program.

As subcontractor to GAC, Battelle Memorial Institute (BMI), Columbus, Ohio, processed the basic Nitinol rod into diameters of 100, 20, 15, and 10 mils under the direction of Dr. Curtis M. Jackson and Mr. David C. Drennen.

The contractor's number for this report is GER 14188.



SUMMARY

Goodyear Aerospace Corporation has determined the physical, mechanical, and electrical characteristics of nominal 55-Nitinol, a nickel-titanium alloy, to enable evaluation of its suitability for potential applications in space. Materials from three different melts were fabricated into rods, wire, and foil for the investigation, and the tests summarized in table I were accomplished.

The three different compositions had martensite transformation starting temperatures (M_s)* as follows: Type A, -60°F ; Type B, 65°F ; and Type C, 105°F . The starting materials for this program are defined in table II. A rod diameter of 100 mils, nominal wire diameters of 20, 15, and 10 mils, and foil thicknesses of 6 and 3 mils were evaluated during the study.

Complete process records were kept to ensure detection of the critical variables and repeatability of the material fabrication and performance characteristics.

As indicated in table I, several tests were repeated during the program, with different samples of the same type Nitinol resulting in consistent or explainable data. In addition, effects of such parameters as sample width, sample length, temperature, loading, and blocking were investigated sufficiently to define design criteria. Cooling and heating effects on the stress-strain behavior of Nitinol were investigated in detail. Sufficient comparison tests were made to substantiate the expected Nitinol behavior based on the tension data.

Substantial design information is now available for utilization of 55-Nitinol in many varied applications. The processing techniques necessary to preserve NiTi "memory" characteristics are better understood and seem somewhat controllable. Ways have been developed to predict and improve this unique memory phenomenon of Nitinol. Program results showed that the material can be processed into rod, wire, and foil shapes and still maintain the desired memory, physical, and structural properties.

This program represents a big coordinated step. Earlier test data could be considered exploratory - limited for general use and applied with caution for many applications. Many tests and cross checks were possible with the present program, since the raw data was thoroughly analyzed by cognizant specialists from government and industry to verify the data and direct further testing.

The characterization tests conducted during this program provide adequate information to facilitate the design of expandable or erectable structures in particular, and many other applications in general.

* M_s values shown are for hot-swaged bar stock in the "as-received" condition.

TABLE II. - STARTING MATERIALS^a FOR NITINOL CHARACTERIZATION STUDY PROGRAM

Composition	Original alloying ^b	Heat No.	Original ingot weight, lb	M _s temperature, °F ^c		
				Swaged rod	3-mil foil	6-mil foil
A - TiNi _{0.935} , Co _{0.065} ^d	NOL	NOL-1015	Approx 10	-60	-85	-80
B - C 0.07, Ni 55.0, Ti balance ^e	SMC	D-4028	Approx 100	65	75	76
C - C 0.06, Ni 54.6, S 0.006, Ti balance ^e	SMC	D-4006	Approx 100	105	105	105

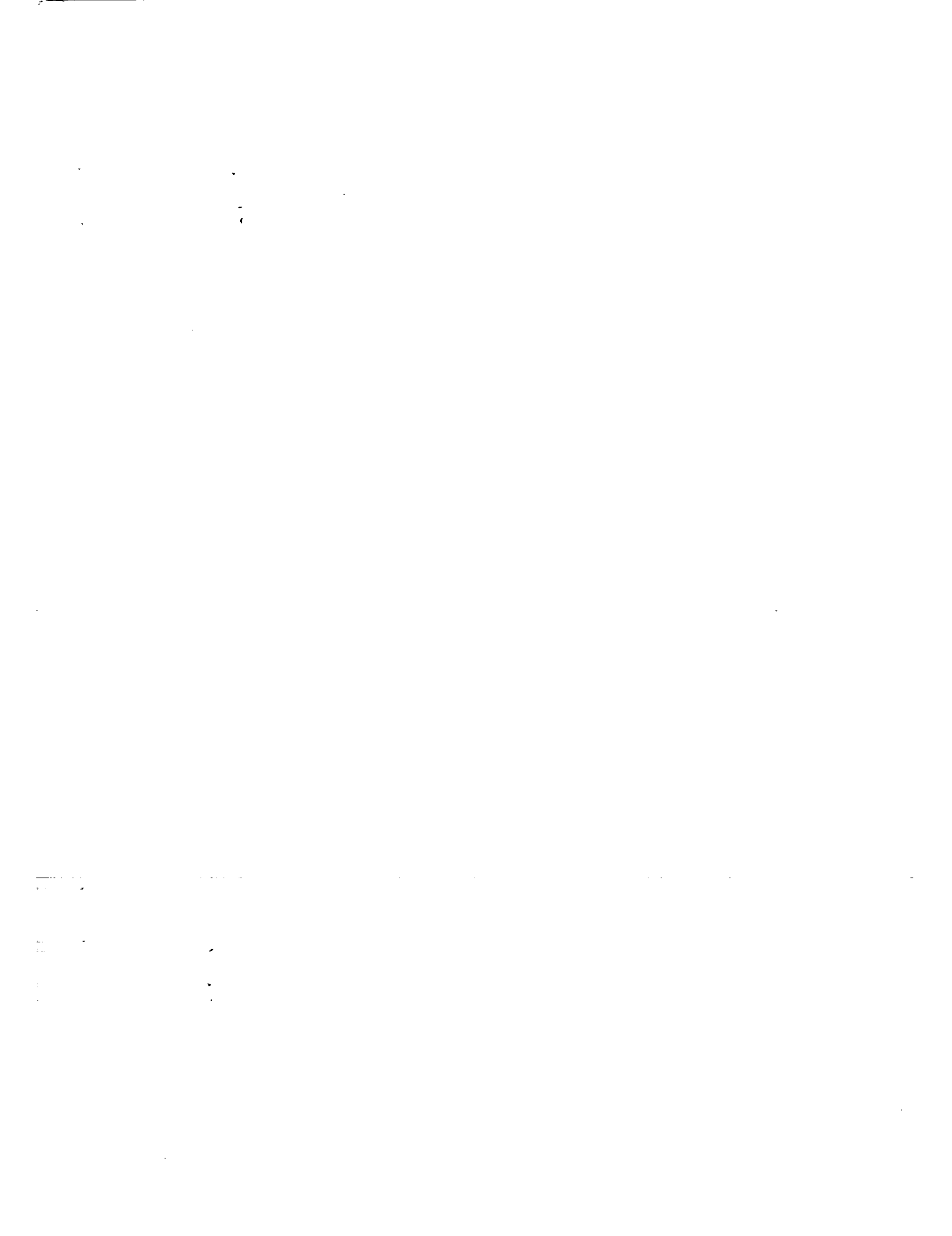
^a Supplied by U.S. Naval Ordnance Laboratory (NOL), Silver Spring, Maryland.

^b All heats were melted by induction and contained in a graphite crucible.

^c Determined from electrical resistance versus temperature measurements made on "as-received" material in the case of the swaged rod and on final annealed material in the case of foil.

^d Heat D-4006 modified by cobalt and titanium additions to attain approximately the chemical formula shown.

^e Special Metals Corporation (SMC), New Hartford, New York, ingot analysis.



CONTENTS

	Page
FOREWORD	iii
SUMMARY	v
SYMBOLS AND ABBREVIATIONS	xii
INTRODUCTION	1
REVIEW OF NITINOL PROPERTIES AND UNIQUE BEHAVIOR	2
MATERIAL INVESTIGATION	4
General	4
Swaged Rods	4
Rolled Thin Sheet (Foil)	4
Drawn Wire	5
EXPERIMENTAL PROCEDURE	10
EXPERIMENTAL RESULTS AND DISCUSSION	11
Direct Observation of Transformation	11
General	11
Electrical resistance versus temperature	11
Uniaxial dimensional change	20
Mechanical Behavior	23
Stress versus elongation curves	23
Degree of shape recovery	27
Recovery stress	40
Mechanical work	42
Shape recovery fatigue	51
Thermal cycling effects	53
CONCLUSIONS	57
REFERENCES	59
BIBLIOGRAPHY	59

ILLUSTRATIONS

Figure		Page
1	Block diagram of wire drawing schedule	6
2	Microstructures of longitudinal sections of as-received hot-swaged Nitinol alloys	7
3	Microstructures of longitudinal sections of as-drawn Nitinol alloys	8
4	Microstructures of longitudinal sections of annealed Nitinol alloys	9
5	Typical electrical resistivity versus temperature curves for drawn NiTi wire annealed at 932°F (500°C)	14
6	Effect of post-drawing anneal temperatures on electrical resistance and bend recovery behavior.	15
7	Electrical resistance versus temperature curves for swaged rods	16

Figure		Page
8	Electrical resistance versus temperature curves for Composition A materials	17
9	Electrical resistance versus temperature curves for Composition B materials	18
10	Electrical resistance versus temperature curves for Composition C materials	19
11	Typical uniaxial dimensional change behavior for Composition B and C drawn wire annealed at 932 ^o F	21
12	Uniaxial dimensional change versus temperature curves for 100-mil diameter Composition B and C rods	22
13	Uniaxial dimensional change versus temperature curves for 100-mil diameter Composition A rods	23
14	Stress versus elongation curves for 100-mil diameter Composition B rods during cooling and heating cycles	24
15	Stress versus elongation curves for 20-mil diameter Composition B wire during cooling and heating cycles	25
16	Yield stress and modulus versus temperature curves for 100-mil diameter Composition B rods during cooling and heating cycles	26
17	Tensile shape recovery versus initial strain curves for Composition A materials	28
18	Tensile shape recovery versus initial strain curves for Composition B materials	29
19	Tensile shape recovery versus initial strain curves for Composition C materials	30
20	Compression shape recovery versus initial strain curves for Composition B and C rods	31
21	Strain in outer fiber as a function of bend diameter and specimen thickness	32
22	Bend recovery versus temperature curves for 100-mil diameter Composition A rods	33
23	Bend recovery versus temperature curves for Composition B materials	34
24	Bend recovery versus temperature curves for Composition C materials	37
25	Bend shape recovery versus initial strain curves for Composition A materials	40
26	Bend shape recovery versus initial strain curves for Composition B materials	41
27	Bend shape recovery versus initial strain curves for Composition C materials	41
28	Tensile recovery stress versus temperature curves for 100-mil diameter Composition B rods at various strain levels	42
29	Maximum recovery stress versus initial strain curves for Composition A materials	43

Figure		Page
30	Maximum recovery stress versus initial strain curves for Composition B materials	44
31	Maximum recovery stress versus initial strain curves for Composition C materials	45
32	Mechanical work versus temperature curves for 100-mil diameter Composition A rods	46
33	Mechanical work versus temperature curves for 100-mil diameter Composition B rods	47
34	Mechanical work versus temperature curves for 100-mil diameter Composition C rods	47
35	Maximum mechanical work versus initial strain curves for Composition A materials	48
36	Maximum mechanical work versus initial strain curves for Composition B materials	49
37	Maximum mechanical work versus initial strain curves for Composition C materials	50
38	Tensile recovery versus number of deformation cycles for 20-mil diameter Composition B wire. 6 and 8 percent strain	51
39	Load-elongation curves following shape recovery cycling for 20-mil diameter Composition B wire	52
40	Electrical resistance versus temperature curves following repeated deformation cycles for 20-mil diameter Composition B wire	54
41	Thermal cycling effects on bend recovery for 20-mil diameter Composition B and C wire	56

TABLES

Table		Page
I	Summary of Test Program for Nitinol Characterization Study	vi
II	Starting Materials for Nitinol Characterization Study Program	vii
III	Summary of Physical and Mechanical Properties of Nominal 55-Nitinol	3
IV	Summary of Types of Tests, Specimen Sizes, Gage Lengths, and Load Rates	12
V	Approximate M_d , M_s , M_f' , and A_s Critical Temperature Points for Materials Investigated	20
VI	Degree of Strain Maintained in Thermal Cycling Specimens	55

SYMBOLS

A_S	Start of reverse transformation, NiTi (III) \rightarrow NiTi (II). NiTi (II) and NiTi (III) designate structure variations (phases) produced by diffusionless (martensitic) transformation.
M_d	Maximum temperature for martensite formation by deformation. NiTi (II) structure thermodynamically stable at this point.
M_f'	Temperature where macroscopic atomic shear ceases. (An arrest point, since transformation can be made to proceed through mechanical deformation.)
M_S	Martensite transformation starting point in cooling.

ABBREVIATIONS

BMI	Battelle Memorial Institute
GAC	Goodyear Aerospace Corporation
LRC	Langley Research Center
NOL	Naval Ordnance Laboratory
SMC	Special Metals Corporation

NITINOL CHARACTERIZATION STUDY

By W.B. Cross, A.H. Kariotis, and F.J. Stimler
Goodyear Aerospace Corporation

INTRODUCTION

Nickel-titanium alloys (Nitinol, TiNi, or NiTi) of proper composition exhibit unique mechanical "memory" or restoration force characteristics. 55-Nitinol is an NOL designation for this series of near-stoichiometric intermetallic compound alloys. This designation is used to typify the generic class of shape-recoverable alloys ranging in composition from about 52 to 56 weight percent nickel, the balance titanium. The name is derived from Ni-Ti-NOL. The prefix numerical value indicates the nominal nickel content in weight percent.

The shape recovery performance of this material is phenomenal. The material can be plastically deformed, such as in the simulation of model packaging conditions, and then restored to the original configuration or shape by heating it above the characteristic transition temperatures. Mr. Buehler and his colleagues at NOL have shown qualitatively, using crystallographic techniques, that a martensitic (diffusionless) atomic structure change is responsible for this unique mechanical memory, as well as other anomalous properties (ref. 1).

This unusual behavior is limited to NiTi alloys having near-equiatomic composition. A pure stoichiometric (50 atomic percent) NiTi alloy will have a nickel content of approximately 55 percent by weight. Increasing the nickel concentration lowers the characteristic transformation temperature of the alloy. Nickel concentration increases are limited to about 56.5 percent by weight due to the formation of a detrimental second phase. Further reduction in transformation temperature, with shape memory retention, however, is possible through partial substitution of cobalt for nickel. Using this substitution method, it is possible that a single-phase alloy can be made which will have a transformation temperature approaching -321°F . Without cobalt substitution, the transformation range can be lowered from about 200° to about 15°F .

The present effort was directed toward obtaining large quantities of physical behavior data with three different types of compositions and many specimen forms processed from them. Hundreds of curves of these data have been analyzed and thus provide background for quantitative understanding of the shape recovery performance of NiTi alloys not previously available.

REVIEW OF NITINOL PROPERTIES AND UNIQUE BEHAVIOR

Since the recent discovery, at the U.S. Naval Ordnance Laboratory, of the extraordinary shape recovery or mechanical "memory" property of the equiatomic NiTi intermetallic compound designated 55-Nitinol, considerable interest has been generated in the basic and engineering features of this material. Some of the physical and mechanical properties of nominal 55-Nitinol are listed in table III. (Detailed data may be found in references 1 and 2.)

The mechanical memory of this material is easily demonstrated by plastically deforming an annealed wire or sheet of NiTi at room temperature and then heating it, whereupon it will revert to its original shape. This unusual behavior is attributed to a reversible low temperature diffusionless (martensitic type) transformation which is not complete at room temperature. The transformation, however, can be made to proceed at room temperature by straining the material. Thus it is assumed, when demonstrating mechanical memory, that plastic deformation occurs through transformation and that reverse transformation takes place upon heating. By this process plastic deformation is erased, and the material recovers its original shape.

In order to preset an original shape, the alloy must first (i.e., prior to plastic deformation) have been annealed while constrained in the shape that it is to "remember." These anneals are usually carried out at temperatures from 750° to 1110°F. However, the amount of plastic deformation that the alloy can tolerate, and still revert to its original shape when reheated, depends on the temperature at which it was annealed. Thus there appears to be an optimum annealing temperature, which is a function of the alloy composition and prior processing history.

To understand the cause of the shape memory effect, one must consider the phases that are present in the 55-Nitinols at various temperatures. It is generally agreed that at temperatures above about 1200° - 1300°F these alloys consist of a single-phase body-centered-cubic random solid solution. This phase is not believed to enter into the shape memory phenomenon.

There is much disagreement in the technical literature (ref. 3, 4, 5, 6, and 7) in regard to the phases that exist in the Nitinol alloys from 1200 - 1300°F down to their transition temperatures (M_s). Some investigators believe that the alloy in this temperature range consists of an ordered single-phase NiTi matrix that has a complex structure with a 9 Å repeat distance; others state that it is a single-phase (NiTi) ordered CsCl-type phase with a lattice parameter of about 3 Å; while still others believe that two phases are present. One of the two phases is said to be NiTi with an ordered CsCl-type structure, and the other is either Ni₃Ti (for alloys that are slightly rich in nickel) or Ti₂Ni (in the case of alloys that are slightly rich in titanium).

For the present, it will suffice to say that a phase that is stable or metastable above the M_s temperature can transform to a martensitic-type phase at temperatures below M_s . Transformation occurs below M_s both athermally (on cooling) and by plastic deformation. It appears that the grains that transform athermally do not contribute to the shape memory effect.

Shape memory apparently comes about as a result of the formation of the acicular phase by deformation of the metastable retained higher-temperature phase. When 55-Nitinol is plastically deformed at a temperature near or below the M_s point, the retained phase is transformed into the acicular product. The orientation of the transformed phase depends on the state of stress that caused the transformation. The "memory" arises from the fact that, upon heating (above the A_s point), the oriented grains of acicular phase transform in the reverse direction and assume their original shapes; thus the mechanical plastic deformation is annihilated and the sample returns to the shape it had prior to deformation.

TABLE III. - SUMMARY OF PHYSICAL AND MECHANICAL PROPERTIES OF NOMINAL 55-NITINOL

Density, lb/in. ³	0.234
Melting point, °F	2390
Magnetic permeability	<1.002
Electrical resistivity, microhm-cm	
At 68°F	~80
At 1652°F	~132
Mean coefficient of thermal expansion (75° - 1652°F) per °F x 10 ⁻⁶	5.7
Hardness ^a	
1742°F, furnace-cooled	89 R _B
1742°F, quenched (R. T. water)	89 R _B
Tensile ^a	
Ultimate tensile strength, ksi	125
Yield strength, ksi	See fig. 16
Elongation, percent	60
Young's modulus, millions of psi	See fig. 16
Shear modulus, millions of psi	3.6
Poisson's ratio	0.33
Impact (Charpy) ^a	
Unnotched (R. T.), ft-lb	155
Unnotched (-112°F), ft-lb	160
Notched (R. T.), ft-lb	24
Notched (-112°F), ft-lb	17
Fatigue (Std R.R. Moore Test) ^a	
Stress (10 ⁷ cycles-runout), ksi	70

NOTES: 1. Tests were performed at room temperature except where noted. Room temperature was below the transition temperature range.

2. Detailed data may be found in references 1 and 2.

^aData obtained on hot wrought alloys.

MATERIAL INVESTIGATION

General

Three different compositions designated A, B, and C were evaluated during the course of the program. In each case the basic material was supplied by the U.S. Naval Ordnance Laboratory (NOL), Silver Spring, Maryland, in the form of 0.2- or 0.3-inch diameter swaged rods and 0.003- and 0.006-inch rolled sheet. Prior to testing, the rods were processed into wires of 100, 20, 15, and 10 mils in diameter by Battelle Memorial Institute (BMI) of Columbus, Ohio. The thin sheet (foil) materials, with the exception of final annealing, did not require any additional processing. The chemical composition and martensite start temperatures (M_s) of the materials are given in table II.

Details of the processing steps involved in producing the swaged rod and thin sheet are described in the following paragraphs.

Swaged Rods

Composition A rod was processed by NOL from a sound cast ingot hot-rolled to a thickness of about one inch and then cut into square bars. Three bars were swaged at 1562°F to approximately 0.3 inch in diameter.

Composition B was hot-swaged by NOL at 1562°F to 0.2-inch diameter rod from hot-rolled 1-inch square bars supplied to NOL by Special Metals Corporation (SMC), New Hartford, New York.

Composition C was processed by NOL in a manner similar to Composition B. However, original ingot sections obtained from SMC were first remelted by nonconsumable arc (under a partial atmosphere of argon) into bar stock approximately 5/8 inch in diameter.

Rolled Thin Sheet (Foil)

Compositions A, B, and C were rolled by NOL into 0.006- and 0.003-inch thick sheets as described in the following paragraphs.

Hot-rolled. - All heats were hot-rolled at a temperature of 1562°F for the initial passes. This temperature was progressively lowered, as the sheet became thinner, to a final temperature of 1292°F. Final hot-rolled thickness was 0.040 inch. All hot-rolling was done in a 2-high rolling mill.

Warm-rolled. - Following appropriate shearing, the 0.040-inch strips measuring approximately 3 inches wide were warm-rolled in a 4-high rolling mill. The warm-rolling process consisted of heating the strips in a tube furnace mounted ahead of the rolls and maintained at 1200°F. Heating time varied with the strip thickness and ranged from three minutes for the 0.040-inch thick strip to one minute for the 0.006-inch thick strip. The strip was reheated

after each pass through the rolling mill. Up to 5 mils of "screw-down" was used for each pass on the approximately 0.040-inch thick strip until a smooth surface was attained. As many as four or five passes were made at the same setting when approaching the 0.006-inch thickness. A portion of each heat was processed to 0.006-inch thickness. The remainder were slit longitudinally in 3/4-inch wide strips. The edges, which were of variable thicknesses, were discarded. These strips were then rolled, by repeated passes and heating (1200°F), to a thickness of slightly greater than 0.003 inch.

Cold-rolled. - Following the hot-rolling sequence, strips of Composition B and C material slightly thicker than the desired 0.006 and 0.003 inch were given a reduction by cold-rolling. This resulted in a strip approximately 5 percent longer and desired thicknesses of 0.006 and 0.003 inch. Composition A strips were not cold-rolled since the material is well above its M_s point at room temperatures and therefore difficult to plastically deform.

Studies were conducted on the 0.006- and 0.003-inch thick sheets to determine the final anneal temperature required for good shape recovery performance. The results of this work indicated that 930°F (500°C) was satisfactory for 0.006-inch thick Composition A, 0.006- and 0.003-inch thick Composition B, and 0.006-inch thick Composition C. A slight performance improvement, however, was gained by annealing the 0.003-inch thick Composition A sheet at 1112°F (600°C) and the 0.003-inch thick Composition C sheet at 752°F (400°C).

Drawn Wire

The Composition B and C materials were successfully processed by BMI from 0.2-inch diameter swaged rod into wires of 100, 20, 15, and 10 mils in diameter by utilizing cold-drawing techniques. Drawing was accomplished below the upper range of each alloy's transition temperature. Above the transition temperature, fabrication difficulties arise, in that these materials are stable at a particular phase. The procedures developed by Buehler (ref. 1) were used as a general guide, but were modified in several important respects.

For Composition A, special drawing techniques were developed whereby it could be drawn readily despite its low transition temperature range. Drawing was accomplished at a temperature of about -10°F. The wires were held at the drawing die in an insulated tank containing a mixture of Dow polyglycol P-400 and dry ice. This mixture was maintained at a temperature between -4° and -22°F. Furthermore, the polyglycol served as an effective lubricant; thus no additional lubricant was required.

Studies were conducted on alloy samples of 100, 20, 15, and 10 mils to determine the best annealing temperature required to produce complete shape recovery. The results of these tests indicated that 930°F (500°C) was the optimum temperature for Compositions B and C at each diameter. The optimum annealing temperature for Composition A was found to be 1110°F (600°C). Final "straight" annealing was accomplished by passing the wire, under tension, through a 19-inch long tube furnace. Tension and rate of travel through the furnace were adjusted to the requirements of each particular wire size.

The actual processing schedule employed in converting the alloys into wire is summarized in figure 1.

Figures 2 through 4 show typical microstructures of Compositions A, B, and C in the as-received hot-swaged (fig. 2), as-drawn (fig. 3), and annealed (fig. 4) conditions. In general, the microstructures consist of a single acicular phase containing a random dispersion (as well as some stringers) of nonmetallic inclusions. The inclusions are presumed to be

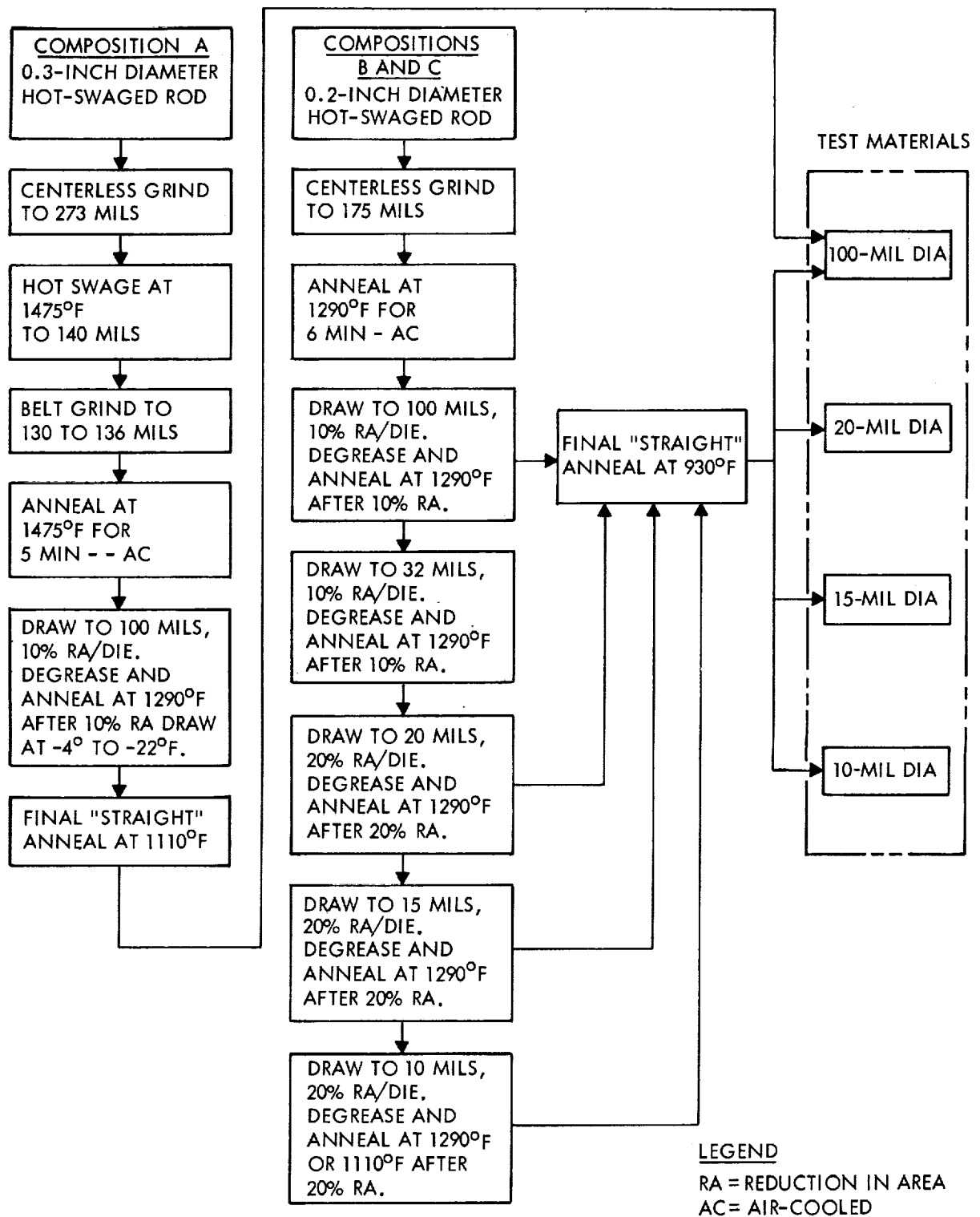
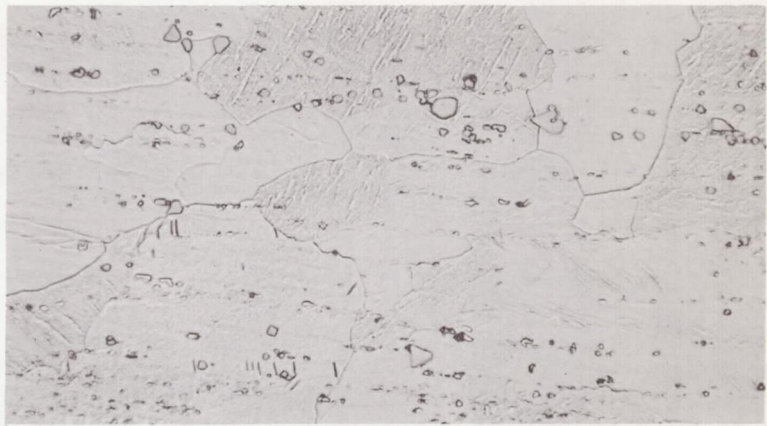


Figure 1. - Block diagram of wire drawing schedule.

(A) COMPOSITION A NITINOL ROD,
273-MIL DIAMETER



500X

82H₂O-14HNO₃-4HF

9C799

(B) COMPOSITION B NITINOL ROD,
205-MIL DIAMETER



500X

82H₂O-14HNO₃-4HF

9C803

(C) COMPOSITION C NITINOL ROD,
205-MIL DIAMETER

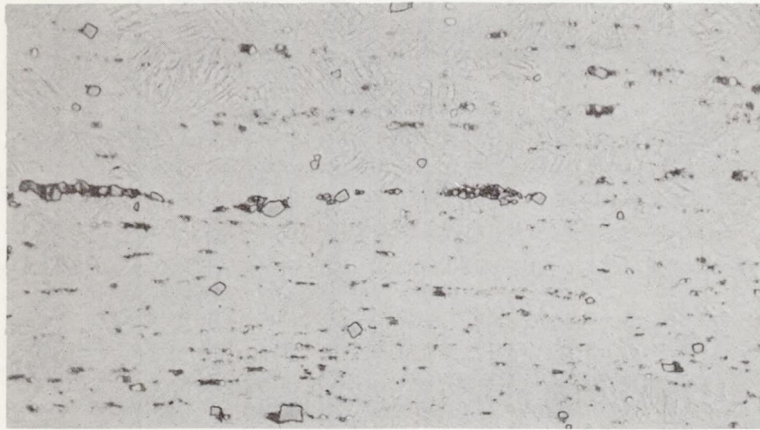


500X

82H₂O-14HNO₃-4HF

9C802

Figure 2. - Microstructures of longitudinal sections of as-received hot-swaged Nitinol alloys. Alloys were hot-swaged at NOL.

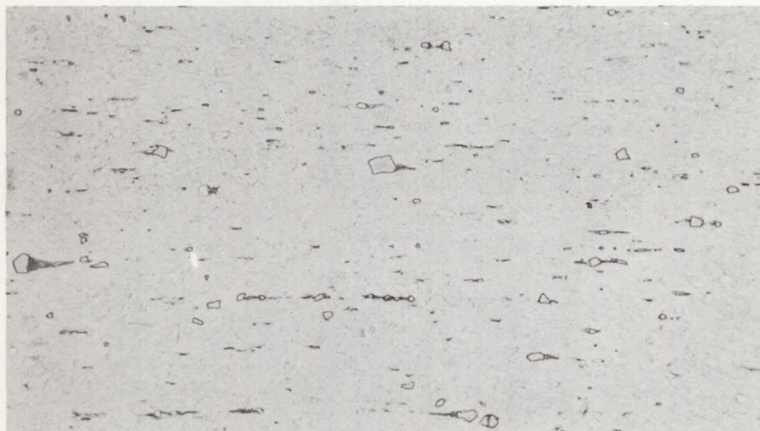


(A) COMPOSITION A NITINOL WIRE,
100-MIL DIAMETER, 10% REDUC-
TION

500X

$82\text{H}_2\text{O}-14\text{HNO}_3-4\text{HF}$

9C798



(B) COMPOSITION B NITINOL WIRE,
20-MIL DIAMETER, 20% REDUC-
TION

500X

$82\text{H}_2\text{O}-14\text{HNO}_3-4\text{HF}$

9C794



(C) COMPOSITION C NITINOL WIRE,
100-MIL DIAMETER, 10% REDUC-
TION

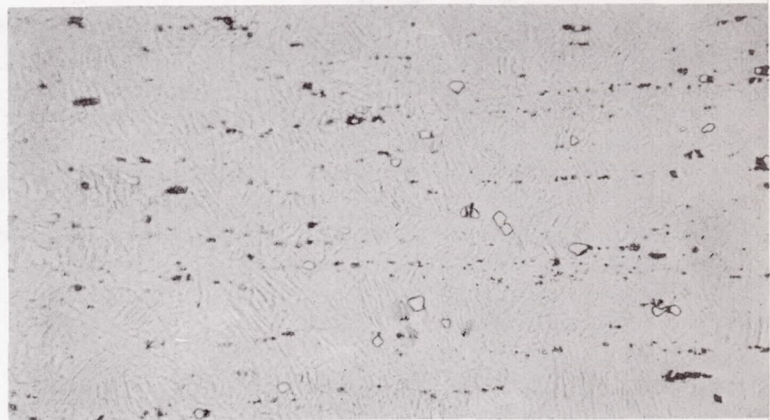
500X

$82\text{H}_2\text{O}-14\text{HNO}_3-4\text{HF}$

9C797

Figure 3. - Microstructures of longitudinal sections of as-drawn Nitinol alloys.

(A) COMPOSITION A NITINOL WIRE,
100-MIL DIAMETER, 10% REDUC-
TION + STRAND ANNEALED AT
1110°F (AIR-COOLED)

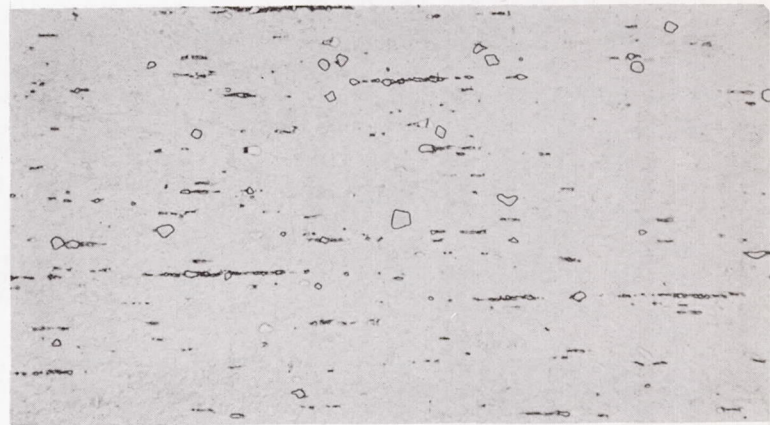


500X

82H₂O-14HNO₃-4HF

9C796

(B) COMPOSITION B NITINOL WIRE,
20-MIL DIAMETER, 20% REDUC-
TION + STRAND ANNEALED AT
930°F (AIR-COOLED)



500X

82H₂O-14HNO₃-4HF

9C795

(C) COMPOSITION C NITINOL WIRE,
100-MIL DIAMETER, 10% REDUC-
TION + STRAND ANNEALED AT
930°F (AIR-COOLED)



500X

82H₂O-14HNO₃-4HF

9C805

Figure 4. - Microstructures of longitudinal sections of annealed Nitinol alloys.

primarily titanium carbonitrides, with a few nickel-titanium oxides. The stringers of inclusions are aligned with the axis of the rod or wire, as would be expected.

A comparison of figures 2A and 2B shows that the microstructures of as-received Compositions A and B are very similar. By comparing these compositions with that of Composition C in figure 2C, it may be seen that they contain larger, but fewer, inclusions.

A comparison of the as-drawn and the annealed microstructures of each alloy in figures 3 and 4 shows that there is a tendency for the acicular appearance of the matrix to be partially eliminated. No other changes were apparent during examination under the light microscope at magnifications up to 800X.

EXPERIMENTAL PROCEDURE

Evaluation of the unique properties of Nitinol required the development of special testing techniques. In general, the type of apparatus utilized consisted of commercially available equipment. Preliminary tests were conducted to establish the most acceptable methods that would produce meaningful and repeatable data.

As shown in table I, the test program consisted of evaluation of the following mechanical, thermal, and electrical properties:

- (1) Stress-strain characteristics in tension and compression as a function of temperature
- (2) Shape recovery from tensile, compressive, and bending deformation as a function of initial strain level
- (3) Recovery stress (or force) from tensile deformation as a function of initial strain level
- (4) Mechanical work potential from tensile deformation as a function of initial strain level
- (5) Shape recovery fatigue, or degree of recovery from tensile deformation as a function of percent strain and number of cycles
- (6) Thermal cycling effects, or degree of recovery from exposure to temperature extremes as a function of percent strain, number of cycles, and degree of restraint
- (7) Uniaxial dimensional change as a function of temperature
- (8) Electrical resistance as a function of temperature

Specimens were tested in wire and foil forms. Wires were 100, 20, 15, and 10 mils in diameter. The foil specimens were 3- and 6-mil thick and were tested in 0.12- and 0.25-inch wide strips, respectively. Three Nitinol compositions having different transformation temperatures were tested. Wire was received in coils, and when uncoiled retained a curvature. After the test specimens were cut to length, they were strain-relieved by submerging them in boiling water.

Except for bending tests, all testing was conducted in an Instron universal testing machine equipped with an X-Y chart recorder system capable of recording load versus time or strain. Interchangeable load cells permitted selection of proper cells for maximum accuracy. The load-measuring system was calibrated using dead weights. Strains at elevated or reduced temperatures were measured with a linear variable differential transformer (LVDT) type extensometer, Baldwin Model PS-6M, modified for use at temperatures ranging from -320° to $+500^{\circ}$ F. The LVDT extensometer and an Instron strain gage extensometer, Model G-51-13, were used for room temperature tests. Both extensometers are accurate to within ± 0.5 percent of full-scale range. Tests at temperatures other than ambient were conducted in a controlled-temperature chamber capable of providing temperatures from -300° to $+1000^{\circ}$ F with an accuracy of $\pm 1^{\circ}$ F.

Wherever possible, testing was conducted in accordance with the following standards:

- (1) ASTM E8-61T, "Tension Testing of Metallic Materials"
- (2) ASTM E9-61, "Compression Testing of Metals"
- (3) ASTM D1906-62T, "Test for Gage Length in Single Fiber Testing"

Testing for properties such as shape recovery, recovery stress, mechanical work potential, shape recovery fatigue, and thermal cyclic fatigue necessitated the supplementation of the above standards with special test methods. Extensometers used to measure initial strain and degree of recovery were mounted on test specimens and insulated electrically to allow heating of the specimen while passing electrical current through it. Mechanical work was measured by applying a constant force with either a pneumatic actuator or dead weights, measuring the amount of displacement with an extensometer, and recording both force and displacement on the Instron machine recorder. Thermal cycling effects required that strained specimens be held rigidly during cyclic exposure to temperature extremes. This was accomplished by winding the wire specimens over a mandrel of the necessary diameter and spot welding the ends of the specimen to the mandrel. Degree of recovery after thermal cycling was calculated using the measured radius of curvature of the tested specimen after transformation recovery. Table IV summarizes the specimen lengths, gage lengths, load rates, and percent of initial strain where applicable to each of the types of test.

EXPERIMENTAL RESULTS AND DISCUSSION

Direct Observation of Transformation

General. - A number of experimental methods can be applied to the quantitative observation of transformation. Direct observation during transformation obtained by monitoring a change in some physical property as a function of temperature has been used successfully by investigators (ref. 8). Properties often monitored include electrical resistance, uniaxial dimensional change (controlled dilation), and mechanical damping. In the present study, quantitative data was obtained by applying the first two methods. The third method, although not used in this program, has been successfully applied by NOL to establish the approximate M_S and A_S points.

Electrical resistance versus temperature. - Equipment was set up to measure electrical resistance as a function of sample temperature so that an accurate determination of the

TABLE IV. - SUMMARY OF TYPES OF TESTS, SPECIMEN SIZES, GAGE LENGTHS, AND LOAD RATES

Shape	Dimension	Tensile Tests														
		Stress-strain			Shape recovery			Recovery-stress			Mechanical work			Shape recovery fatigue		
		Total length	Gage length	Load rate	Total length	Gage length	Load rate	Total length	Gage length	Load rate	Total length	Gage length	Load rate	Total length	Gage length	Load rate
Rod	100-mil dia	6.0	2.0	0.05	6.0	2.0	0.05	6.0	2.0	0.05	6.0	2.0	0.2	---	---	---
Wire	20-mil dia	8.0	5.0	0.5	7.0	2.0	0.2	7.0	2.0	0.5	7.0	2.0	0.2	6.0 10.0	2.0 6.0	0.05 1.0
	15-mil dia	8.0	5.0	0.5	7.0	2.0	0.2	7.0	2.0	0.2	7.0	2.0	0.2	---	---	---
	10-mil dia	8.0	5.0	0.5	7.0	2.0	0.2	7.0	2.0	0.2 0.5	11.0	8.0	0.2	---	---	---
Foil	6-mil x 1/4	6.0	3.0	0.2	6.0	2.0	0.2	6.0	2.0	0.2	6.0	2.0	0.2	---	---	---
	3-mil x 1/8	5.0	2.0	0.2	---	---	---	5.0	2.0	0.2	5.0	2.0	0.2	---	---	---

Shape	Dimension	Compression			Bending						Dimensional change		Electrical resistance	
		Stress-strain, shape recovery, recovery stress			Shape recovery		Thermal cycling effects			Total length	Gage length	Before optimum anneal	After final anneal	
		Total length	Gage length	Load rate	Total length	% strain	Total length	Gage length	% strain			Total length	Total length	
Rod	100-mil dia	3.22	2.0	0.5	5.0 to 8.0	4.0 to 14.0	---	---	---	1.0	1.0	6.0	6.0	
Wire	20-mil dia	---	---	---	5.0	4.0 to 18.0	4.0	3.0	6.0 8.0	---	---	6.0	12.0	
	15-mil dia	---	---	---	6.0	3.0 to 18.0	---	---	---	---	---	6.0	10.0	
	10-mil dia	---	---	---	4.5	2.0 to 16.0	---	---	---	---	---	6.0	14.0	
Foil	6-mil x 1/4	---	---	---	5.5	1.0 to 10.0	---	---	---	---	---	4.0	6.0	
	3-mil x 1/8	---	---	---	5.0	3.0 to 12.0	---	---	---	---	---	6.0	5.0	

- Notes: 1. All lengths are in inches.
2. All load rates are in inches/minute crosshead speed.

transformation start temperature in cooling (M_S) and heating (A_S) could be established for each composition.

The general interpretation of the electrical resistance versus temperature curves is based in part on the work of Wang, et al (ref. 8). This work, combined with the large quantity of resistance versus temperature data gathered during the present effort, has led to a better understanding of the transformation process. A typical resistivity (resistance) versus temperature profile obtained on cold-drawn wire annealed at 932°F (500°C) is presented in figure 5. The characteristic changes associated with transformation during cooling and heating are shown. It is important to consider here that the general shape of the resistance versus temperature curves can be significantly altered by prior cold work or area reduction (in the case of drawn wire) and final annealing temperatures.

As the program progressed, the usefulness of the resistance versus temperature profiles was expanded beyond that of determining M_S and A_S points. These profiles were ultimately used as a reliable indicator of relative shape recovery performance.

Prior to the investigation, it was noted that shape recovery performance quite frequently varied from one wire sample to another even though they were drawn from the same alloy. Deformation and heating would produce rapid and precise recovery in one specimen while showing signs of sluggishness and incomplete recovery in another.

Careful investigations indicated that post-drawing anneal temperature had a significant effect on the shape recovery behavior and that a small variation in temperature could have a marked effect on performance. Furthermore, it was established that a relationship exists between the shape of the resistance versus temperature profile and shape recovery performance. Figure 6 depicts this unique relationship. The experimental data for figure 6 were obtained by first giving a single wire specimen 10 to 20 percent final area reduction by drawing. This drawn wire was then cut into four sections of about equal length. Each section was annealed for three minutes under slight tension to yield a specimen with straight configuration. One section was annealed at each of the four temperatures of 752°F (400°C), 932°F (500°C), 1112°F (600°C), and 1292°F (700°C). After annealing, the resistivity profile of each wire was measured. Each annealed wire specimen was then bent around a mandrel, at room temperature, producing an outer fiber strain of about 9 percent. As would be expected, more elastic spring-back was noted for the lower annealing temperatures. Following bending, each wire was heated above the transformation temperature range and allowed to freely recover. The ultimate recovery behavior was found to correspond to the area encompassed within the resistivity loop. The best recovery was produced by the 932°F anneal, which showed a large area encompassed, while very poor recovery was obtained at the 1292°F anneal temperature. The latter produced a profile where very little area was encompassed within its resistivity loop.

Through the use of an automatic electrical resistance versus temperature plotting system, highly reliable and repeatable data were obtained on a large number of Composition A, B, and C alloys prior to and during the various drawing stages. Curves were also obtained on the 6- and 3-mil foils. A summary of the tests conducted is given in table I. A selected group of curves (reproduced from actual recorded data sheets) is included for reference purposes. The effect of various anneal temperatures (752°F, 932°F, 1112°F, and 1292°F) on 100-mil diameter Composition B alloy is shown in figure 6. These anneal temperatures were also investigated for the wires and foils to determine the final anneal condition for optimum performance. The resistance versus temperature curves for the unannealed hot-swaged rods of Composition A, B, and C starting materials are shown in figure 7. Finally, the profiles obtained on each material type and size following final processing are shown in figures 8, 9, and 10. Using the technique illustrated in figure 5 for selecting critical temperature points (M_d , M_S , M_f , and A_S), and applying it to figures 7, 8, 9, and 10, quantitative values were obtained for each of the materials investigated. A complete summary of these data is given in table V.

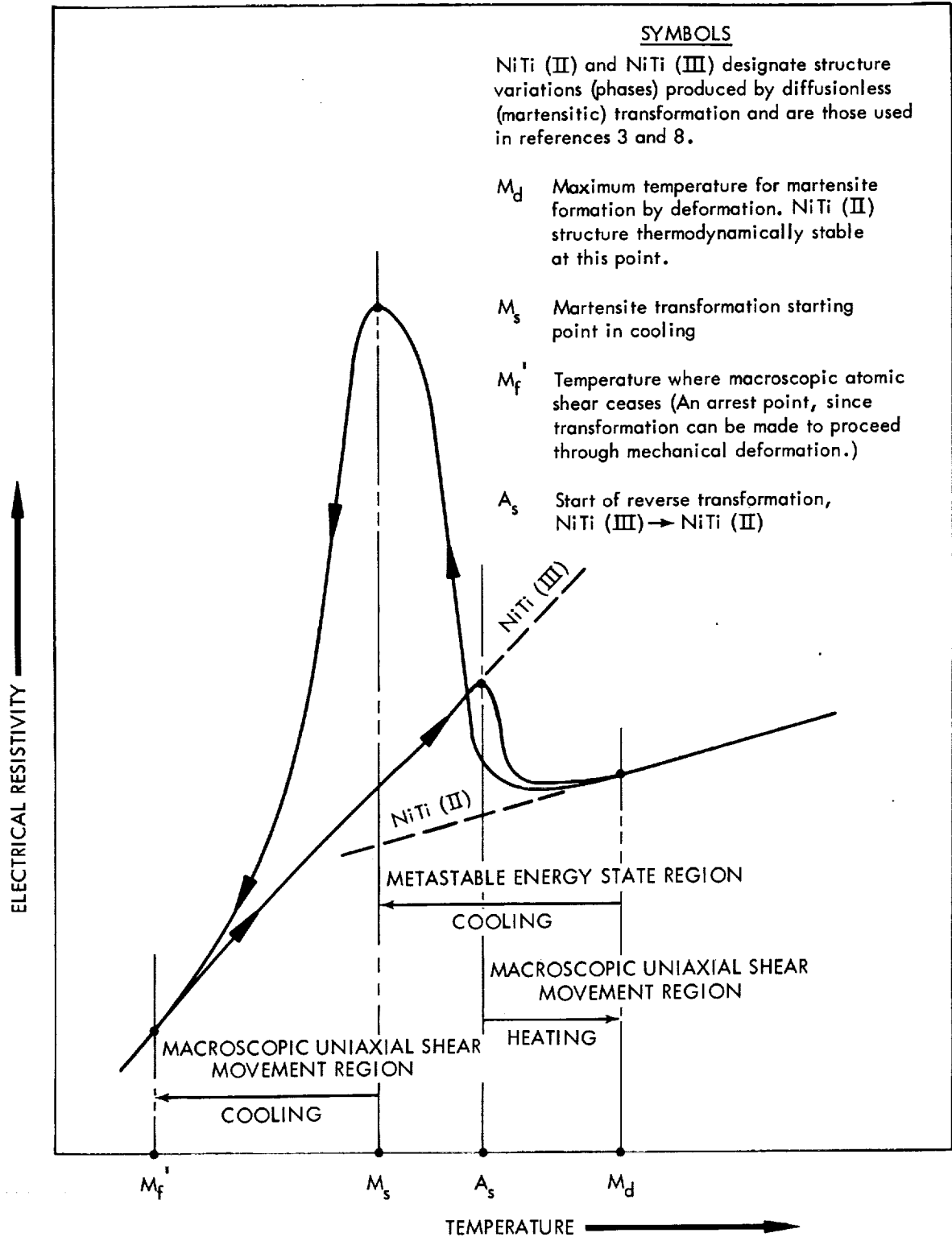
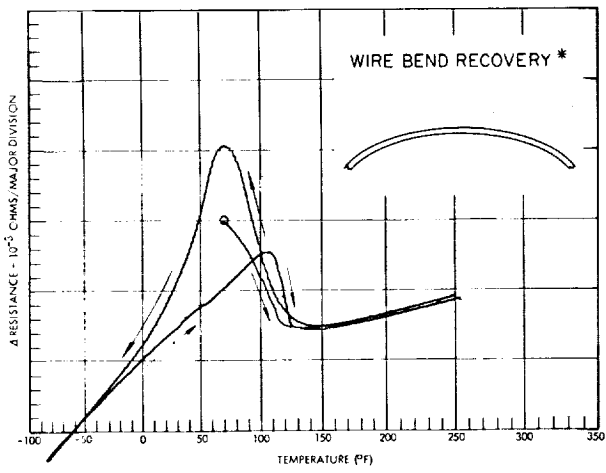
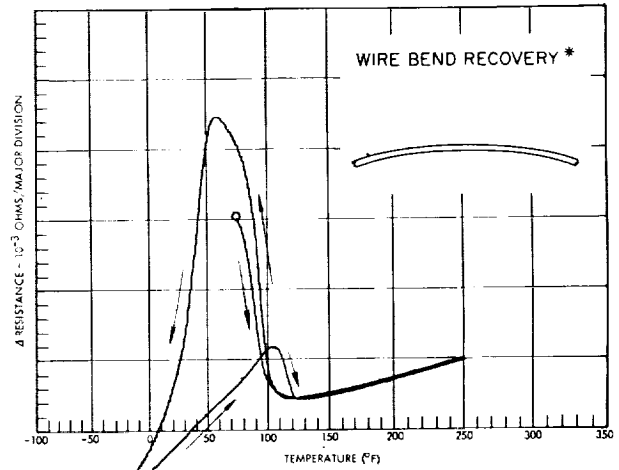


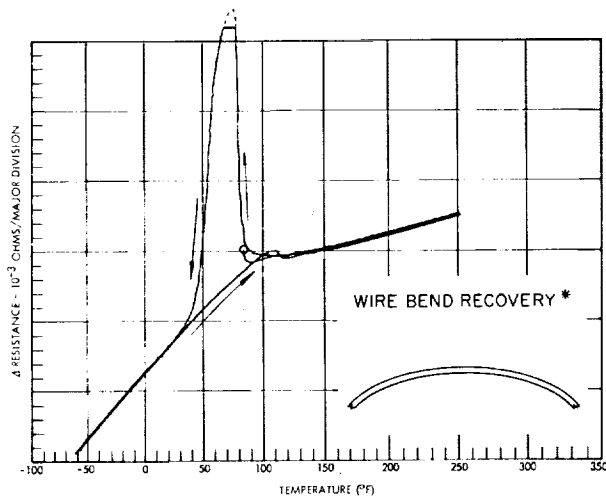
Figure 5. - Typical electrical resistivity versus temperature curves for drawn NiTi wire annealed at 932°F (500°C).



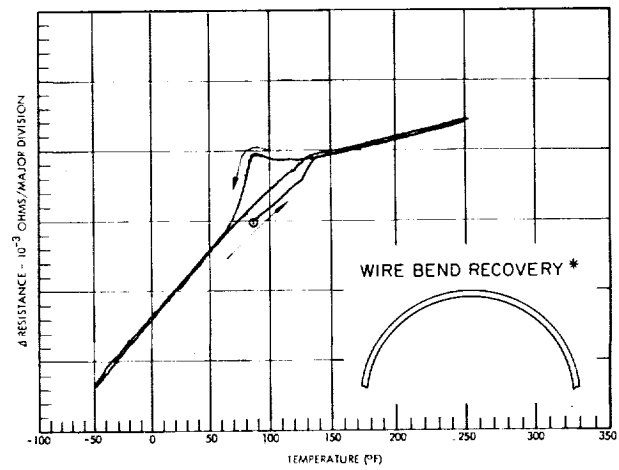
752°F (400°C)



932°F (500°C)



1112°F (600°C)



1292°F (700°C)

* WIRES WERE HEATED ABOVE TRANSFORMATION TEMPERATURE AFTER 360-DEGREE BEND. DEFORMATION REPRESENTS 9% STRAIN IN OUTSIDE FIBERS.

Figure 6. - Effect of post-drawing anneal temperatures on electrical resistance and bend recovery behavior.

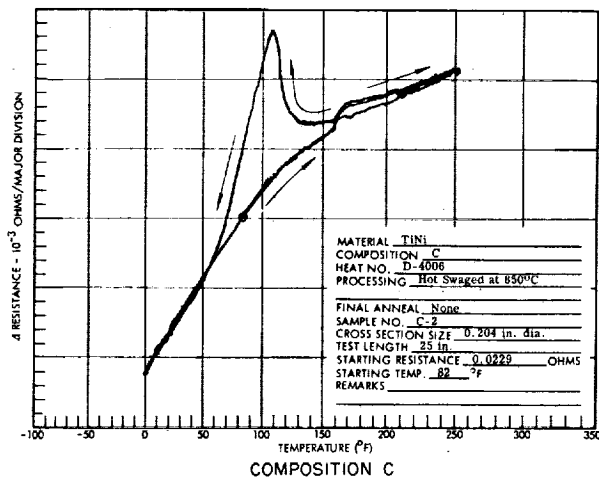
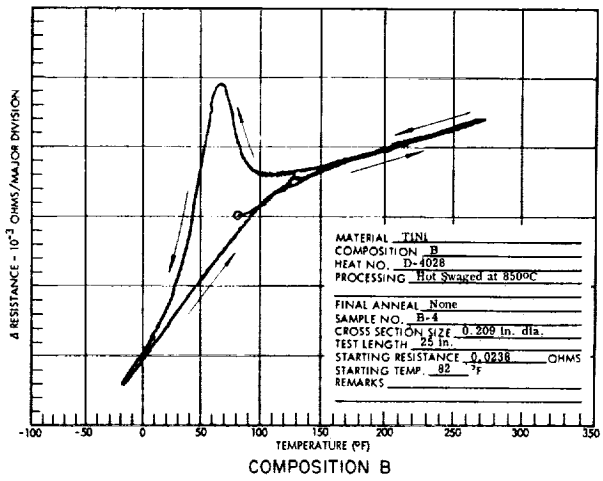
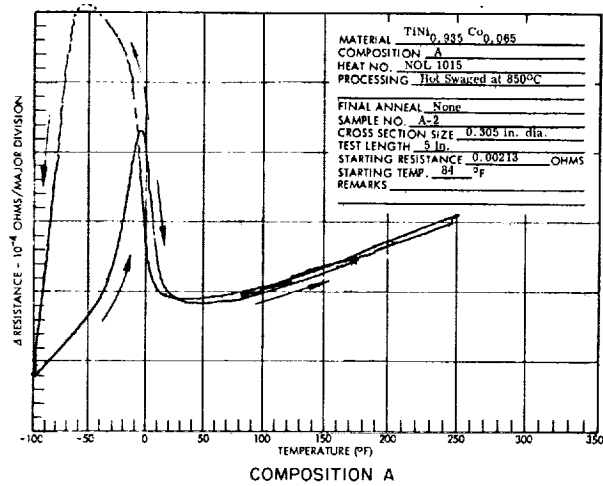


Figure 7. - Electrical resistance versus temperature curves for swaged rods.

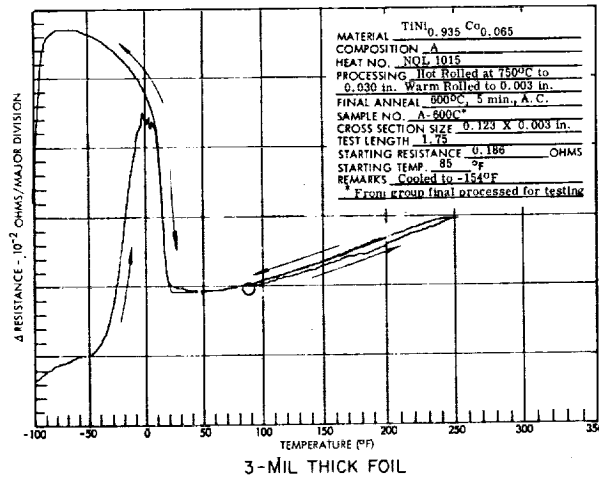
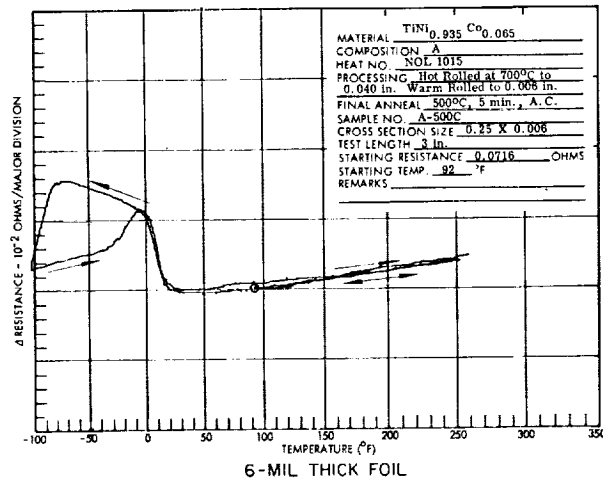
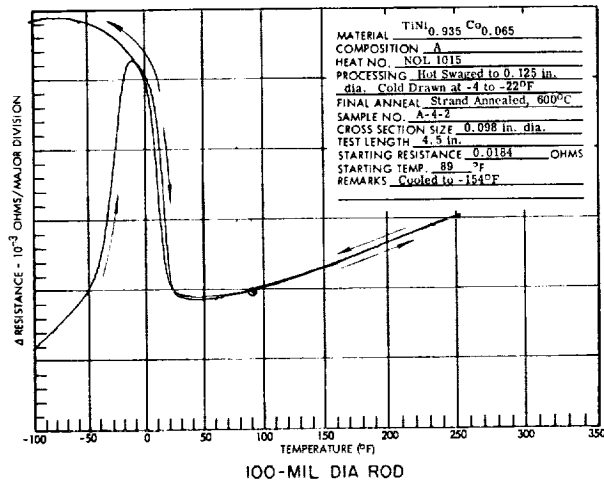


Figure 8. - Electrical resistance versus temperature curves for Composition A materials.

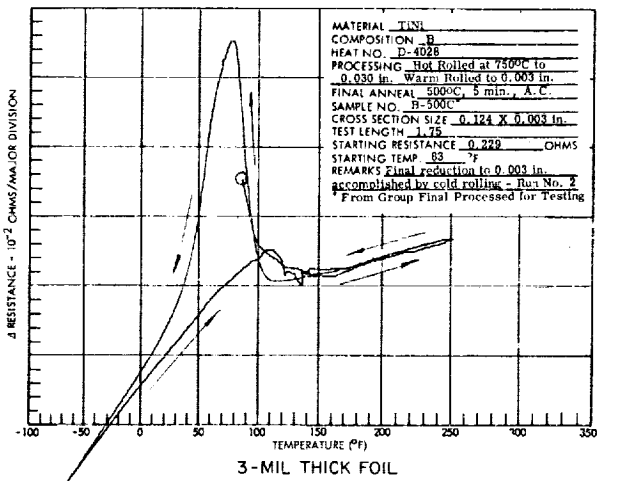
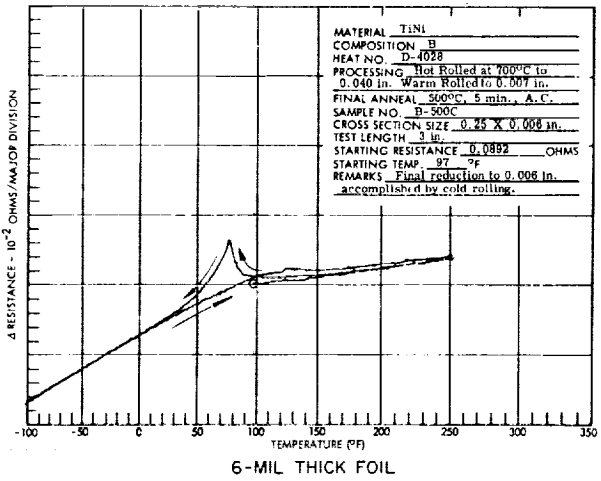
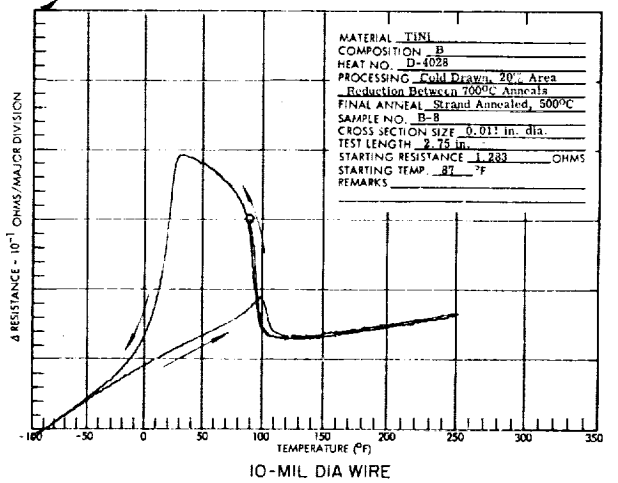
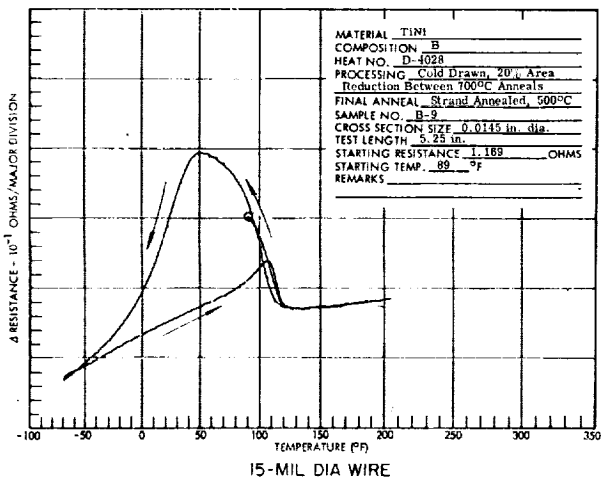
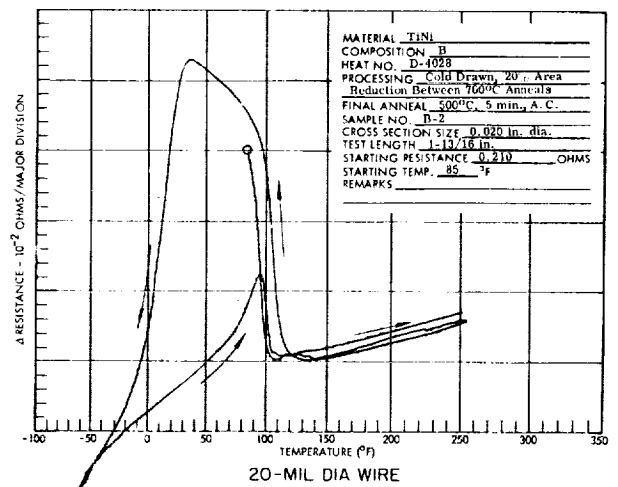
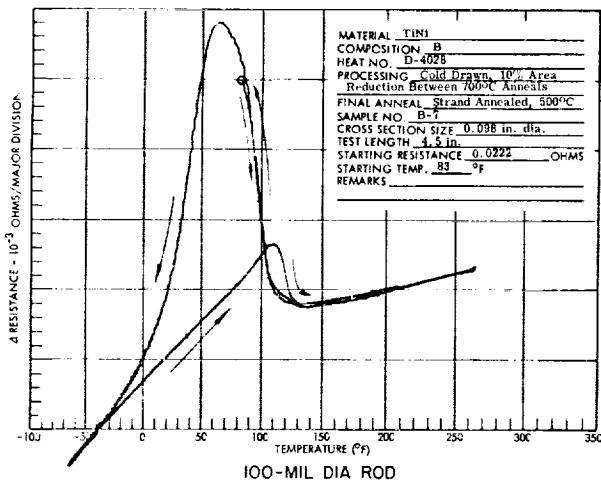


Figure 9. - Electrical resistance versus temperature curves for Composition B materials.

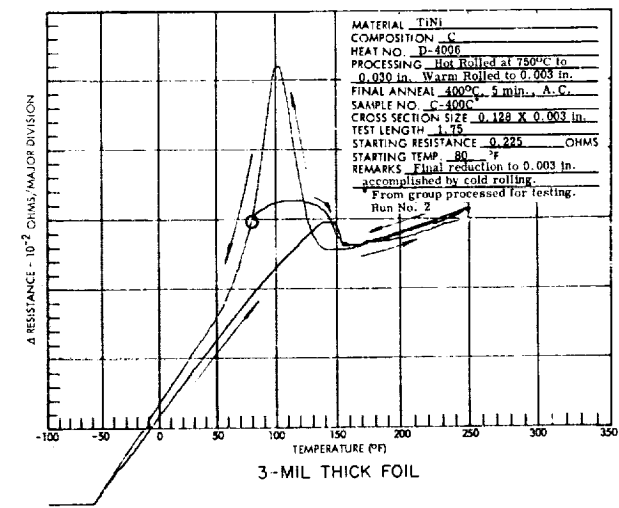
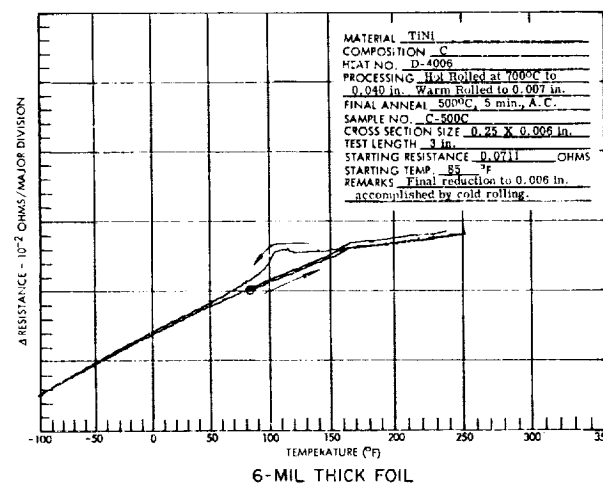
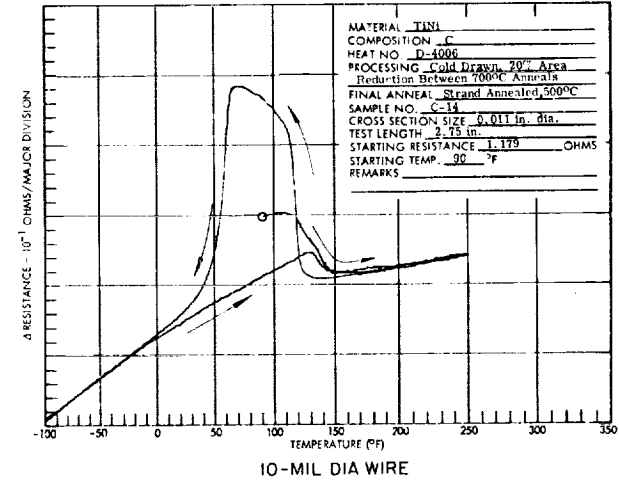
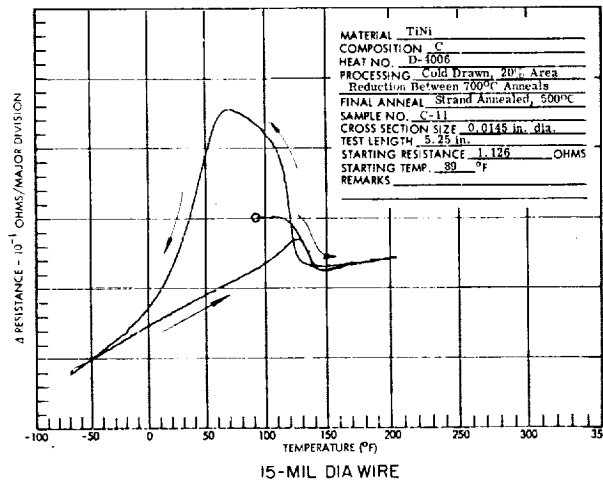
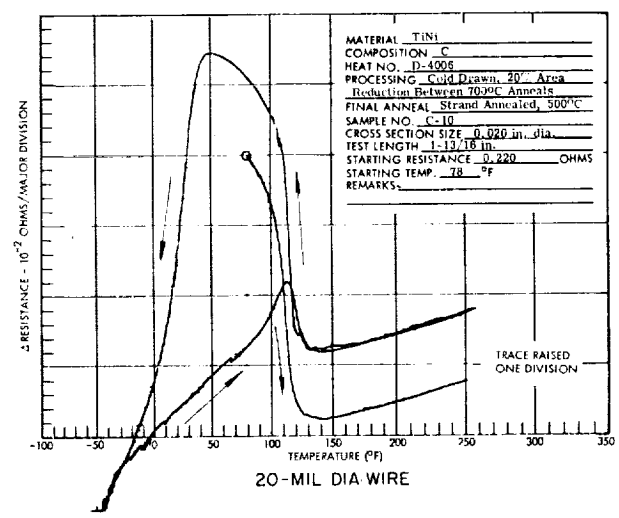
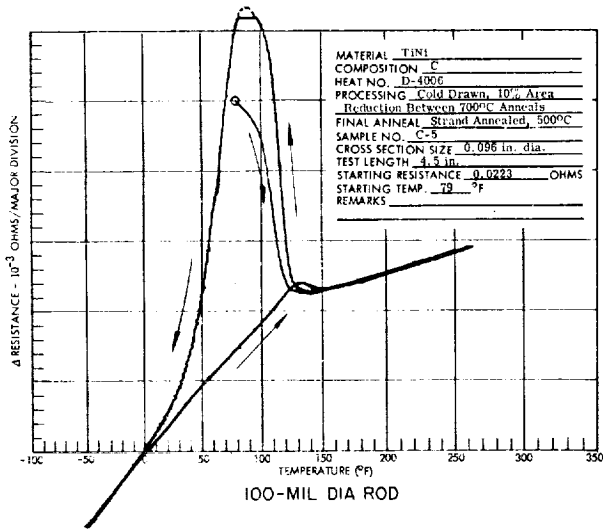


Figure 10. - Electrical resistance versus temperature curves for Composition C materials.

TABLE V. - APPROXIMATE M_d , M_S , M_f' , AND A_S CRITICAL TEMPERATURE POINTS^a FOR MATERIALS INVESTIGATED

Critical points	Temperature, °F, for indicated critical point						
	Hot-swaged bar	Cold-drawn wire				Rolled sheet	
		100-mil dia	20-mil dia	15-mil dia	10-mil dia	6-mil thick	3-mil thick
COMPOSITION A							
M_d	90	100				100	100
M_S	-60	-100				-80	-85
M_f'	(b)	(b)				(b)	(b)
$A_S^{(c)}$	-40/-10	-60/-10				-30/-5	-50/0
COMPOSITION B							
M_d	160	160	160	150	160	150	160
M_S	70	65	35	50	30	78	80
M_f'	0	-30	-40	-50	-50	25	-40
A_S	140	110	95	110	100	125	110
COMPOSITION C							
M_d	190	170	170	160	160	160	180
M_S	110	90	45	70	70	105	100
M_f'	60	0	-25	-40	-10	40	-10
A_S	160	130	115	130	130	170	150

^a Approximate M_d , M_S , M_f' , and A_S critical temperatures determined from electrical resistance versus temperature measurements.

^b M_f' below range plotted; therefore could not be determined.

^c Two values are given since a very large increase in the slope of the heating curve is obtained prior to the decrease point (A_S). This point is shown first and may represent more accurately the start point for reverse transformation in Composition A material.

Uniaxial dimensional change. - Uniaxial dimensional change (controlled dilation) experiments were conducted to gain a better understanding of the transformation process and its effect on the dimensional characteristics of drawn 100-mil rods. In addition, in certain cases the data provided an accurate measurement of M_S , A_S , M_d , and M_f' points that agreed very closely with those obtained using the electrical resistance versus temperature measurement technique. Figure 11 illustrates a profile of a typical uniaxial dimensional change of drawn wire that had been post-annealed at 932°F. Examination of the heating and cooling cycles showed that as the wire is cooled from a temperature above the M_d point, it contracts in a normal fashion until the martensite start temperature (M_S) is reached. The slope of this line agrees favorably

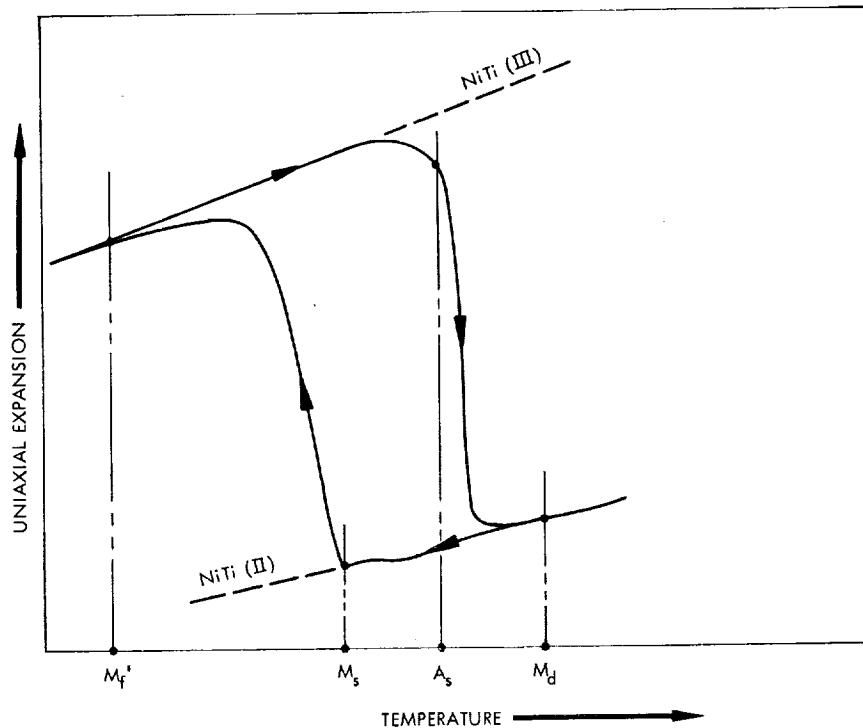


Figure 11. - Typical uniaxial dimensional change behavior for Composition B and C drawn wire annealed at 932°F.

with published thermal expansion data. Further cooling below this point results in large uniaxial expansion that terminates at approximately the M_f' point. (M_f' is defined as the limiting point associated with spontaneous atomic shear.) Cooling below the M_f' point produces normal contraction in an amount equal to that predicted by thermal expansion and contraction.

Heating the sample from a point below M_f' produces normal expansion behavior until the approximate A_s point is reached. At this point reverse transformation is initiated and atomic shear (contraction) begins. Shearing continues until about the M_d point.

The typical heating and cooling curves shown in figure 11 are those obtained when the sample is cooled from a temperature above the M_d point to a point at or below the M_f' point or heated from a point below M_f' to above the M_d point. It should be acknowledged that, in cooling, the path $M_d \rightarrow M_s$ is reversible, but $M_s \rightarrow M_f'$ is not. Likewise, in heating, the path $M_f' \rightarrow A_s$ is reversible, but $A_s \rightarrow M_d$ is not. Reversible behavior is obtained when the sample is heated or cooled in the region above the M_d point and below the M_f' point. If during cooling along the path $M_s \rightarrow M_f'$ or heating along path $A_s \rightarrow M_d$, temperature change ceases and the direction of change is reversed, a new path between lines $M_s - M_f'$ and $A_s - M_d$ will be established.

The previously described behavior was found to be characteristic of the Composition B and C alloys that were cold-drawn and post-annealed at 752°, 932°, and 1112°F. Furthermore, it was established that the magnitude of spontaneous dimensional change diminished as anneal temperatures were increased. However, it was found that at 1292°F, the highest post-drawing anneal temperature, little or no change occurred in the sample. This relationship is clearly seen in figure 12.

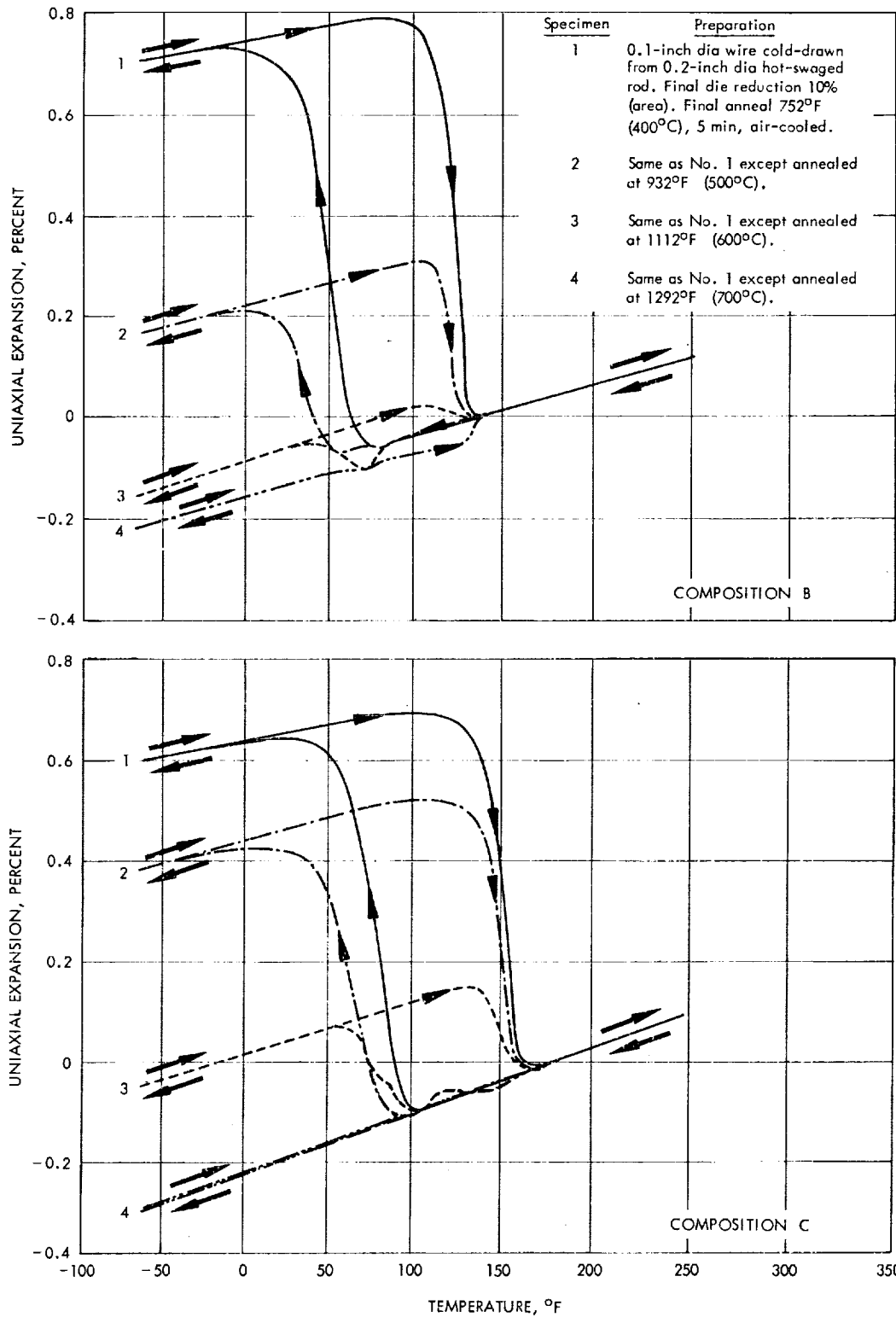


Figure 12. - Uniaxial dimensional change versus temperature curves for 100-mil diameter Composition B and C rods.

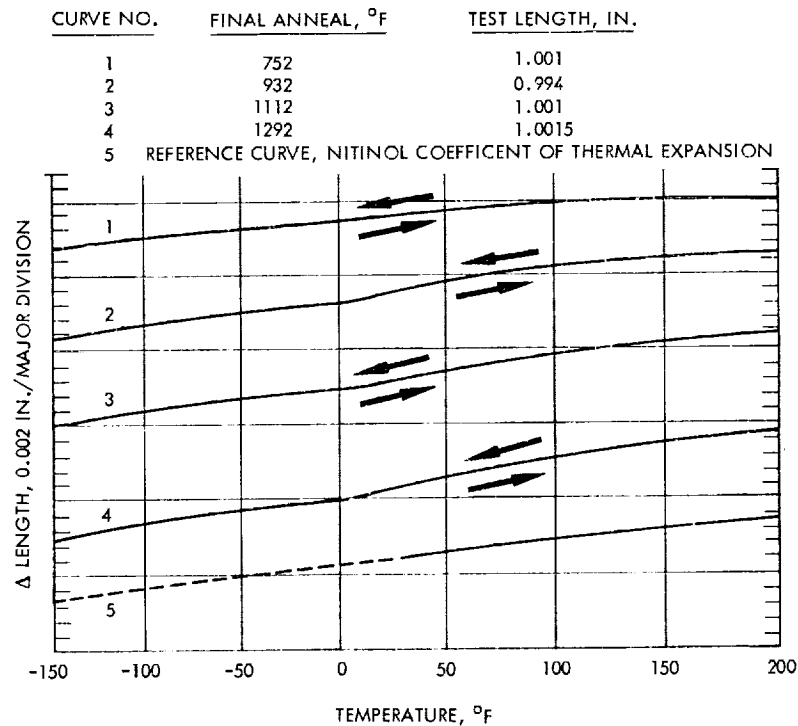


Figure 13. - Uniaxial dimensional change versus temperature curves for 100-mil diameter Composition A rods.

Uniaxial dimensional tests were also performed on Composition A rods post-annealed at temperatures of 752^o, 932^o, 1112^o, and 1292^oF. The results of these tests are shown in figure 13. It can be seen that little, if any, dimensional change occurred in any of the samples tested. Although the reason for this is yet unknown, it is possible that it is linked with the temperature level at which wire drawing was performed. This temperature, although maintained at -4^o to -22^oF during drawing, was well above the M_S point of -60^oF determined for hot-swaged bar. Since it appears that this material was at a higher energy state during drawing than Compositions B or C, a slightly different structure may have developed. This is confirmed somewhat by the fact that some distinctive variation between drawn Composition A material and drawn Composition B and C materials can be noted in the resistance versus temperature profiles. It is also possible that a much lower post-drawing anneal range would have produced a different behavior.

Mechanical Behavior

Stress versus elongation curves. - Stress versus elongation curves were obtained at various temperatures, above and below the transformation zone, during heating and cooling cycles for each type of material as indicated in table I.

Each set of data provides important and useful quantitative information required for the successful utilization of each type of wire and sheet in a structural design. Detailed examination of these curves with regard to how modulus and yield point properties change with temperature adds to the overall understanding of the transformation in Nitinol alloys.

Two typical sets of stress versus elongation curves obtained on 100-mil and 20-mil diameter Composition B material when cooling from 300° to -100°F (cooling cycle) and when heating from -100° to 300°F (heating cycle) are presented in figures 14 and 15. The modulus and 0.2 percent offset yield stress obtained from the data in figure 14 and presented in figure 16 show graphically how these two properties are affected by temperature.

With reference to the stress-strain data, the modulus of elasticity (E) and yield strength (F_y) were obtained from the 100-mil diameter material, whereas the ultimate strength (F_{ult}) and ultimate elongation (e_{ult}) were determined from the wire sizes of 20-mil diameter and under as a function of temperature.

Referring to figure 16A, it can be seen that as the temperature is lowered below about 180°F (the approximate M_d point), yield stress is progressively lowered until a minimum is reached at the M_S point (60°F). The 60°F M_S point was verified from the electrical resistance versus temperature curves shown in figure 9. Continued cooling below the M_S point produces a small continuous increase in yield stress.

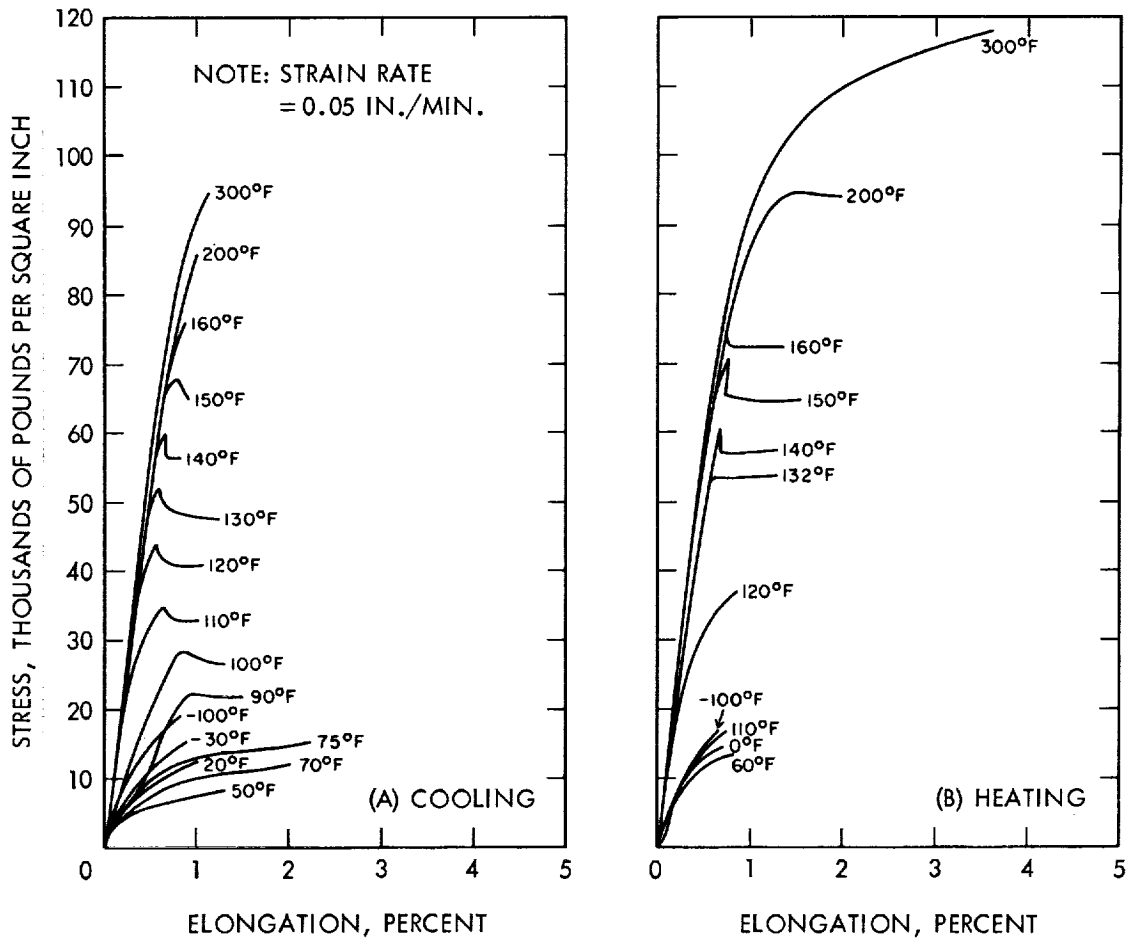


Figure 14. - Stress versus elongation curves for 100-mil diameter Composition B rods during cooling and heating cycles.

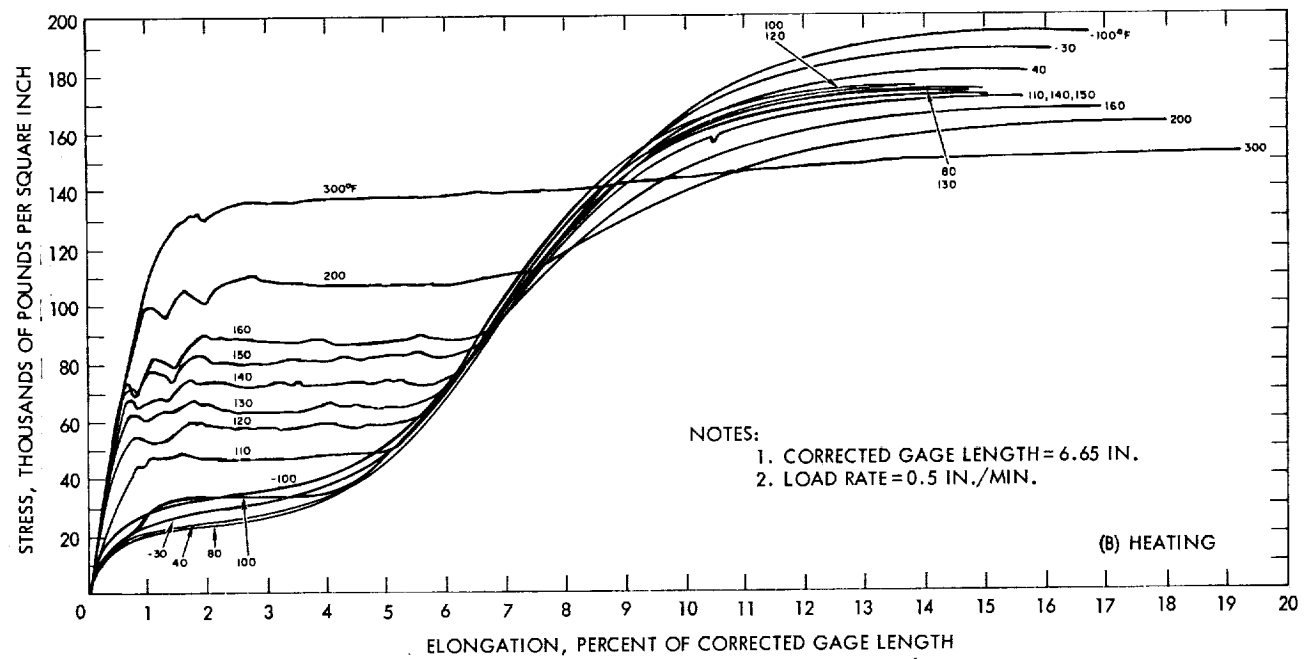
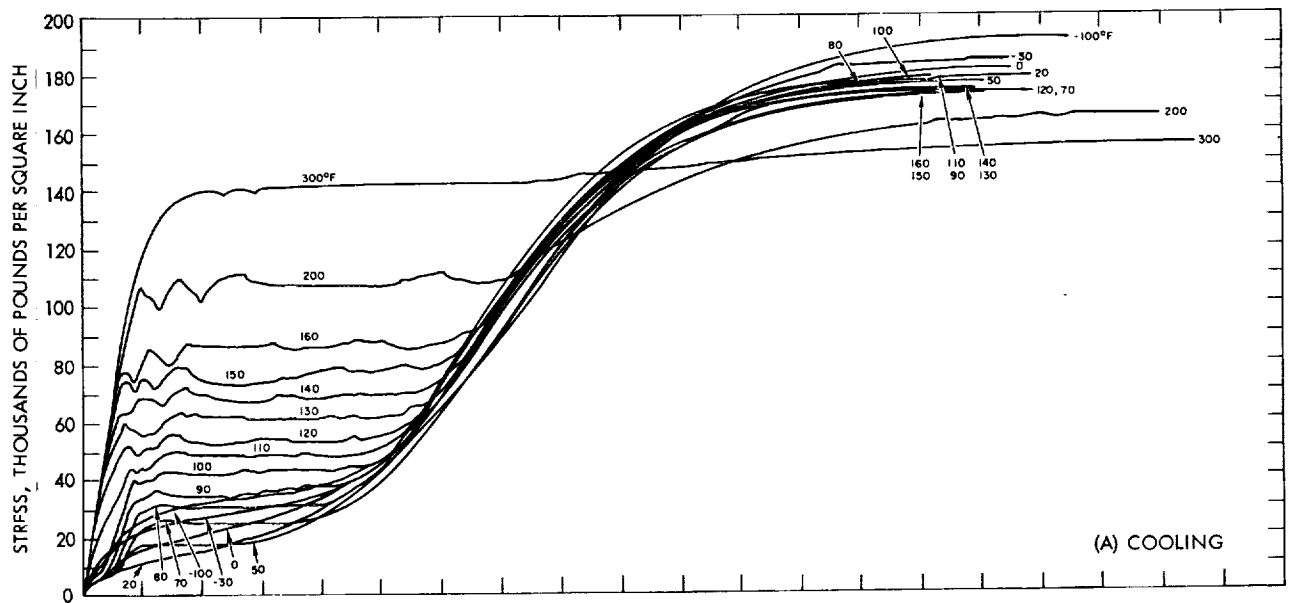


Figure 15. - Stress versus elongation curves for 20-mil diameter Composition B wire during cooling and heating cycles.

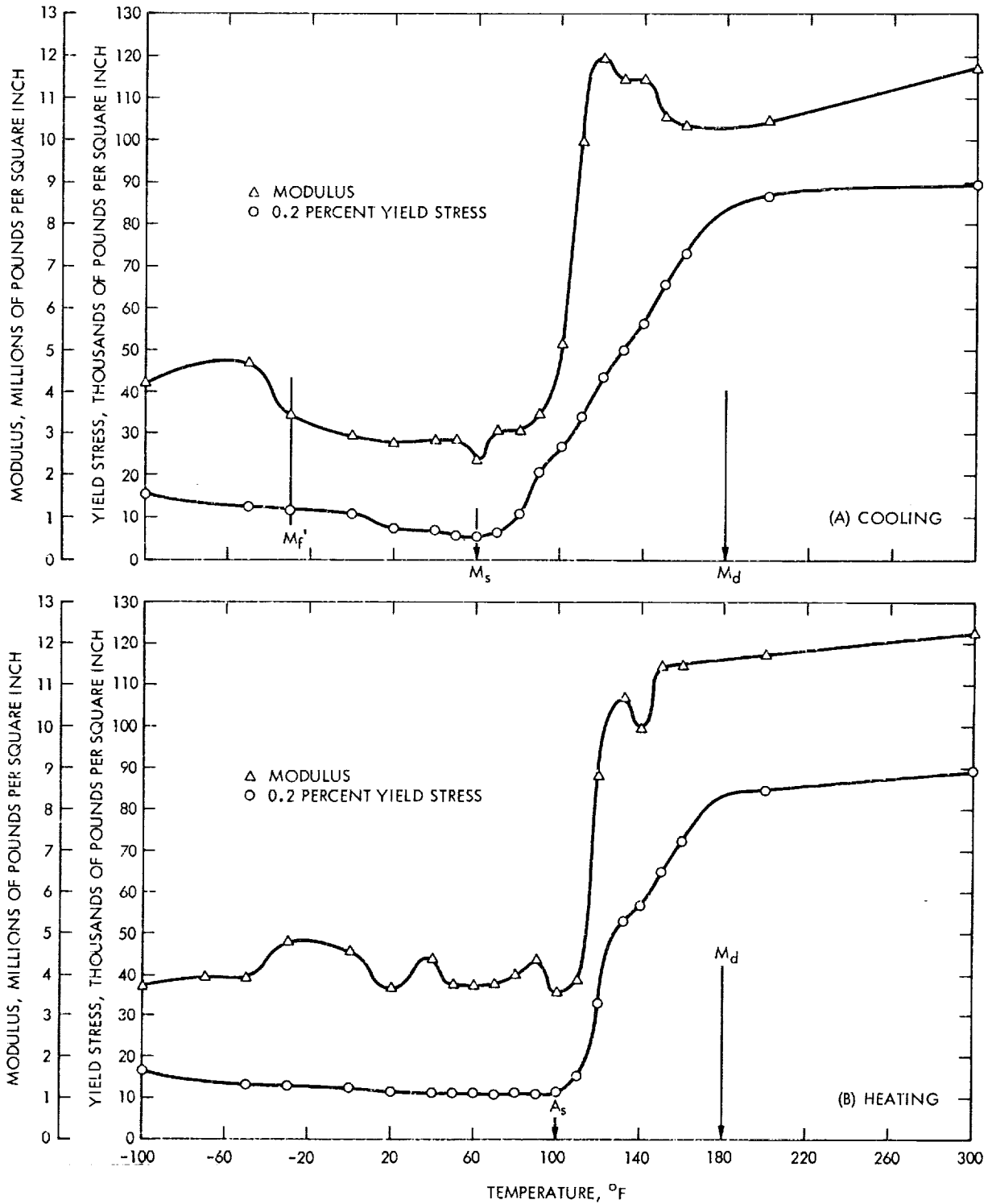


Figure 16. - Yield stress and modulus versus temperature curves for 100-mil diameter Composition B rods during cooling and heating cycles.

Increasing the temperature from a level considerably below the M_S point produces a small gradual decrease in the yield stress until about 100°F (the approximate A_S point). Beyond this point, yield stress sharply increases until a plateau is reached at about 180°F (the M_D point).

Since it is known that decreasing temperature leads to thermodynamic instability, it would be expected that elastic modulus would also decrease as the M_S point is approached. The postulated behavior is confirmed in figure 16A, which shows that modulus declines as temperature approaches the M_S point. However, an anomalous rise in modulus, starting at approximately the M_D point and continuing to 120°F , precedes a sharp decline to its minimum level at the M_S point. Continued cooling produces only a slight increase in modulus until about -30°F . At this point a rise in modulus is noted in the data obtained. The -30°F point appears to coincide with the M_f' point derived from the electrical versus temperature measurements.

Heating following cooling considerably below the M_S point, as shown graphically in figure 16B, does not significantly change the modulus until the temperature is increased above 100°F , the A_S point. At this point a slight increase in temperature greatly increases the elastic modulus. Examination of the data shows that modulus increases are largely confined between the A_S temperature and about 180°F , the M_D temperature.

The preceding discussion describing the behavior of 100- and 20-mil diameter Composition B materials applies, in general, to the other compositions and forms tested.

Degree of shape recovery. - Testing was conducted to determine the ability of Composition A, B, and C wire and foil to recover to its annealed shape after being plastically deformed near its M_S point. No external load was applied during recovery.

Tensile recovery: A typical tensile recovery test sequence consisted of uniaxially elongating a specimen to a predetermined strain level. The straining force was then removed and the amount of elastic recovery (spring-back) was measured and recorded. Composition A materials were deformed at -65°F while Composition B and C materials were deformed at 75°F .

This data is summarized in figures 17, 18, and 19, which show both elastic recovery (measured at the deformation temperature) and the total degree of recovery (consisting of elastic and thermal recovery) as a function of strain. The recovery limit was found to vary between 6 and 8 percent strain for the different compositions of wire 100, 20, 15, and 10 mils in diameter. Variations, although not large, are thought to result from the different processing histories, such as the amount of cold-drawing prior to final annealing, etc. The effects of processing are more clearly seen by comparing the performance of Composition B and C foil material with that of the wire. The foils that had little cold reduction prior to final anneal exhibited full recovery up to about two percent strain level. The behavior of Composition A foil was superior to that of Composition B and C foils in that it recovered completely up to the six percent strain level. This behavior was not unexpected, since the cooling and heating cycles of the electrical resistance versus temperature curves (fig. 8) encompassed more area than the B and C foil material (figs. 9 and 10). Performance differences, however, may not result totally from processing history variations and may be partly attributed to the composition of the alloy.

Compressive recovery: Recovery tests similar to the tensile recovery tests were also conducted in the compressive mode. The test data obtained on 100-mil diameter Composition B and C rods are presented in figure 20, which shows the degree of shape recovery as a function of initial compression strain. Comparing the data obtained on the two compositions, it is seen that full recovery from compression was obtained up to about four percent strain in the case of Composition B, while Composition C was somewhat less, since considerable degradation in recovery occurred after about two percent strain.

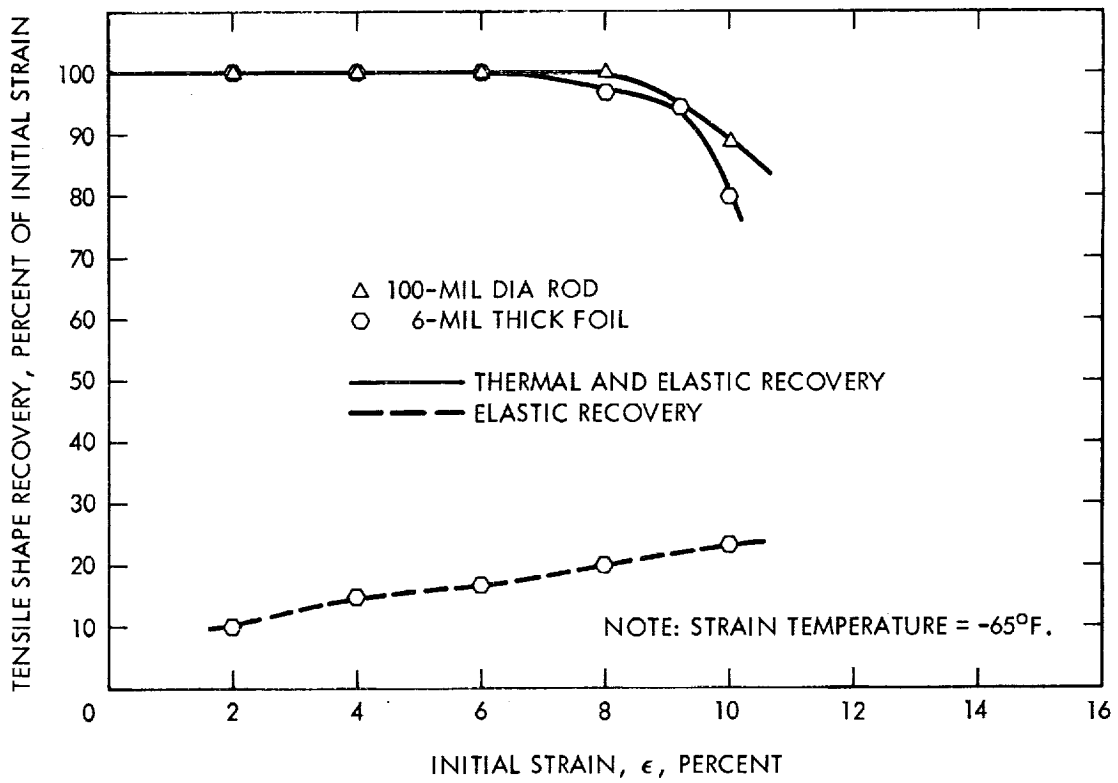
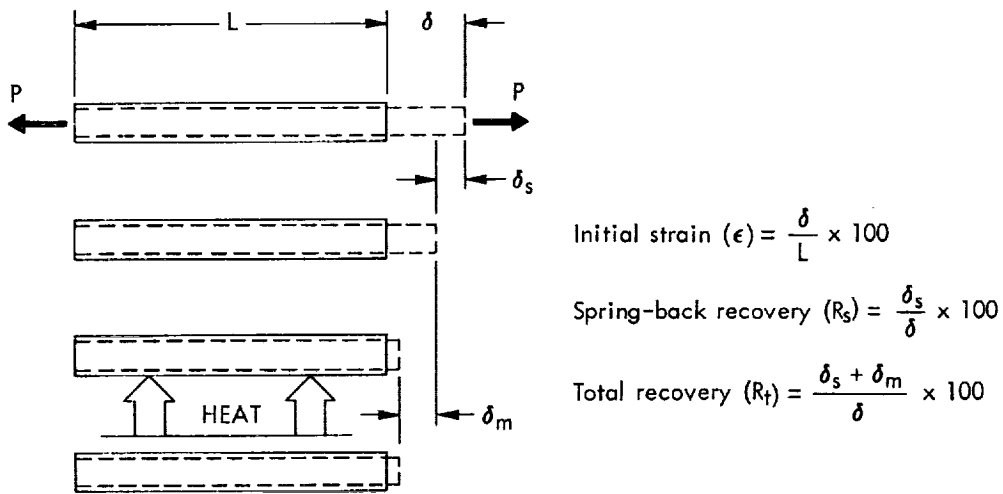


Figure 17. - Tensile shape recovery versus initial strain curves for Composition A materials.

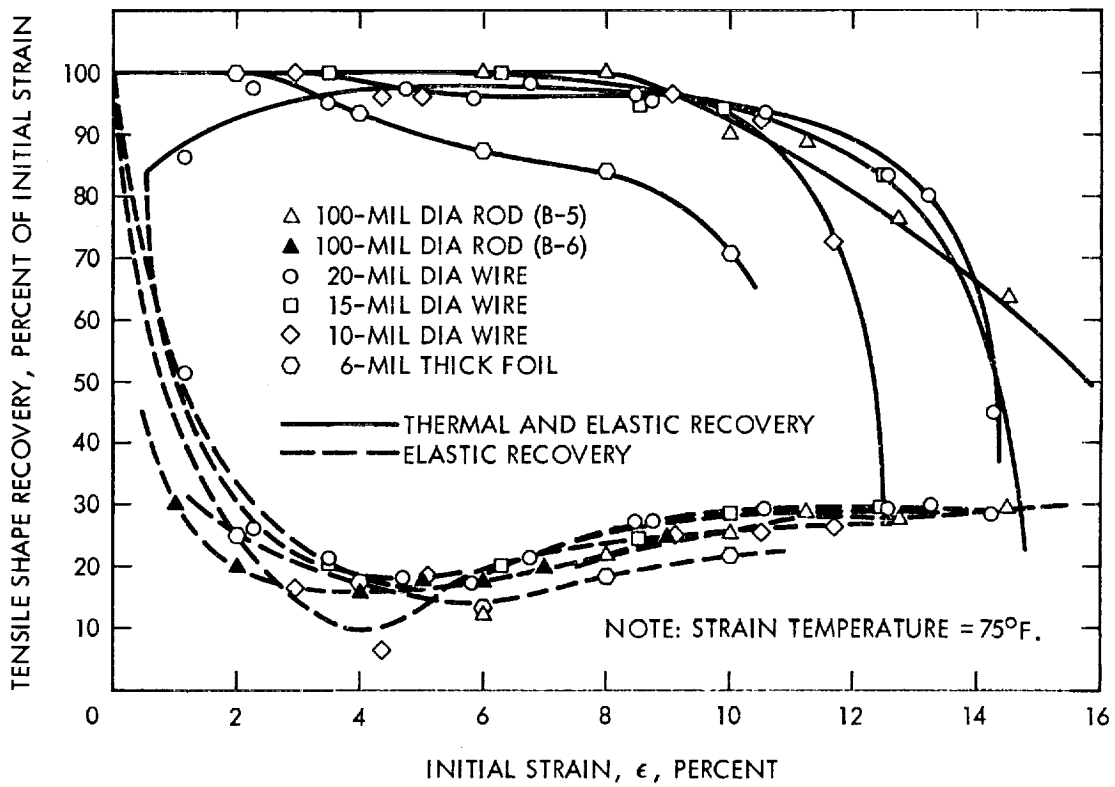
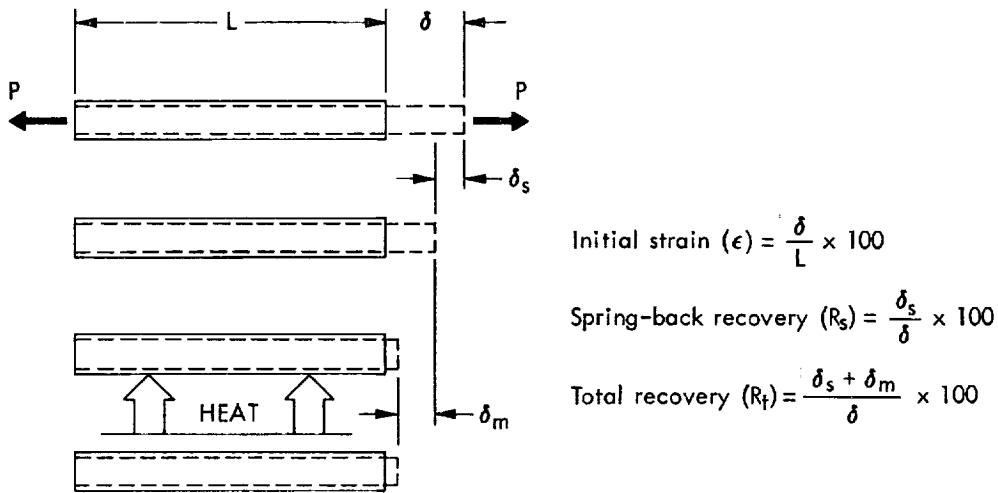


Figure 18. - Tensile shape recovery versus initial strain curves for Composition B materials.

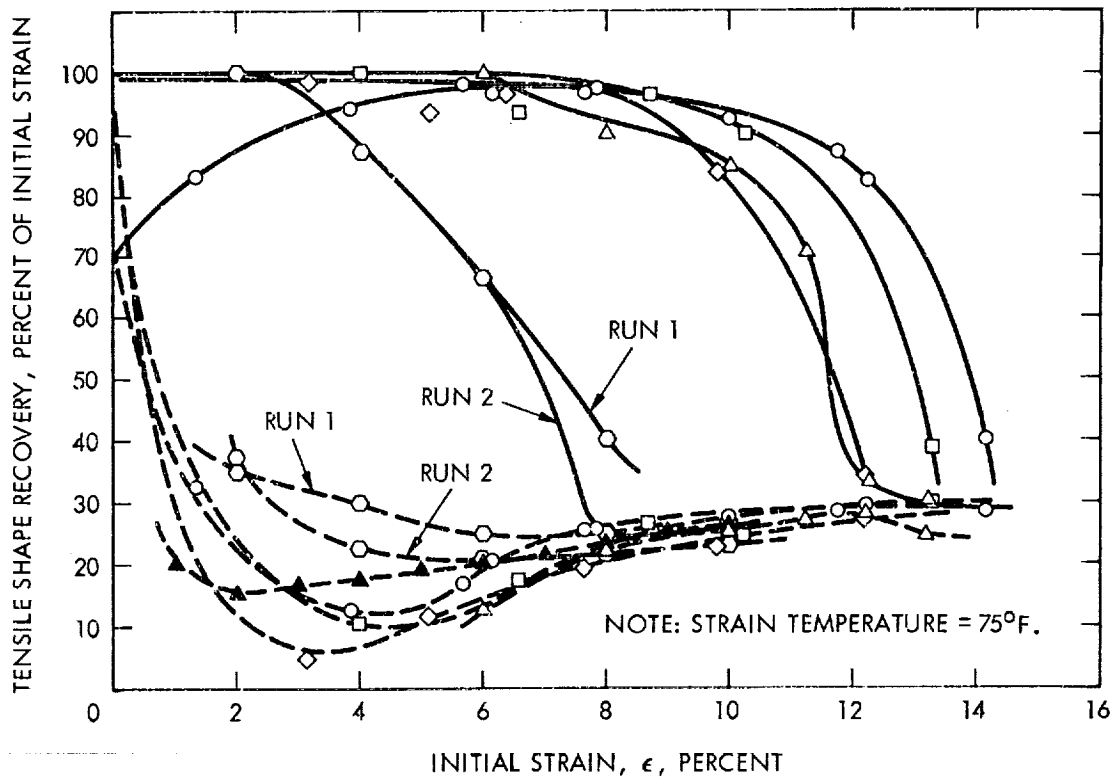
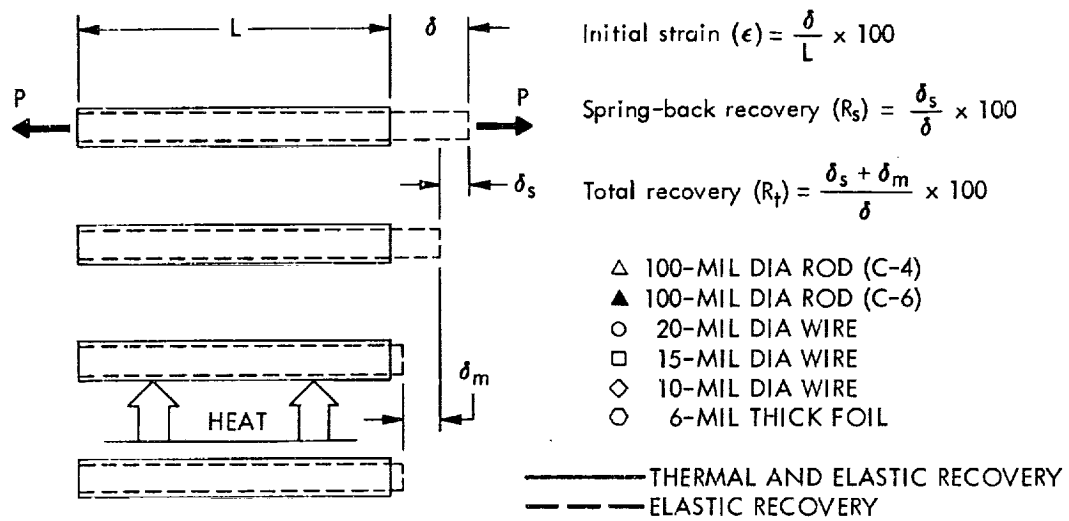


Figure 19. - Tensile shape recovery versus initial strain curves for Composition C materials.

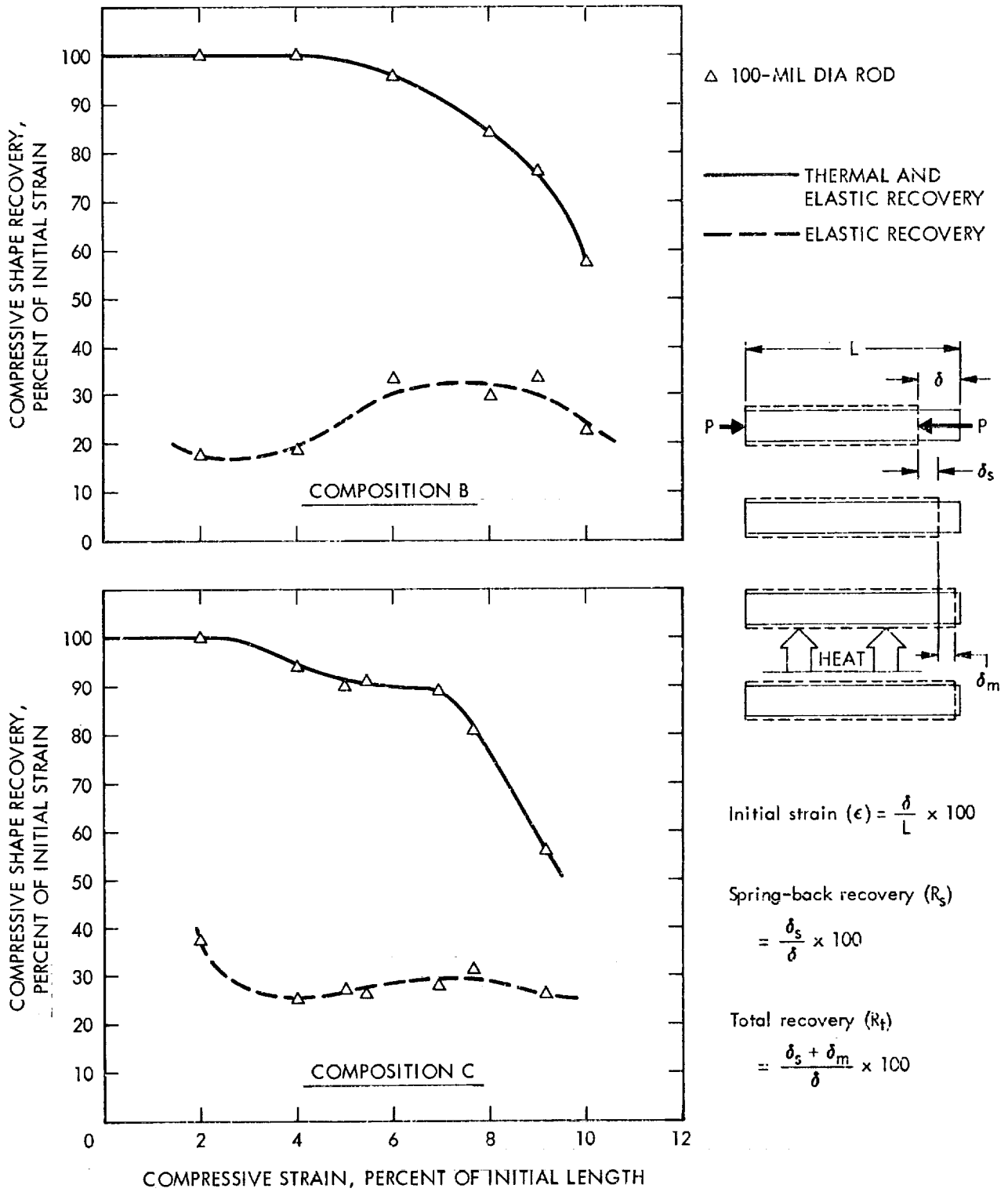


Figure 20. - Compression shape recovery versus initial strain curves for Composition B and C rods.

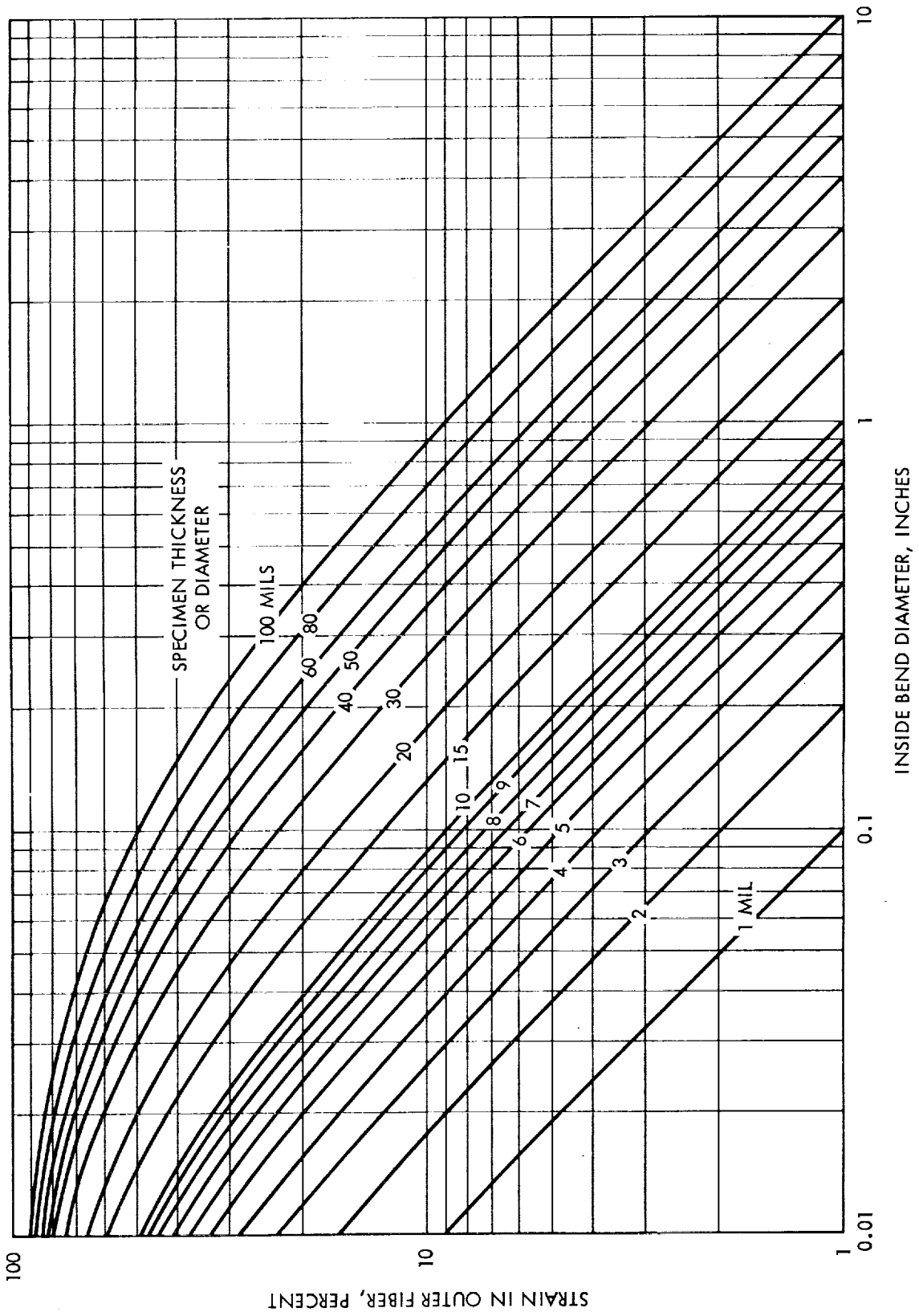


Figure 21. - Strain in outer fiber as a function of bend diameter and specimen thickness.

Bend recovery: Of the possible deformation modes, bending perhaps holds the most interest because it is through this means that a large surface area structure, such as a parabolic antenna or passive communications satellite, could be tightly packaged for subsequent self-erection in outer space.

Bend recovery data were obtained on 100-mil diameter Composition A wire and 100-, 20-, 15-, and 10-mil diameter Composition B and C wire. Data were also obtained on 6- and 3-mil Composition A, B, and C rolled sheet (foils).

Tests were performed by bending the specimens 180 degrees about mandrels of varying diameters. Actual mandrel diameters were selected so that the effect of varying degrees of outside fiber strain could be evaluated. Figure 21 shows how outside fiber strain varies as a function of inside bend diameter. Following deformation, the specimen was released and the elastic recovery (spring-back) was measured. Composition A specimens were bent at -65°F and Composition B and C specimens were bent at 75°F prior to heating. Martensitic recovery was then brought about by increasing the specimen temperature until full recovery was obtained or until it was noted that an increase in temperature did not produce any additional recovery. Where possible, simultaneous measurements of sample temperature and degree of recovery were taken so that the degree of recovery could be closely related to specimen temperature. Due to the fast heating response obtained when 6- and 3-mil thick Composition A specimens were exposed to room air temperatures, simultaneous measurements on the group were not obtained.

Figures 22, 23, and 24 show the bend recovery of Composition A, B, and C specimens

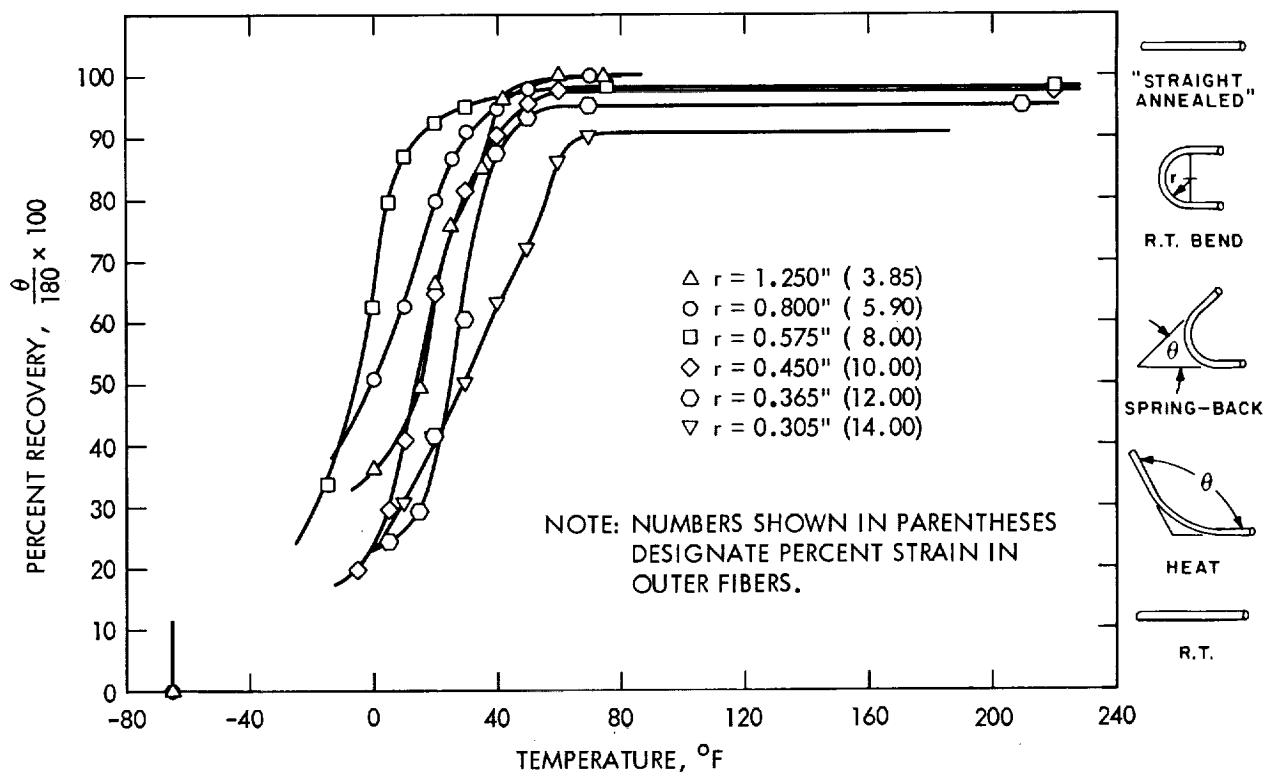


Figure 22. - Bend recovery versus temperature curves for 100-mil diameter Composition A rods.

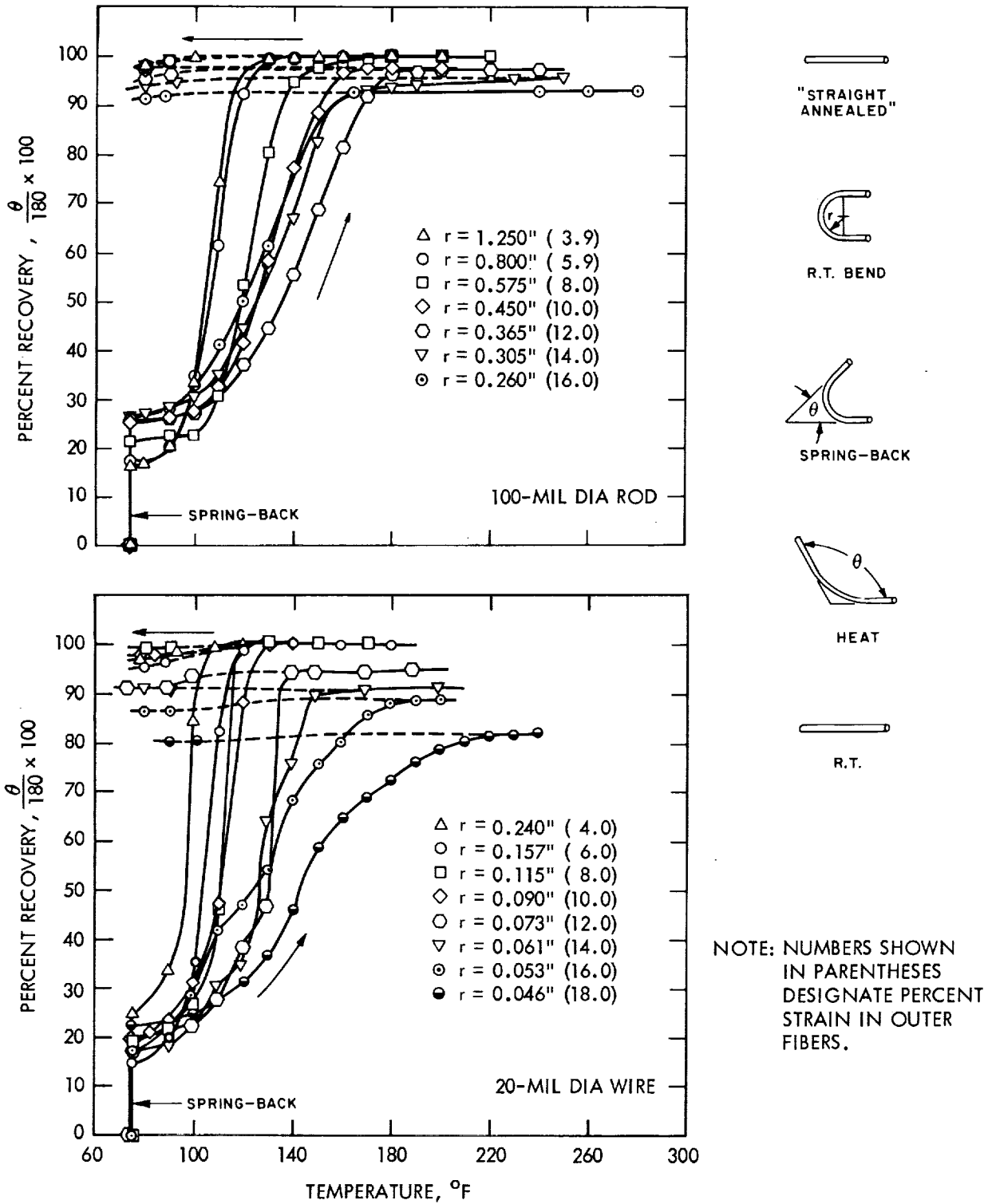


Figure 23. - Bend recovery versus temperature curves for Composition B materials.

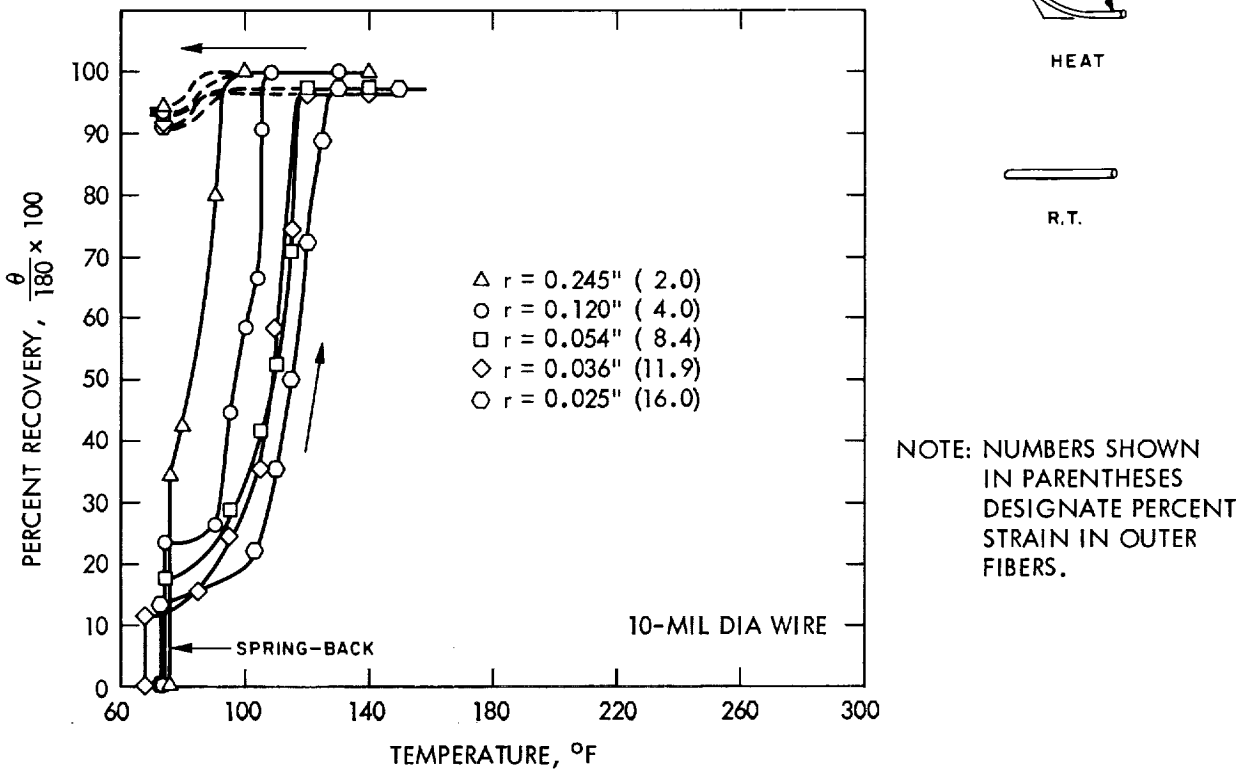
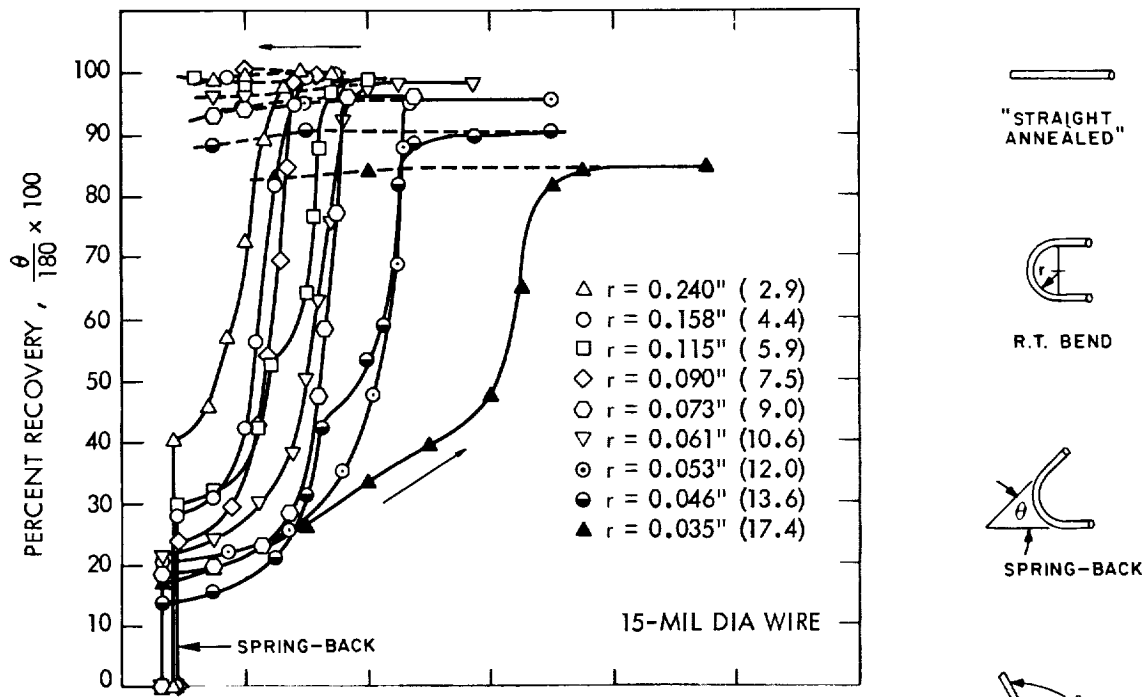
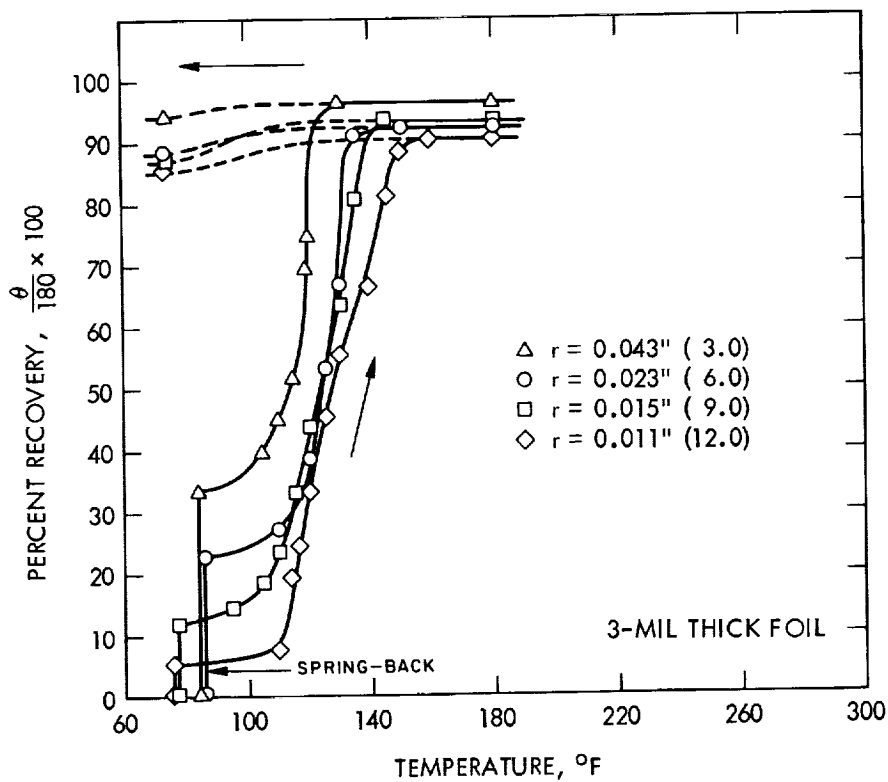
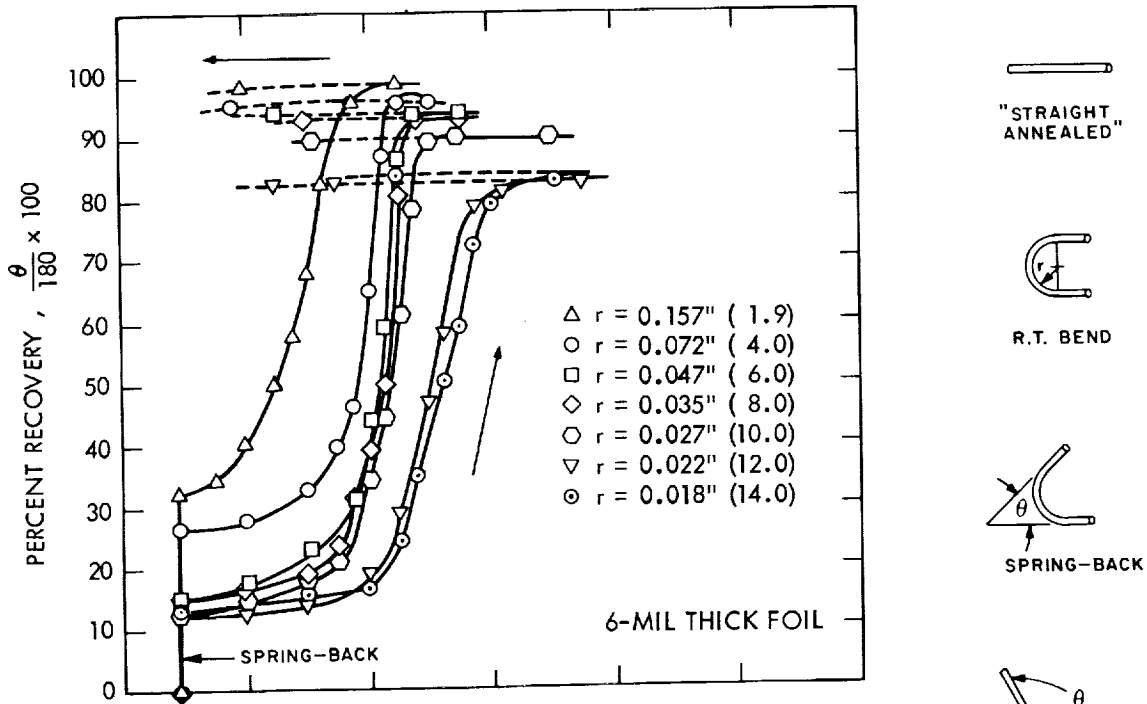
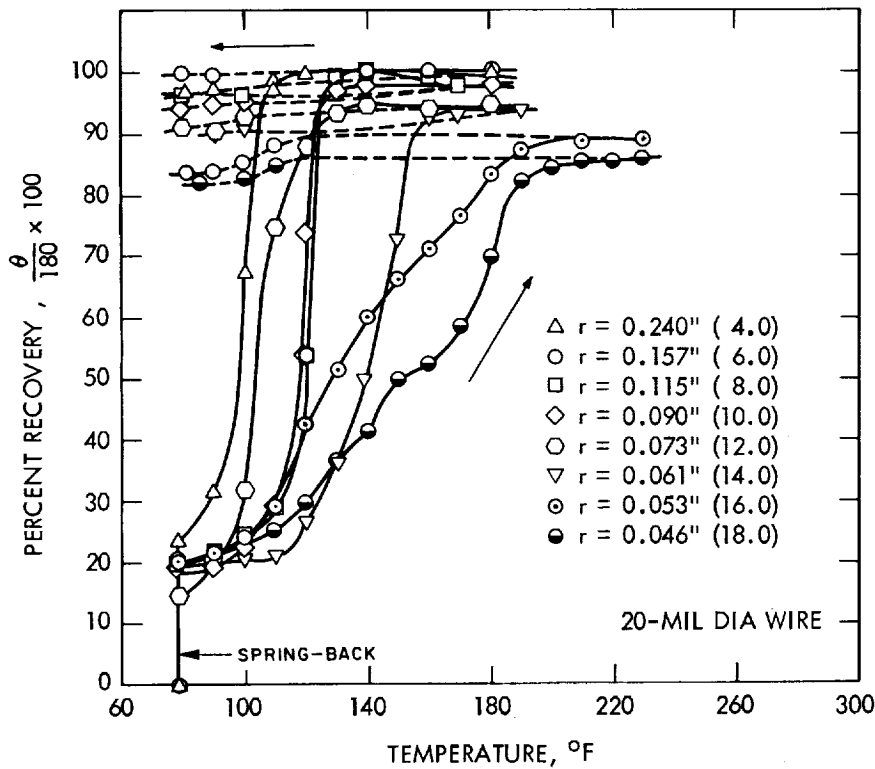
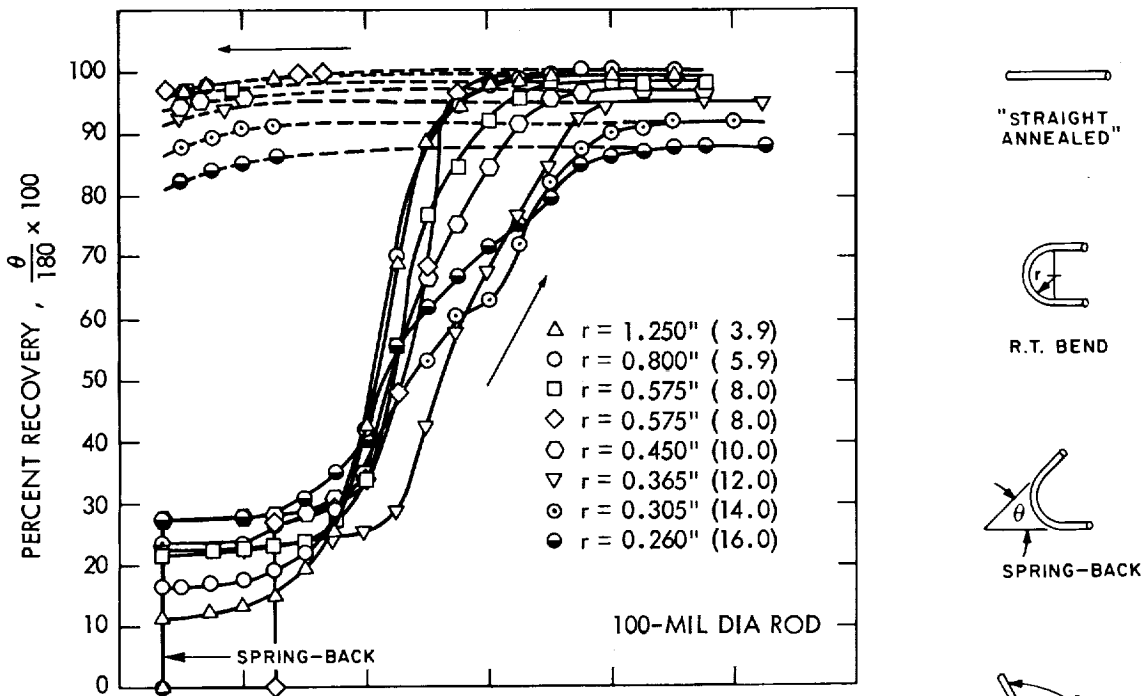


Figure 23. - Continued.



NOTE: NUMBERS SHOWN IN PARENTHESES DESIGNATE PERCENT STRAIN IN OUTER FIBERS.

Figure 23. - Concluded.



NOTE: NUMBERS SHOWN IN PARENTHESES DESIGNATE PERCENT STRAIN IN OUTER FIBERS.

Figure 24. - Bend recovery versus temperature curves for Composition C materials.

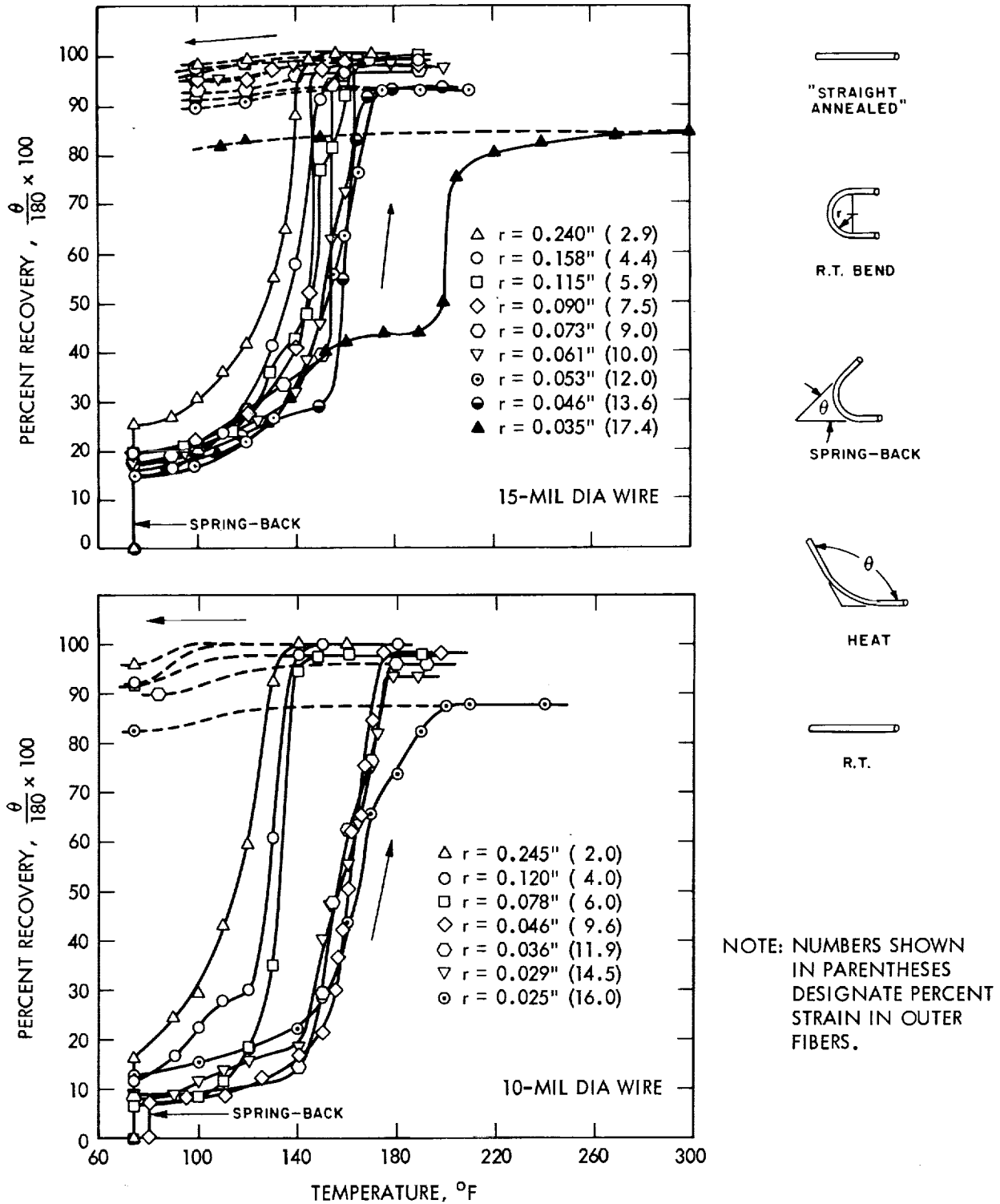
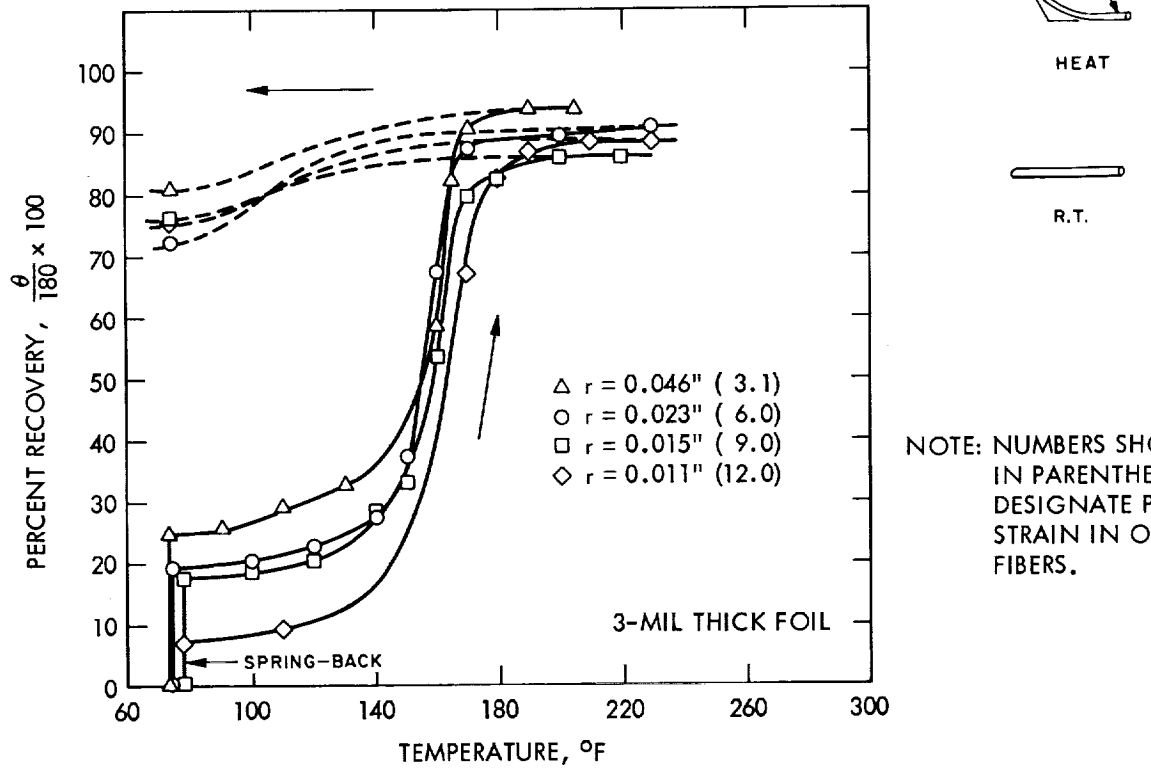
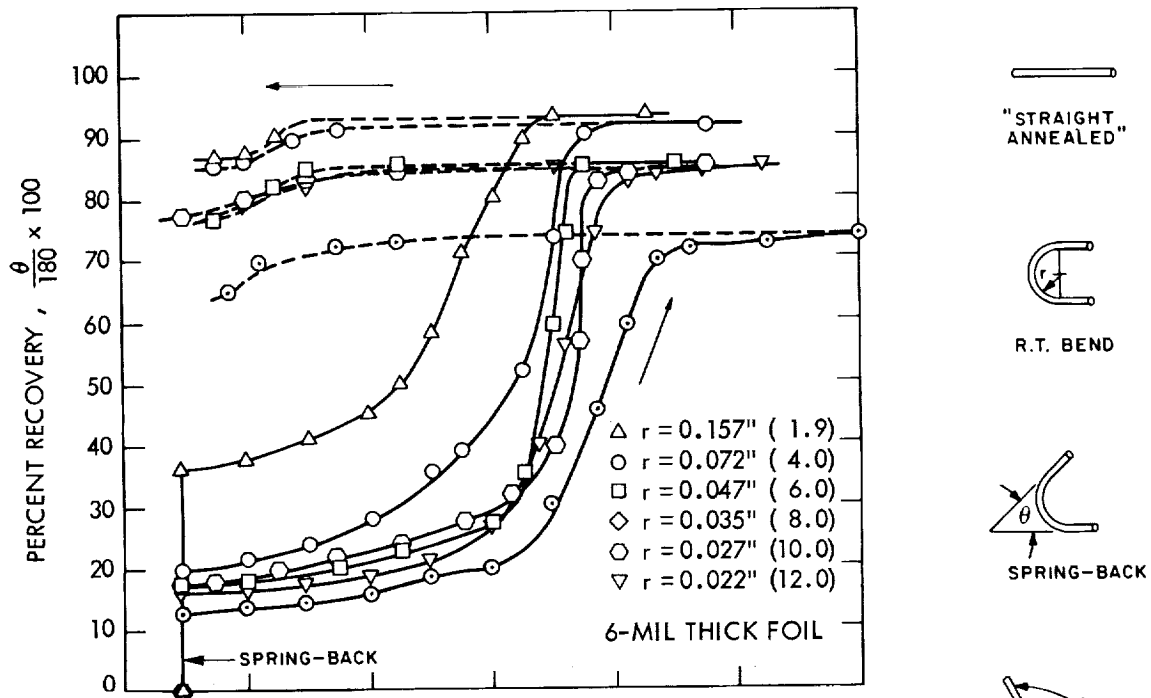


Figure 24. - Continued.



NOTE: NUMBERS SHOWN IN PARENTHESES DESIGNATE PERCENT STRAIN IN OUTER FIBERS.

Figure 24. - Concluded.

as a function of sample temperature. Examination reveals that increasing the temperature results in a slight increase in recovery until the A_S point is reached, whereupon small temperature increases produce large recovery rates. In general, the A_S point agrees favorably with that predicted on the basis of electrical resistance versus temperature tests; however, some increases are apparent in the highly deformed specimens.

Another interesting type of behavior that can be noted in examining these curves is that specimens tend to return slightly to their bend shape as the temperature is lowered from the level where the highest recovery was obtained.

Figures 25, 26, and 27 show the effects of strain (in the outside fibers) on martensitic and elastic recovery (spring-back) of Compositions A, B, and C.

It can be seen from these curves that complete bend recovery varies from 6 to 10 percent outside fiber strain for the types of wire tested. Furthermore, the fall-off is gradual beyond the full recovery point, so that many of the specimens exhibited as much as 90 percent recovery at strain levels as high as 14 to 16 percent. Recovery performance of the foils was considerably below that of the wires. It was found that specimens could be strained only 1 to 1.5 percent before full recovery was lost. Outside fiber strain in excess of this amount produced gradual but constant fall-off in recovery.

Recovery stress. - To gain a better understanding of the forces associated with the shape recovery process, tensile recovery stress characteristics of each of the compositions and processed forms were determined. To accomplish this, each specimen was uniaxially strained (elongated) a predetermined amount. After the load was removed, each wire was heated and the force (stress) required to prevent recovery was measured as a function of temperature.

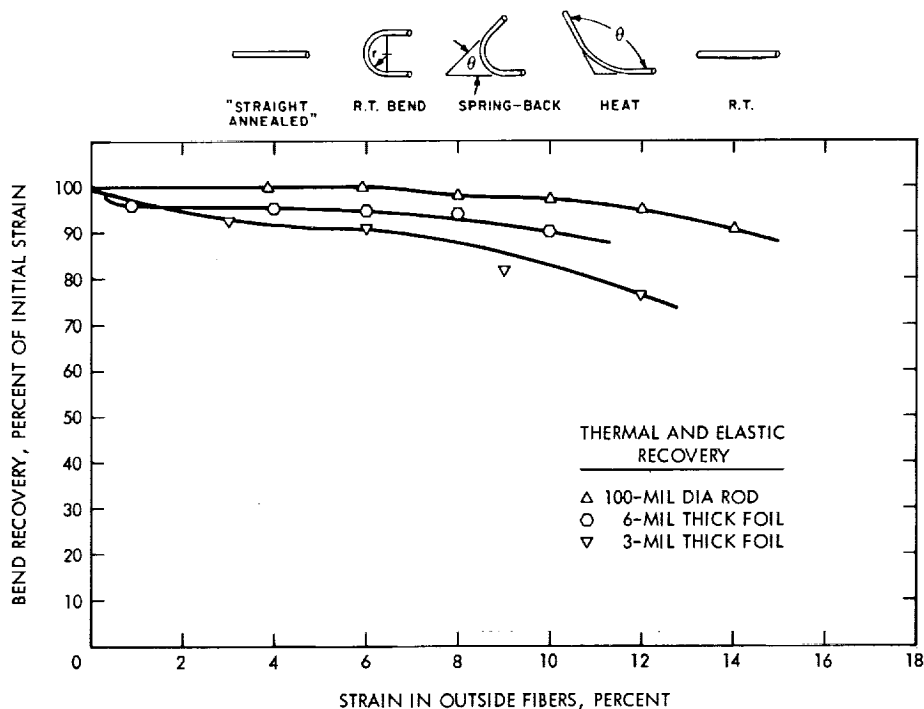


Figure 25. - Bend shape recovery versus initial strain curves for Composition A materials.

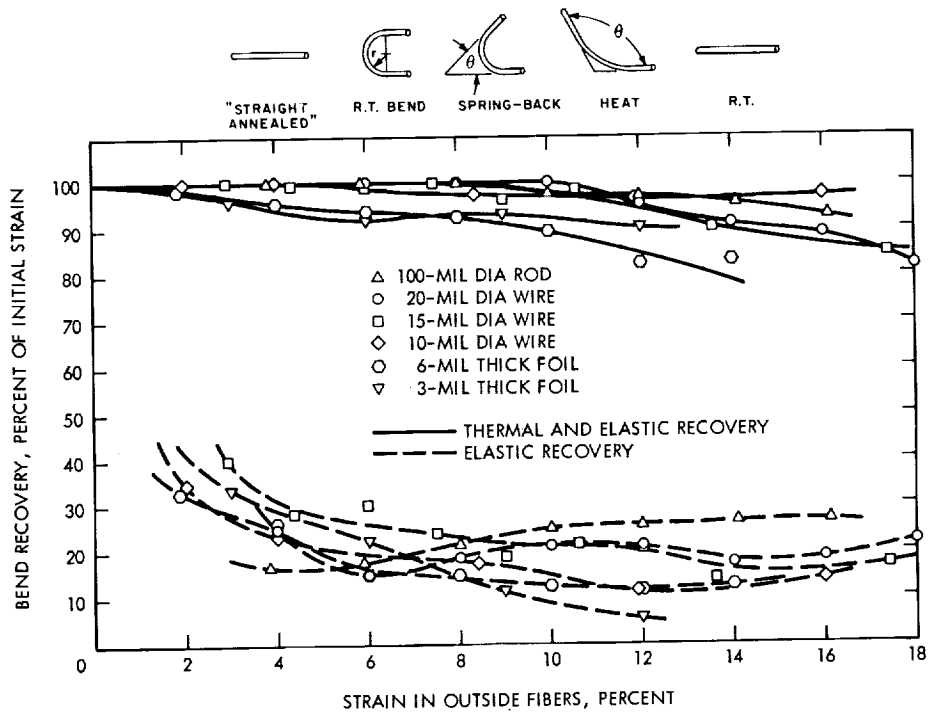


Figure 26. - Bend shape recovery versus initial strain curves for Composition B materials.

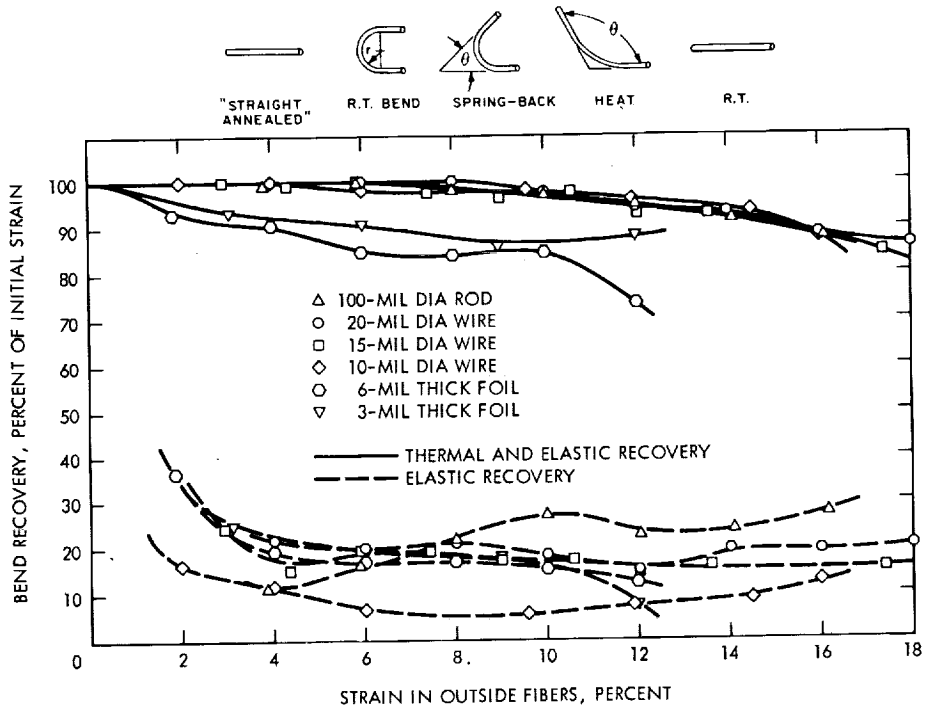


Figure 27. - Bend shape recovery versus initial strain curves for Composition C materials.

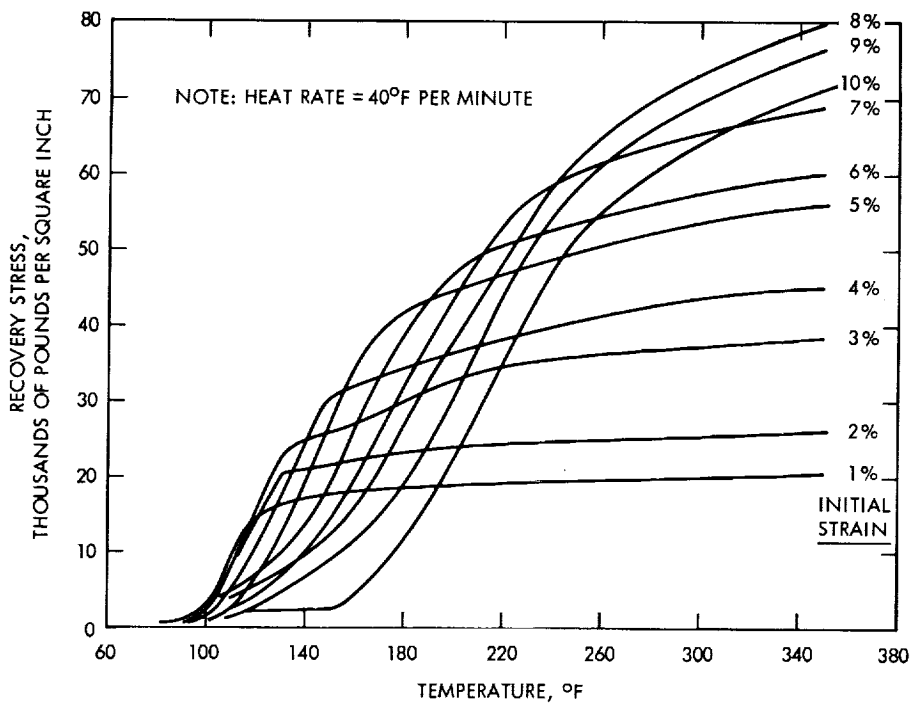


Figure 28. - Tensile recovery stress versus temperature curves for 100-mil diameter Composition B rods at various strain levels.

A representative set of curves obtained in this manner is shown in figure 28. These curves show the tensile recovery stress performance of 100-mil diameter Composition B rods at various strain levels. It can be seen that higher initial strain produces a higher recovery stress. Furthermore, as initial strain is increased, higher temperatures are required to attain maximum recovery stress. A maximum recovery stress of 110 000 psi was recorded for 20-mil diameter Composition B wire strained initially to 8 percent. This stress was produced by a force of 34.5 pounds. This stress was the highest value recorded of all the materials tested. A summary of the recovery stress performance of each specimen is presented in figures 29, 30, and 31. Maximum recovery stress obtained upon heating is plotted as a function of initial strain (elongation). From the data it is clearly seen that a maximum strain level (approximately 8 percent) beyond which recovery stress diminishes is inherent in each specimen. It is believed that these variations are the result of the initial processing histories.

Mechanical work. - The ability of each specimen to perform mechanical work was measured by applying a constant force to the end of a vertical specimen. The force (weight) uniaxially strained the wire. Following straining, the specimen was heated while the force was maintained, and the recovered strain (deflection) was measured as a function of temperature. The product of the deflection times the constant force per unit of material volume (specific work) was then plotted as a function of temperature for both the heating and cooling cycles. A family of curves was obtained for each material by varying the constant load (initial strain).

An interesting observation was made in connection with the cooling cycle. As the specimen was cooled, with the constant load imposed, it would elongate plastically beyond the initial starting length if a suitable stop were not provided. This "super" plastic behavior is initiated when the temperature is lowered to the M_S point and the specimen becomes very soft and

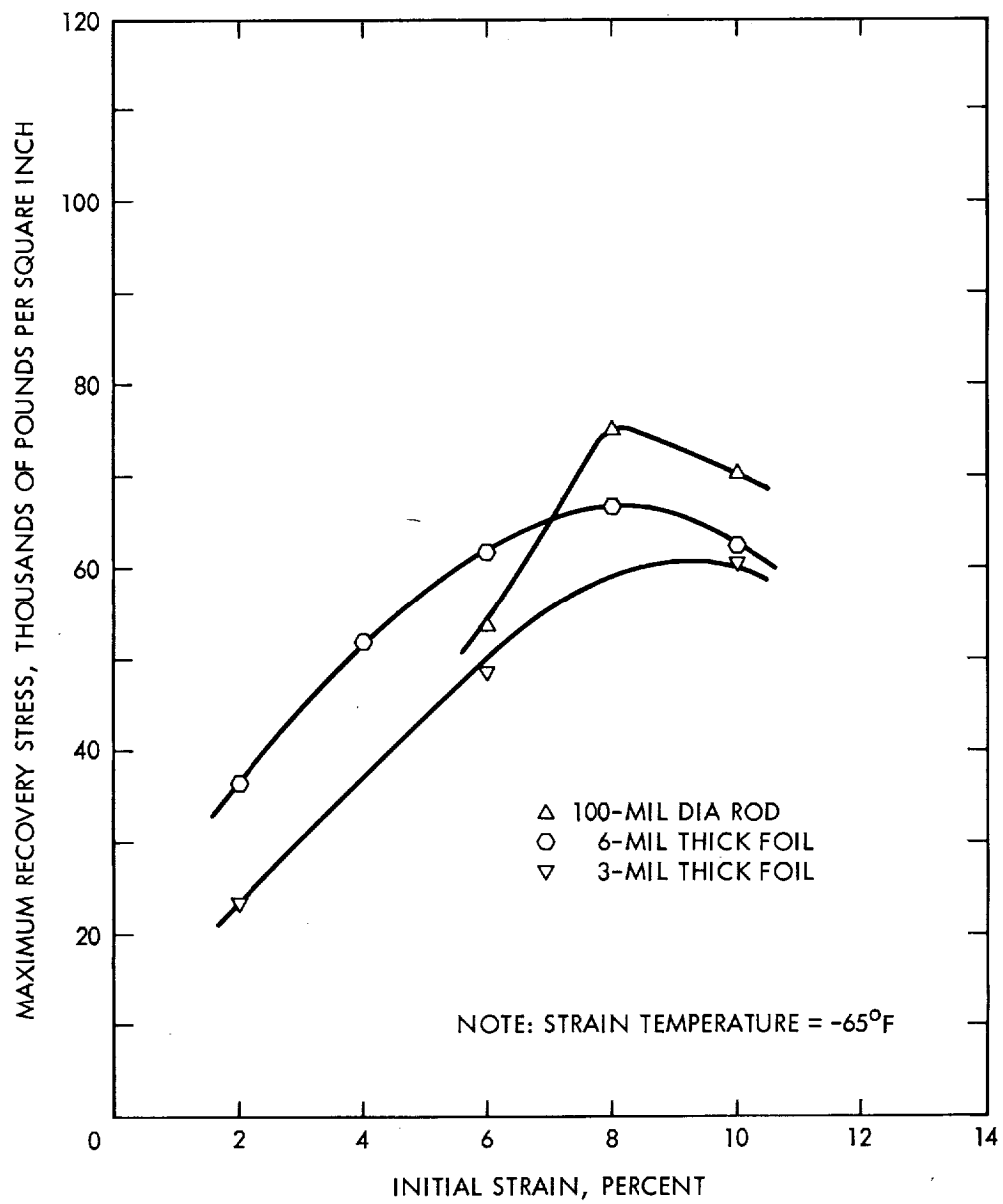


Figure 29. - Maximum recovery stress versus initial strain curves for Composition A materials.

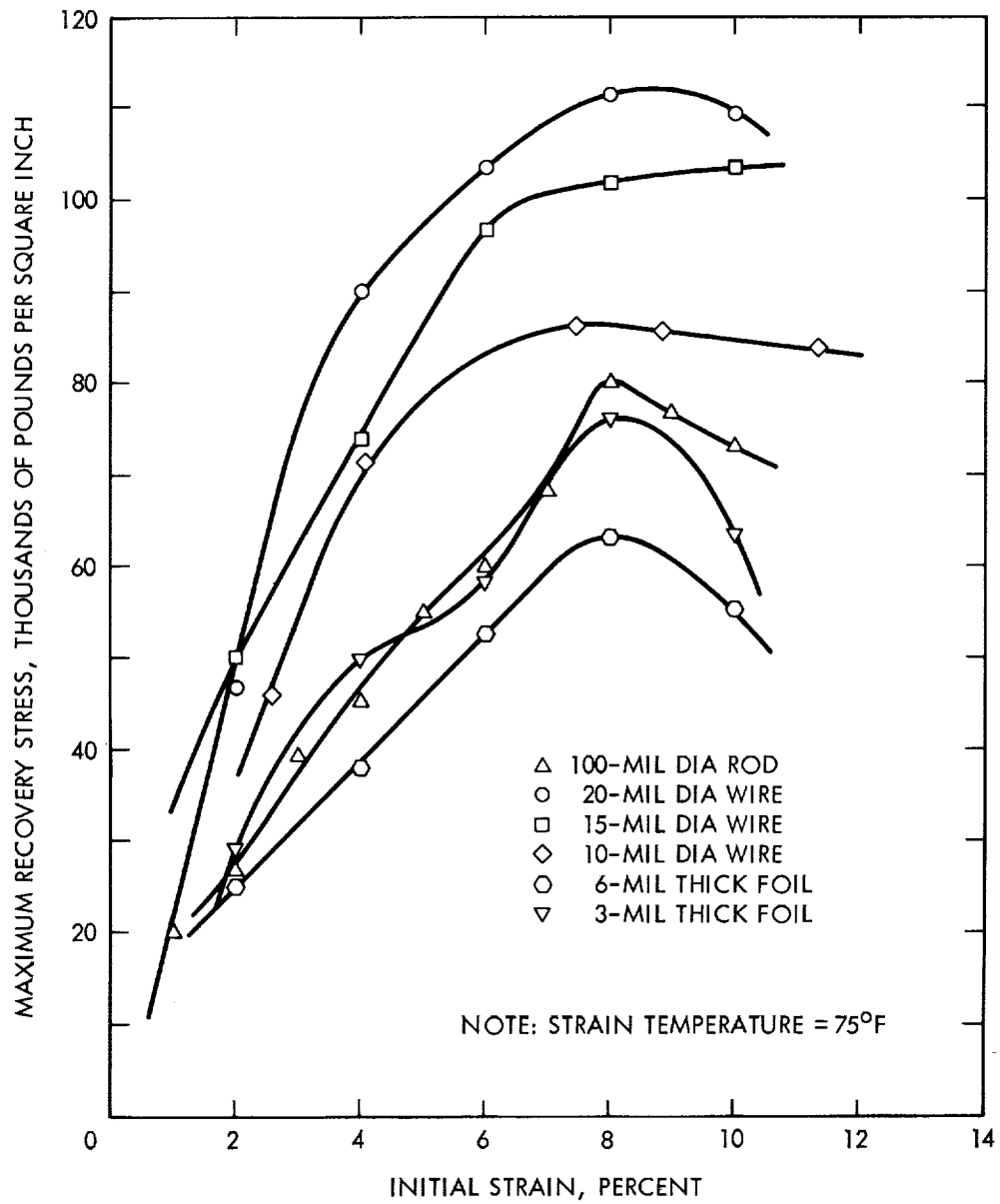


Figure 30. - Maximum recovery stress versus initial strain curves for Composition B materials.

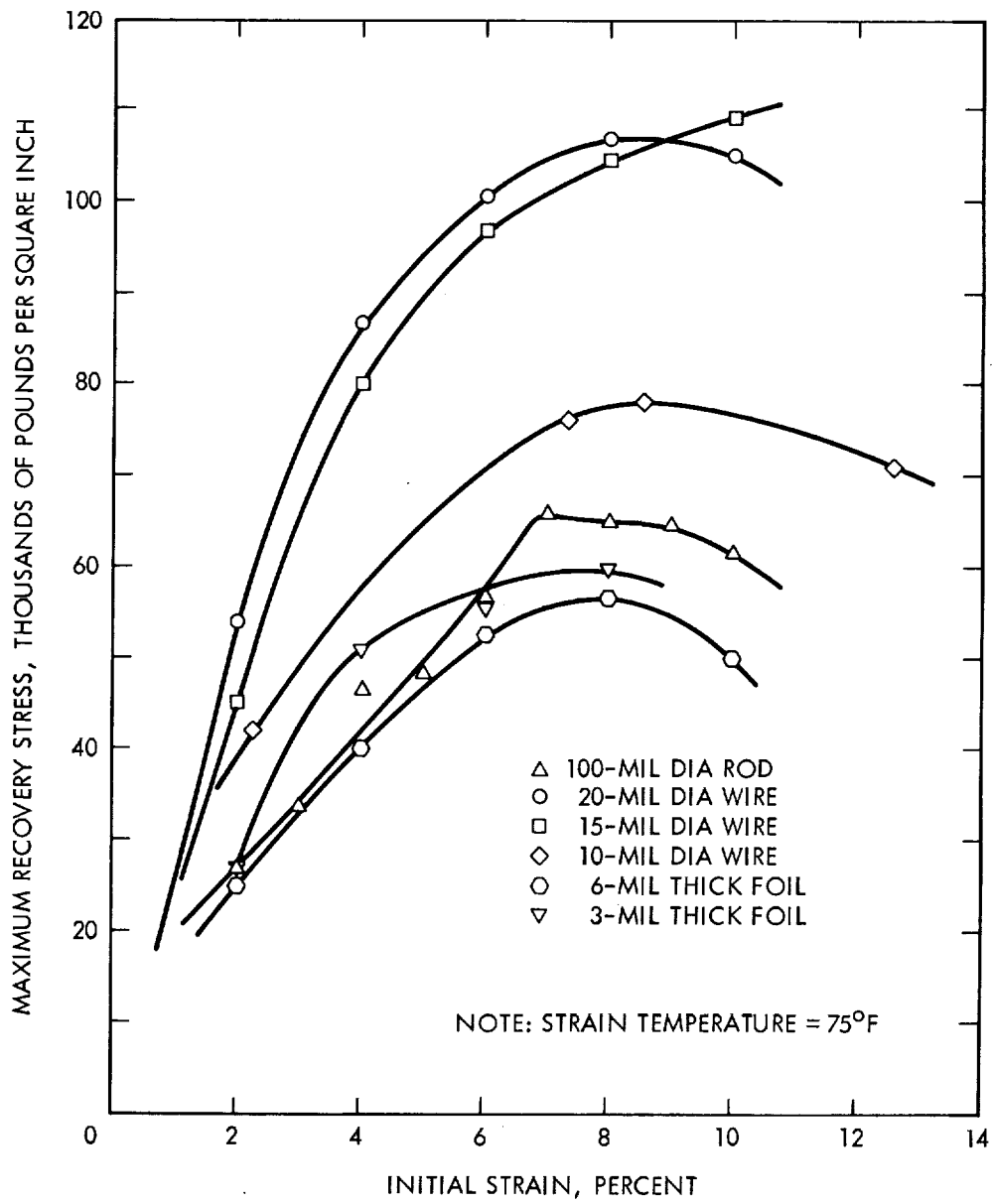


Figure 31. - Maximum recovery stress versus initial strain curves for Composition C materials.

easily subjected to plastic deformation. The M_S' point is somewhat higher than M_S and represents the martensitic transformation temperature for the material under stress.

The data obtained on 100-mil diameter Composition A, B, and C specimens are presented in figures 32, 33, and 34. A close examination of these curves shows that the maximum mechanical work output increases with increasing initial strain until about 7 percent. Beyond this strain level a sharp decline occurs in the maximum mechanical work. A summary of the maximum mechanical work as a function of initial strain level for the specimens tested is presented in figures 35, 36, and 37. Since there is a considerable variation in the maximum mechanical work output among the various specimens tested, the relative performance of each specimen can be established.

In general, the mechanical work performance of the 20-mil wire was superior to all other sizes. The 20-mil Composition C material recorded the highest value - 2900 inch-pounds per cubic inch. The performance of the 15-mil wire closely followed that of the 20-mil wire, whereas the 10-mil wire performance fell considerably below that of the 15-mil wire, but slightly above that of the 100-mil rod. The 100-mil Composition A rod followed this group; however, it exceeded the performance of the 6- and 3-mil foils, with the 3-mil foils showing the poorest performance.

The data obtained shows improvement in performance as the result of drawing and proper annealing and the overall importance that processing had on final material behavior. It is seen

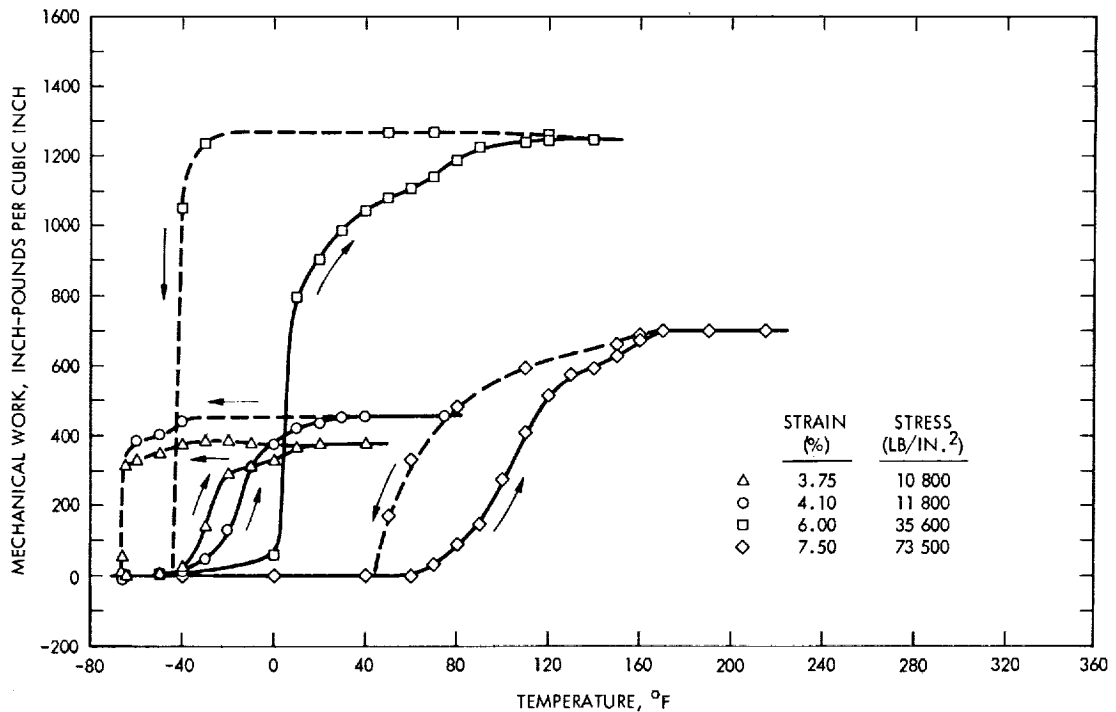


Figure 32. - Mechanical work versus temperature curves for 100-mil diameter Composition A rods.

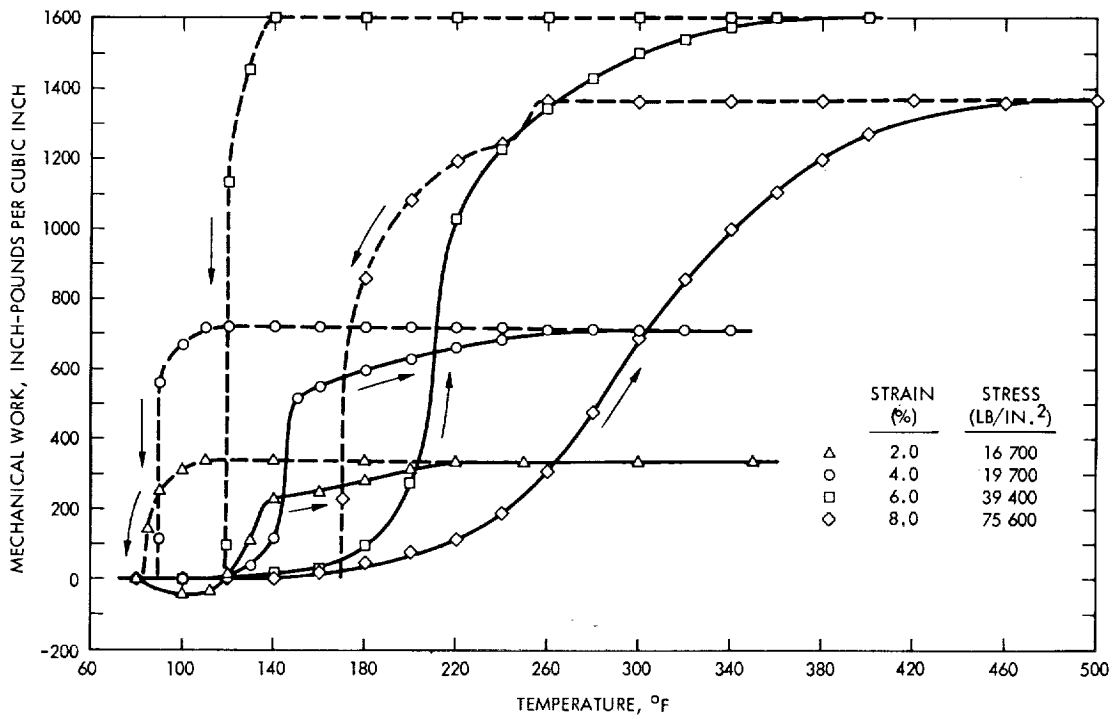


Figure 33. - Mechanical work versus temperature curves for 100-mil diameter Composition B rods.

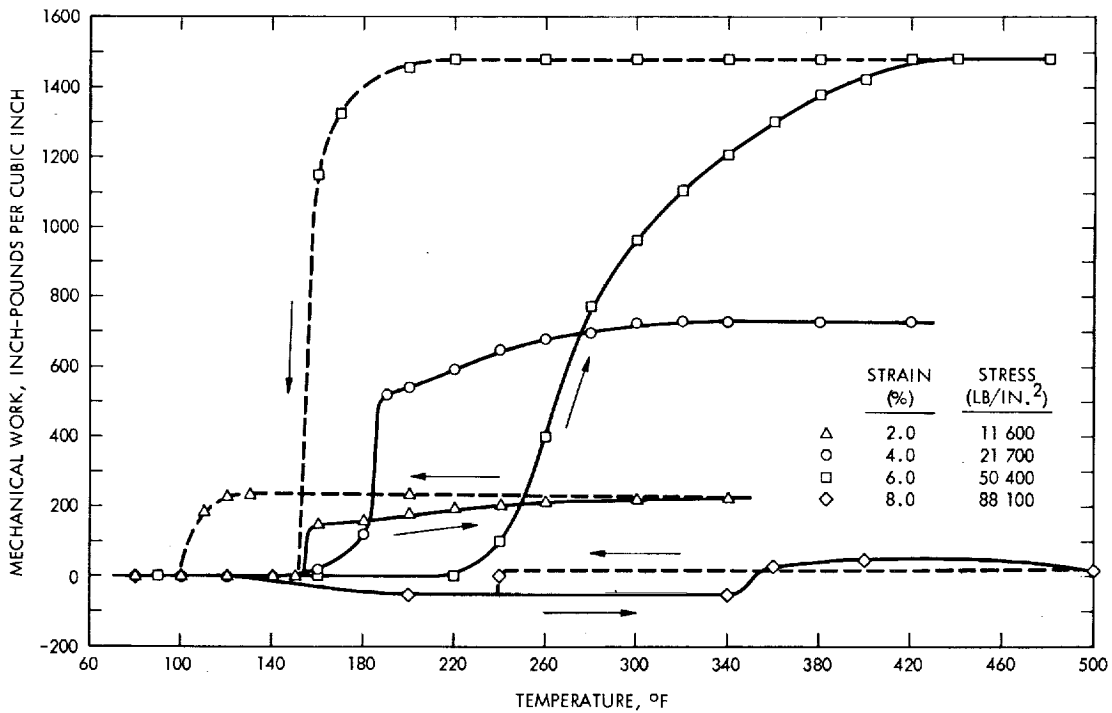


Figure 34. - Mechanical work versus temperature curves for 100-mil diameter Composition C rods.

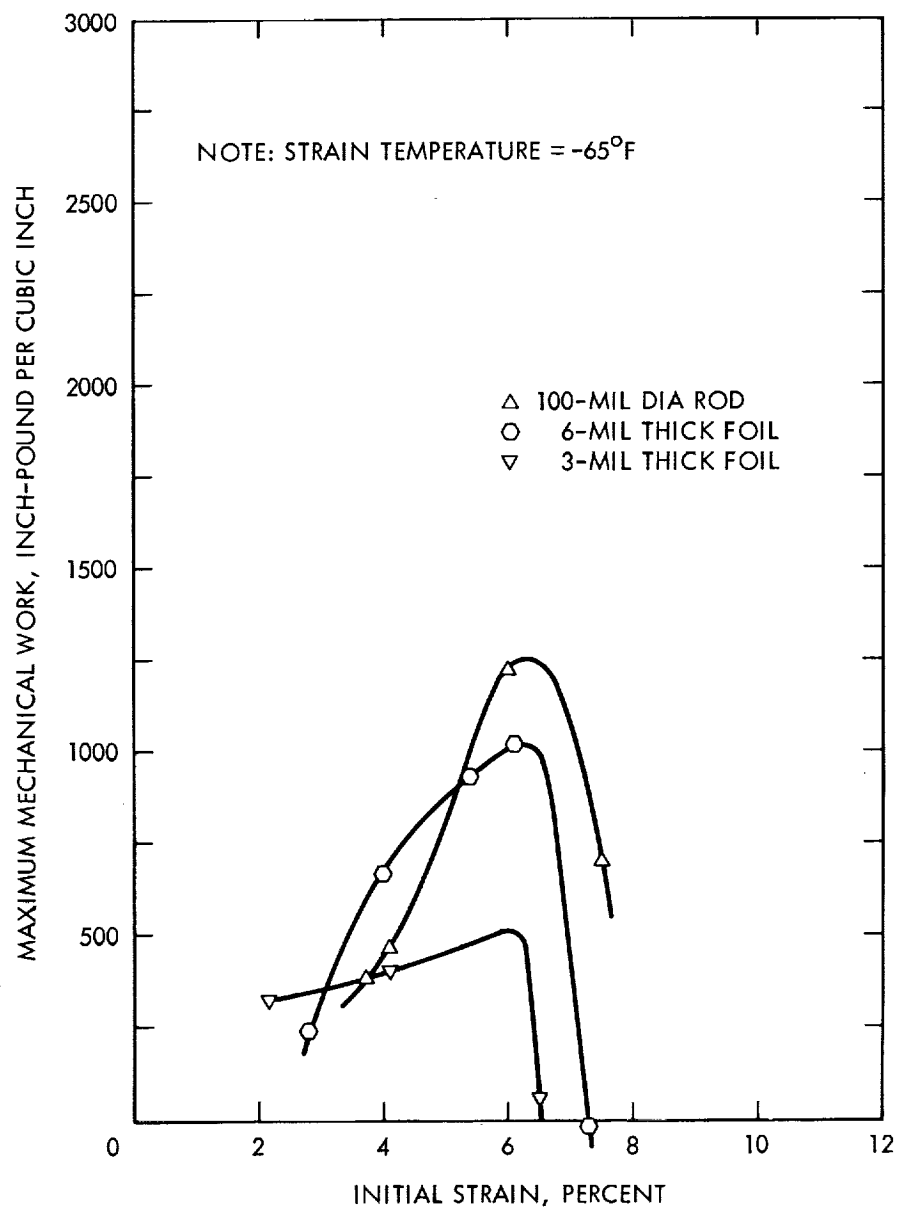


Figure 35. - Maximum mechanical work versus initial strain curves for Composition A materials.

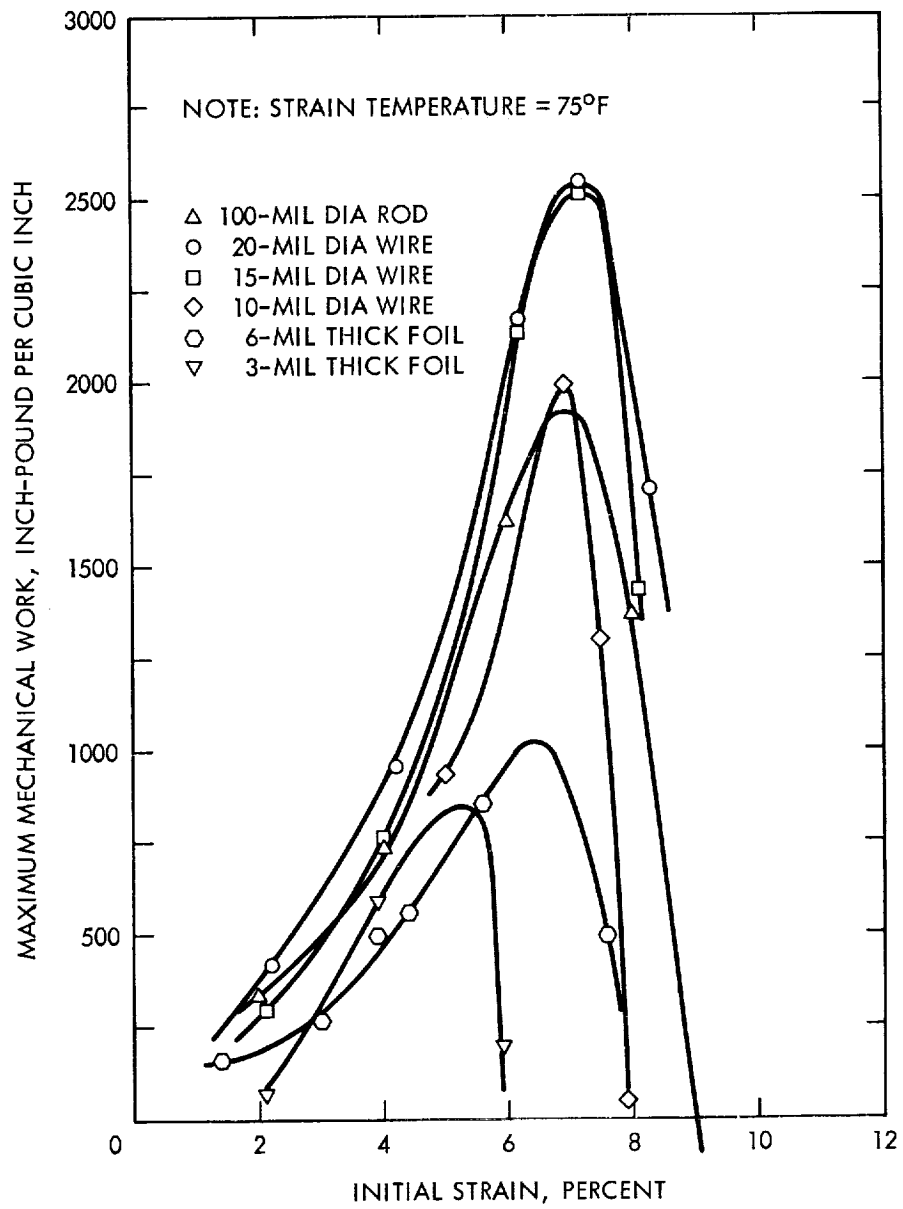


Figure 36. - Maximum mechanical work versus initial strain curves for Composition B materials.

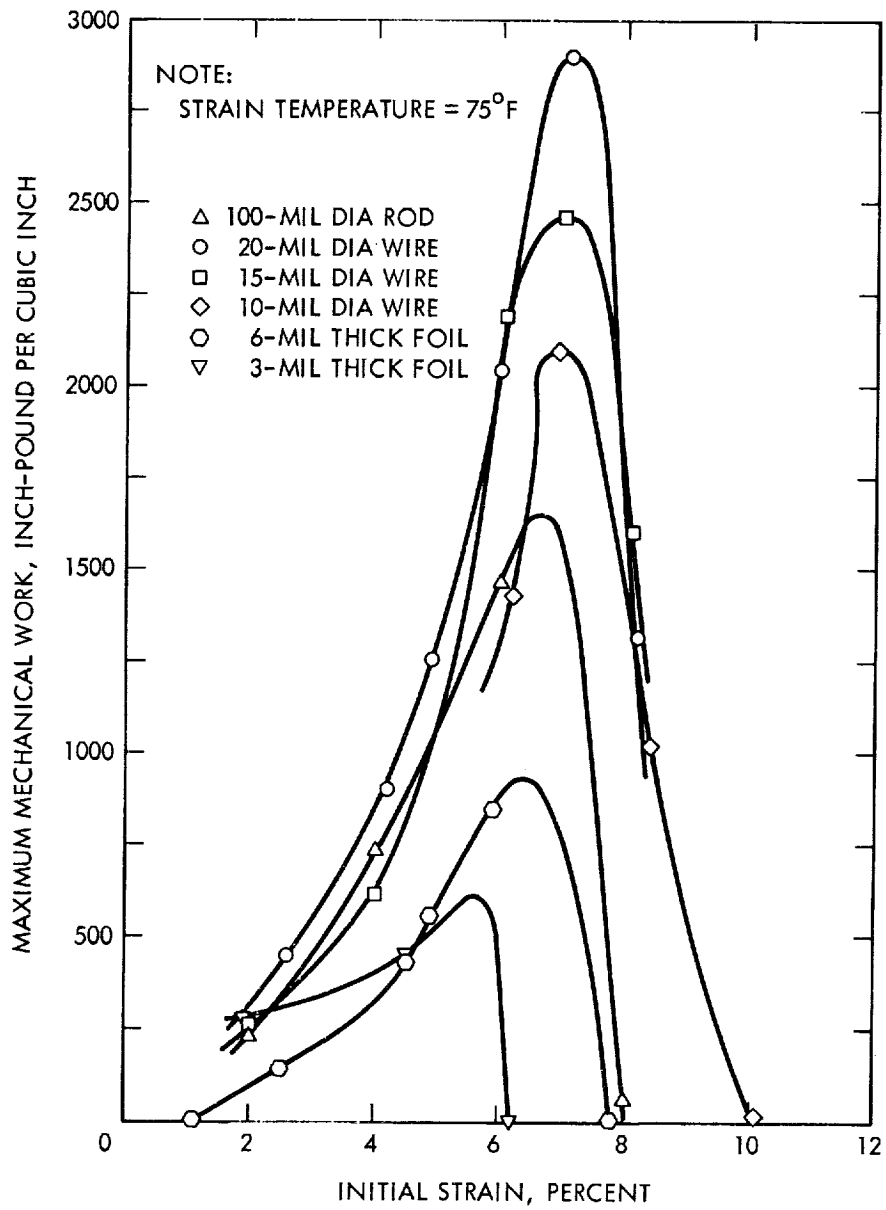


Figure 37. - Maximum mechanical work versus initial strain curves for Composition C materials.

that cold work in the form of drawing and perhaps rolling improves performance, the maximum being reached at the 20-mil diameter level. Further reduction beyond this point appears to lower performance somewhat. The reason for this is not clearly understood. However, it is possible that a reduction in performance of the 10-mil diameter material is brought about by oxidation during annealing. This would have a more significant effect on fine diameter wire and would also help explain the very low performance seen in the 3-mil foils.

Shape recovery fatigue. - To gain a better understanding of the repeatability of the tensile shape recovery process, testing was performed to measure the effects of a repeated deformation and heat recovery cycle. Three indicators were used to monitor changes:

- (1) Degree of no load recovery after heating above the M_d point
- (2) Change in the load versus elongation curve
- (3) Change in the electrical resistance versus temperature curve

These items will be discussed in more detail later in this subsection. Testing was performed on 20-mil wire for the two strain levels of 6 and 8 percent. A maximum strain level of 8 percent was selected on the basis of previous tensile recovery tests (figs. 17, 18, and 19), which indicated that full recovery could be anticipated up to about this point.

Degree of recovery: The degree of recovery as a function of the number of cycles for the 6 and 8 percent strain levels is shown in figure 38 for Composition B wire. These data show that, following 6 percent strain, the specimen recovered 96 percent after the first cycle and maintained nearly the same degree of recovery following 10 additional cycles. Following 100 cycles, the material still recovered 93.4 percent. Increasing the strain level to 8 percent produced a significant change in recovery behavior. As can be noted in figure 38, the specimen recovered only 91 percent for the first cycle and 86 percent after 10 cycles. After approximately 20 cycles the rate of change declined considerably, so that following 100 cycles the sample recovered only 81 percent.

Change in load elongation curves: The overall changes in load versus elongation curves for the 6 and 8 percent cyclic strain tests are illustrated in figure 39. Examination of these curves indicates that for both strain levels, repeated cycling brings about a small but

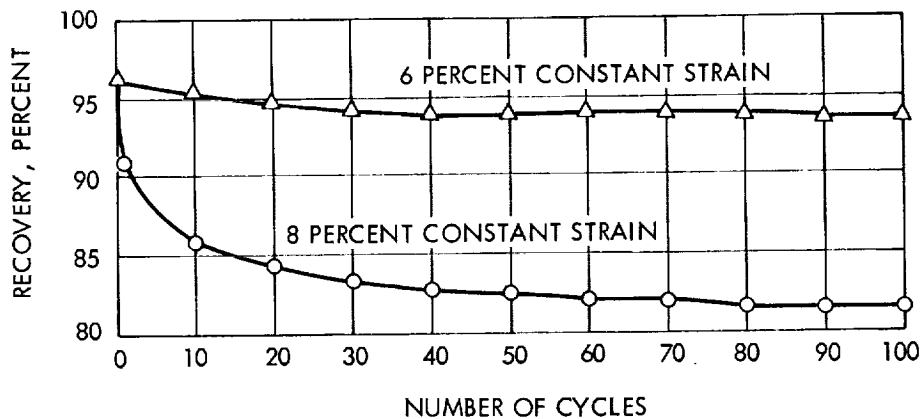
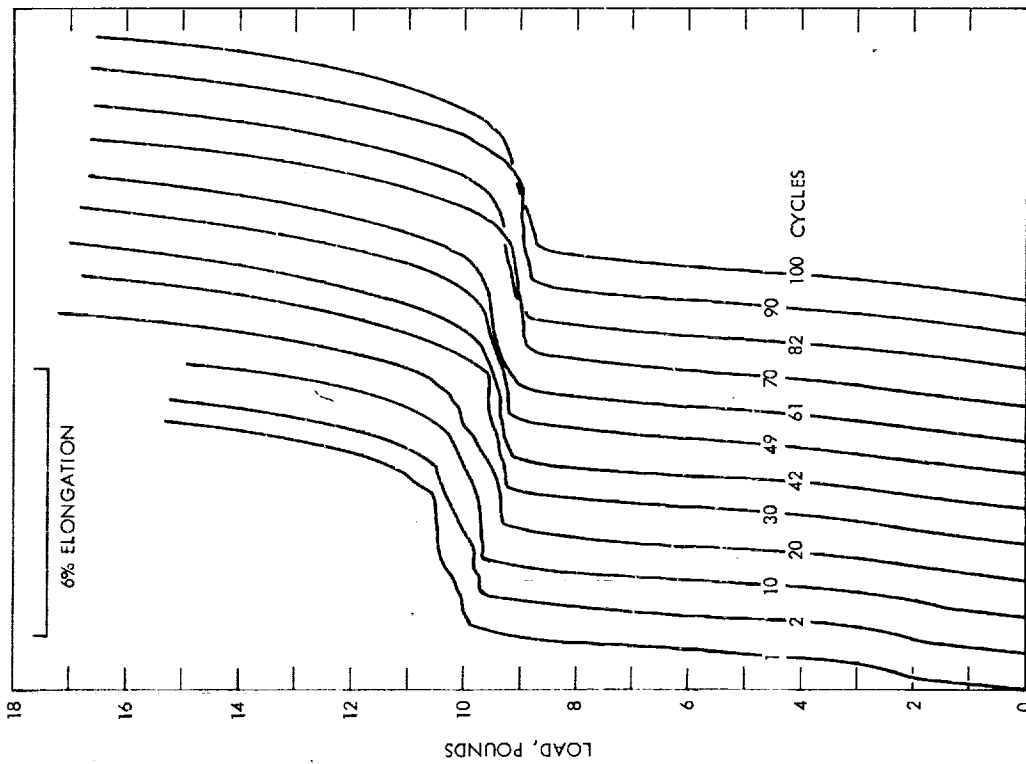
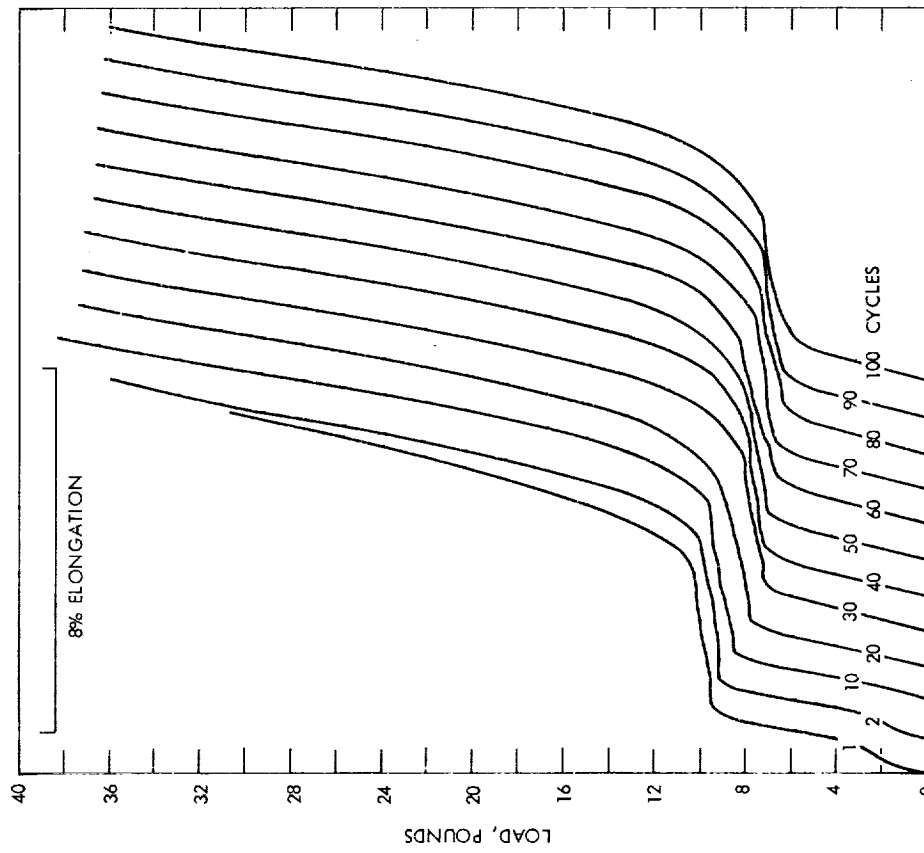


Figure 38. - Tensile recovery versus number of deformation cycles for 20-mil diameter Composition B wire. 6 and 8 percent strain.



(A) 6% ELONGATION EACH CYCLE



(B) 8% ELONGATION EACH CYCLE

NOTES: 1. ALL CURVES START AT ZERO STRAIN AND ARE OFFSET TO SHOW THE EFFECT OF CYCLING.
 2. DATA TAKEN AT ROOM TEMPERATURE (75°F).

Figure 39. - Load-elongation curves following shape recovery cycling for 20-mil diameter Composition B wire.

significant reduction in the yield point characteristics. This change appears to progress at about the same rate as the recovery degradation. In addition, it can be noted that a small anomalous change in the linear portion of the load versus elongation curve disappeared after about 10 to 20 cycles.

Electrical resistance versus temperature curves: The electrical resistance versus temperature curves shown in figure 40 were obtained on the 6 and 8 percent strained wire following 20 and 15 deformation-recovery cycles, respectively. Curves were not obtained on wires with a greater number of cycles. In general, the cycling produced little change in the characteristics. The M_s point for the material remains unchanged; however, a small increase of about 15°F is noted in the A_s point when the data is compared with that of the uncycled wire.

In summary, it appears that repeated 6 percent cycling produces a very small, but measurable, degradation in tensile recovery after the first cycle. At 100 cycles the wire recovered 93.4 percent of its initial gage length. Increasing strain to 8 percent brings about a significant increase in recovery degradation in that, following the first cycle, the specimen recovered only 91 percent and continued to decay to 81 percent recovery at 100 cycles.

Thermal cycling effects. - A series of tests was performed to determine the effect of cyclic exposure to temperature extremes on shape recovery behavior. All testing was conducted on Composition B and C 20-mil wire.

Testing consisted of subjecting specimens to temperature extremes while being held in a predetermined strained condition. A test temperature range of -100° to 300°F was initially selected, but was later modified to -320° and 160°F when it was proven, through preliminary tests (one cycle), that 300°F exposure destroyed a major portion of shape recovery. Lowering the temperature to 212°F brought about less degradation, but still proved to be unsatisfactory. After further testing, 160°F was selected as the upper limit, since it produced insignificant degradation following a single cycle exposure. Recovery after exposure to -320°F was compared with that obtained after -100°F and found to be identical.

Two different levels of deformation in bending (6 and 8 percent outer fiber stress) and three different degrees of restraint were examined as a function of temperature cycles. They were as follows:

- (1) Specimens were fully restrained so that the initial 6 or 8 percent outer fiber stress was maintained throughout the cyclic temperature exposure.
- (2) Specimens were permitted to recover elastically (spring-back) after bending, then restrained at the recovery point throughout the cyclic temperature exposure.
- (3) Specimens were plastically deformed in bending, allowed to spring back, then heated slightly to provide partial martensitic recovery before being restrained.

The degree of strain maintained under each of these restraint conditions is given in table VI.

Specimens were subjected to 0, 1, 10, 50, and 100 thermal cycles by dipping them alternately in liquid nitrogen (-320°F) and hot water (160°F). After the desired number of cycles, specimens were removed from their restraining mandrels and submerged in boiling water (212°F) to bring about martensite shape recovery. They were then removed from the water, allowed to assume room temperature, and measured to determine degree of recovery. It is important to note that the degree of recovery at 75°F (room temperature) is somewhat lower than the level

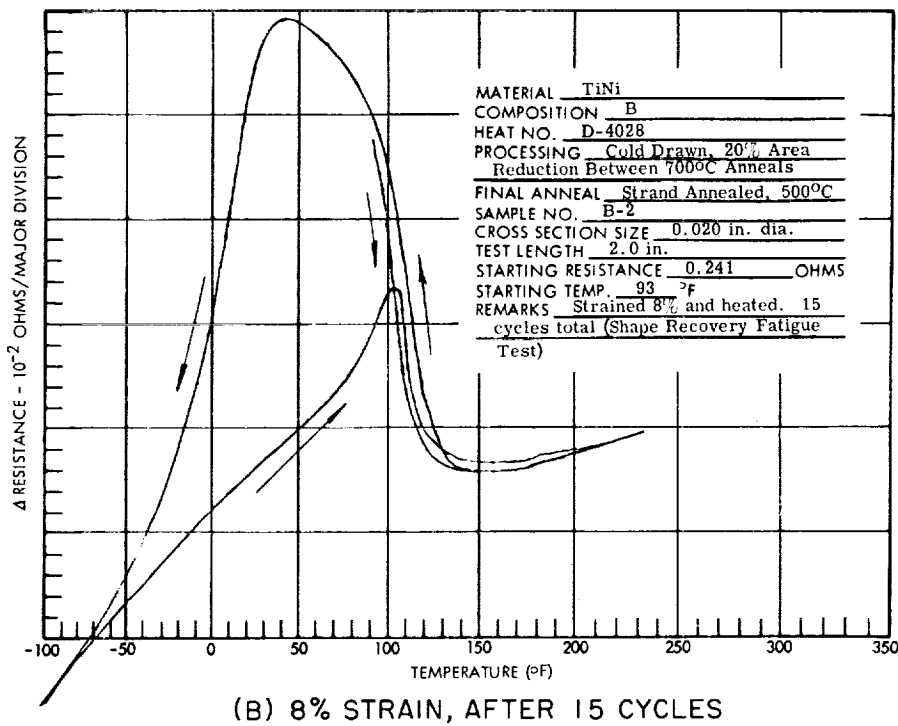
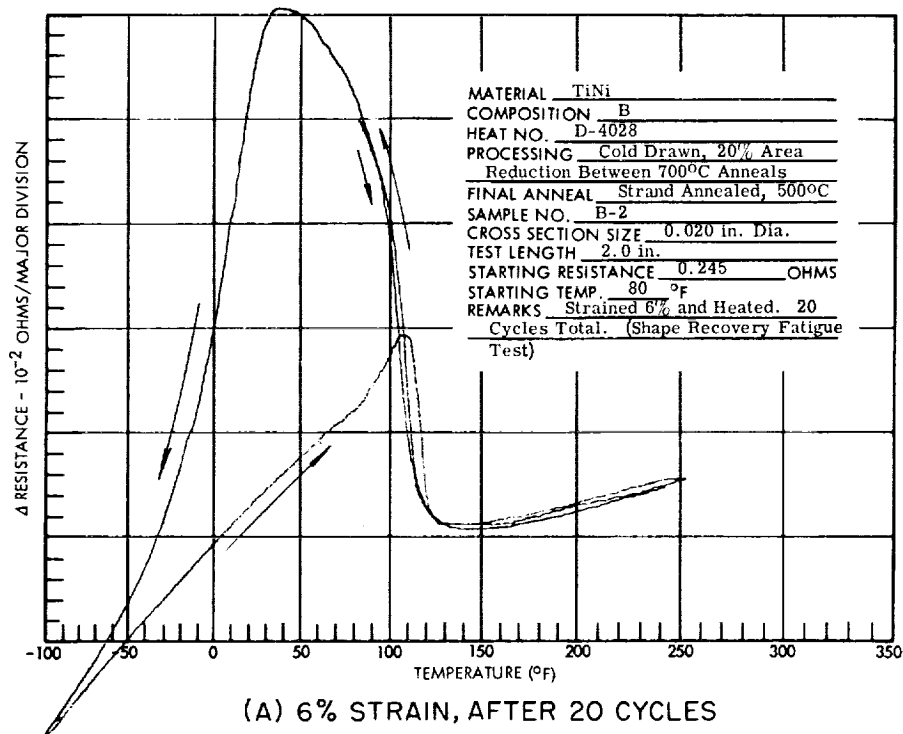


Figure 40. - Electrical resistance versus temperature curves following repeated deformation cycles for 20-mil diameter Composition B wire.

TABLE VI. - DEGREE OF STRAIN MAINTAINED IN THERMAL CYCLING SPECIMENS

Initial strain, percent	Outer fiber strain, percent		
	Fully restrained	After elastic recovery	After partial memory recovery
6	6.0	3.8	1.9
8	8.0	6.0	2.6

reached when the sample was placed in boiling water. The behavior was previously noted and can be clearly seen in the data presented in figures 23 and 24.

The results of the tests performed on 20-mil Composition B and C wire are summarized in figure 41. The curves show the degree of bend recovery as a function of cooling-heating cycles.

Examination of the data obtained reveals that the 6 percent strain condition produces less initial degradation in recovery for both compositions than the 8 percent strain condition. However, after 100 thermal cycles in both strain conditions, recovery is about equal. The highest recovery recorded after 100 cycles was 95.8 percent for Composition B and 95.3 percent for Composition C.

In general, the completely restrained condition produces a greater initial degradation but becomes better than the other two constrained test conditions beyond about 10 to 20 cycles. Following 100 cycles, Composition B specimens, restrained following partial recovery, indicated a slight improvement over the elastic recovered specimens. This may not represent a trend since the same restrained condition produced identical behavior in the Composition C wire.

It has been concluded that while the magnitude of change brought about by thermal cycling below 160°F is small - about 2 percent loss for 100 cycles - a trend exists that should be considered in any future design. Most important is the serious degradation to recovery (memory loss) that occurs if strained materials of the type examined are subjected to temperatures above about 160°F.

Although heating much above 160°F will produce measurable degradation, it should not be construed as a sharp limiting point. While the mechanism surrounding this behavior is not clearly understood, heating above the M_d point (approximately 160°F) appears to introduce a slightly different "remembered" shape and should be avoided whenever a specimen is constrained in a configuration other than that originally introduced.

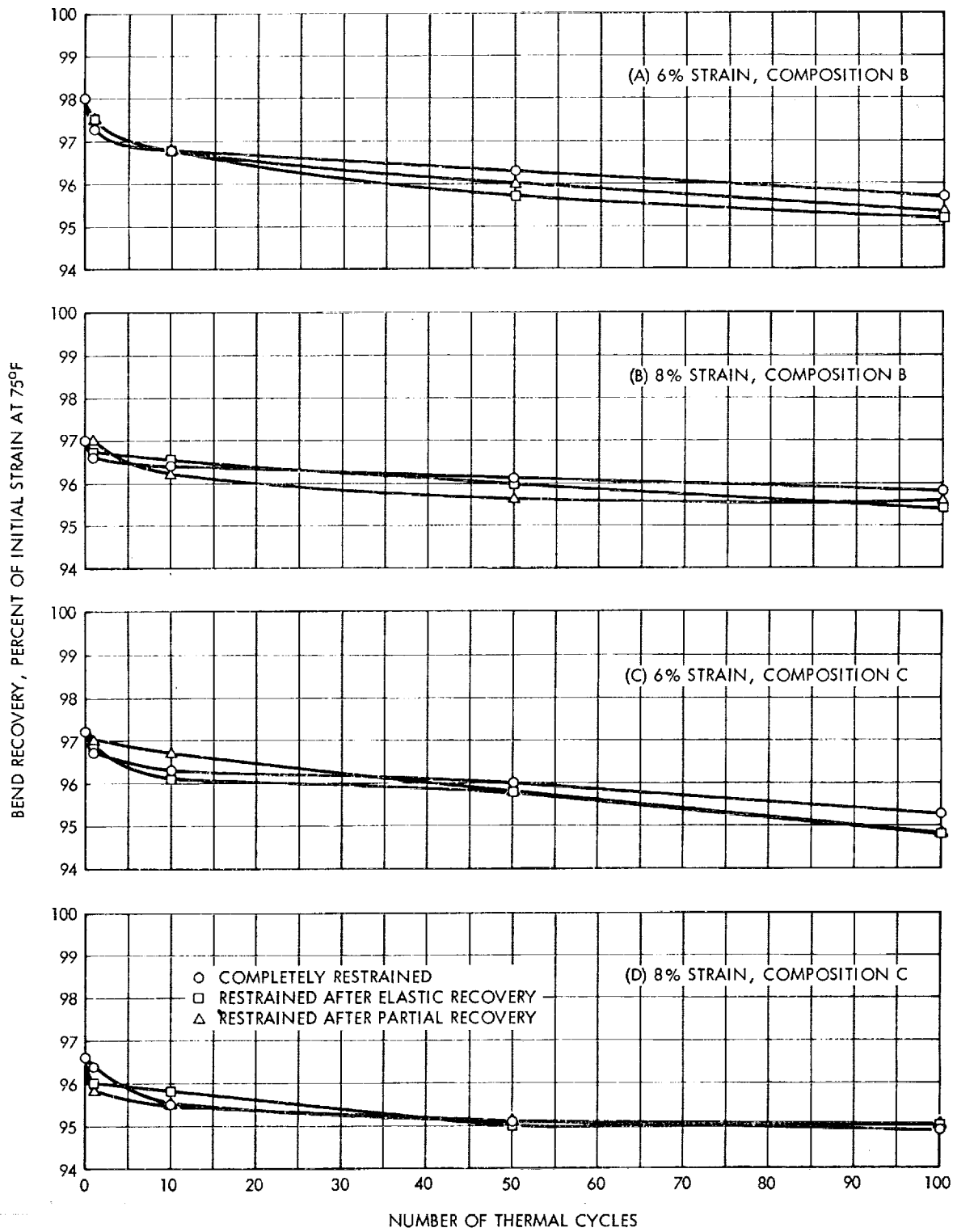


Figure 41. - Thermal cycling effects on bend recovery for 20-mil diameter Composition B and C wire.

CONCLUSIONS

Engineering data has been obtained on typical 55-Nitinol alloy compositions in sufficient quantities and detail to permit NiTi utilization in practical design concepts. Furthermore, it has been proven that when careful processing procedures are utilized, reliable and consistent shape recovery performance can be obtained over a range of material compositions and wire sizes.

Careful processing of the various wire and thin sheet forms has led to a greater understanding of the variables that must be controlled to provide good recovery behavior and has firmly established the relationship between post-drawing annealing temperature and shape recovery performance.

Through the widespread use of electrical resistance versus temperature profiles as a transformation temperature (M_S and A_S) monitor tool, it was possible to broaden the understanding of how processing affects transformation, starting temperatures, and overall recovery performance to such a degree as to make possible qualitative and quantitative predictions of the wire performance on the basis of preliminary small ingot sections.

Therefore, the following conclusions can be drawn from the results of this experimental investigation:

- (1) Nitinol alloys having M_S temperatures that are near room temperature can be processed readily into fine wire and thin sheet by using hot-swaging and cold-drawing or rolling techniques that are customarily used for advanced materials.
- (2) Nitinol alloys having M_S temperatures considerably below room temperature can also be drawn into wire; however, special die cooling procedures must be followed.
- (3) The shape recovery ability of a 55-Nitinol alloy is closely linked to processing history, e.g., prior cold work introduced by cold-drawing or rolling and final annealing temperature. Therefore, processing must be carefully controlled.
- (4) Electrical resistance versus temperature curves provide a reliable means for determining M_S , A_S , and M_D temperature points of the martensitic transformation that occurs in 55-Nitinol alloys. In addition, they provide a means of predicting the relative shape recovery performance of a particular Nitinol alloy.
- (5) A decrease in the elastic modulus is associated with a decrease in temperature and precedes instability and transformation at the M_S point. In the case of 100-mil diameter drawn rod, elastic modulus decreased from a maximum of 12 million psi to a minimum of about 3 million psi at the M_S point. Heating from below the M_S point causes a reverse behavior whereby modulus increases, starting at a temperature (A_S point) somewhat in excess of the M_S point and continuing until a maximum is reached at about the M_D point.
- (6) The 0.2 percent offset yield stress decreases as temperature is lowered below the M_D point and reaches a minimum at M_S . In the case of 100-mil diameter drawn rod, the 0.2 percent offset yield stress decreases from a maximum of 90 000 psi to a minimum of about 5 000 psi. Upon heating, a reverse behavior occurs. However, the increase is initiated at A_S , a temperature point somewhat in excess of M_S .

- (7) Plastic deformation when introduced at temperatures below or somewhat above the M_S point causes transformation in amounts determined by the degree of strain and the strain temperature. The highest degree of transformation for a given degree of deformation occurs at the M_S point. As temperature is increased above the M_S , the amount of transformation for a given degree of deformation continues to diminish to zero at M_D . Deformation below the M_S point appears to provide a high degree of transformation.
- (8) Wire can be strained 6 to 8 percent and still exhibit 100 percent recovery. However, the material can be strained considerably beyond 8 percent and still exhibit over 90 percent recovery, which should be satisfactory for many possible applications.
- (9) Recovery tensile stress over 100 000 psi can be generated by 15- and 20-mil diameter wires strained initially at 8 percent.
- (10) Mechanical work capability of over 2500 inch-pounds per cubic inch was consistently demonstrated with 15- and 20-mil diameter wires that had undergone approximately 7 percent initial strain, with a maximum value of 2900 inch-pounds per cubic inch being reached.

There are indications that these limits could be raised by using improved processing techniques.

From these results it is recognized that 55-Nitinol has many potential applications in advanced space structures, especially where requirements for expandable and erectable structures or self-actuating devices in space are needed.

REFERENCES

1. Buehler, W.J.; and Cross, W.B.: 55-Nitinol Unique Alloy Wire for Self-Erectable Space Structures. Presented at the Wire Association, Inc., Non-ferrous Div. Meeting, Huntsville, Alabama, 3 - 4 April 1968. (To be published in the Wire Journal.)
2. Buehler, W.J.; and Wang, F.E.: A Summary of Research on the Nitinol Alloys and Their Potential Application in Ocean Engineering. *Ocean Engineering*, vol. 1, No. 1, July 1968.
3. Wang, F.E.; Buehler, W.J.; and Pickart, S.J.: Crystal Structure and a Unique "Martensitic" Transition of TiNi. *J. Appl. Phys.*, vol. 36, No. 10, October 1965.
4. Wang, F.E., ed.: Proceedings of Symposium on TiNi and Associated Compounds, held at U.S. Naval Ordnance Laboratory, Silver Spring, Maryland, 3 - 4 April 1967. NOL TR 68-16. (These proceedings have been published in the *J. Appl. Phys.*, vol. 39, 1968.)
5. Dautovich, D.P.; and Purdy, G.R.: Phase Transformations in TiNi. *Canadian Metallurgical Quarterly*, vol. 4, No. 2, April - June 1965, pp. 129-143.
6. Purdy, G.R.; and Parr, J.G.: A Study of the Titanium-Nickel System Between Ti_2Ni and NiTi. *Trans. AIME*, vol. 221, June 1961, pp. 636-639.
7. Wasilewski, R.J.; Butler, S.R.; and Hanlon, J.E.: On the Martensitic Transformation TiNi. *Metal Science Journal*, vol. 1, 1967, pp. 104-110.
8. Wang, F.E.; DeSavage, B.F.; Buehler, W.J.; and Hosler, W.R.: The Irreversible Critical Range in the TiNi Transition, *J. Appl. Phys.*, vol. 39, No. 5, April 1968.

BIBLIOGRAPHY

Bradley, D.: Sound Propagation in Near-Stoichiometric TiNi Alloys. *J. Acoust. Soc. Am.*, vol. 37, No. 4, April 1965, pp. 700-702.

Buehler, W.J.: Intermetallic Compound Based Materials for Structural Applications. Presented at the Seventh Navy Science Symposium, 14-16 May 1963, ONR-16, vol. 1, 1963.

Buehler, W.J.; and Wang, F.E.: Martensitic Transformation in the TiNi Compound. *Reactivity of Solids*. Fifth International Symposium, Munich, 1964.

Buehler, W.J.; and Wang, F.E.: Study of Transition Element Intermetallic Compounds. Presented at the Ninth Navy Science Symposium, 5-6 May 1966.

Buehler, W.J.; and Wiley, R.C.: The Properties of TiNi and Associated Phases. *Trans. Am. Soc. Metals*, vol. 55, No. 2, June 1962.

Buehler, W.J.; and Wiley, R.C.: TiNi - Ductile Intermetallic Compound. *Trans. Am. Soc. Metals*, vol. 55, 1962, pp. 269-276.

- Buehler, W.J.; Wiley, R.C.; and Wang, F.E.: Nickel-Base Alloys. Patent No. 3,174,851, March 23, 1965.
- Buehler, W.J., et al: Effect of Low-Temperature Phase Changes on the Mechanical Properties of Alloys Near Composition TiNi. *J. Appl. Phys.*, vol. 34, No. 5, May 1963, pp. 1475-1477.
- Cooper, J.E.; Bowker, D.E.; and Cross, W.B.: Investigation of the Unique Memory Properties of 55-Nitinol Alloy. (To be presented at the 15th National SAMPE Symposium on 29 and 30 April and 1 May 1969 at the Statler Hilton Hotel, Los Angeles, California.)
- Goff, J.F.: Thermal Conductivity, Thermoelectric Power, and Electrical Resistivity of Stoichiometric TiNi in the 3° to 300°K Temperature Range. *J. Appl. Phys.*, vol. 35, No. 10, October 1964.
- Goldstein, D.M., et al: Effects of Alloying Upon Certain Properties of 55.1 Nitinol. NOL TR 64-235, U.S. Naval Ordnance Laboratory, Silver Spring, Maryland, May 1965.
- Hanlon, J.E.; Butler, S.R.; and Wasilewski, R.J.: Effect of Martensitic Transformation on the Electrical and Magnetic Properties of NiTi. *Transactions of the Metallurgical Society of AIME*, vol. 239, September 1967, pp. 1323-1326.
- Rozner, A.G.; and Buehler, W.J.: Effect of Cold Work on Room-Temperature Tensile Properties of TiNi Intermetallic Compound. *Trans. Am. Soc. Metals*, vol. 59, 1966.
- Rozner, A.G.; and Buehler, W.J.: Low Temperature Deformation of the TiNi Intermetallic Compound. NOL Technical Report 66-38, March 1966.
- Rozner, A.G.; and Wasilewski, R.J.: Tensile Properties of NiAl and NiTi. *J. Inst. Metals*, vol. 94, 1966, pp. 169-175.
- Rozner, A.G., et al: Effect of Addition of Oxygen, Nitrogen, and Hydrogen on Microstructure and Hardness of Cast TiNi Intermetallic Compound. *Trans. Am. Soc. Metals*, vol. 58, No. 3, September 1965.
- Schuerch, H.J.: Certain Physical Properties and Applications of Nitinol. NASA CR-1232, November 1968.
- Spinner, S.; and Rozner, A.G.: Elastic Properties of NiTi As A Function of Temperature. *J. Acoust. Soc. Am.*, vol. 40, No. 5, November 1966, pp. 1009-1015.
- Wang, F.E.: Equiatomic Binary Compounds of Z_T with Transition Elements R_u, R_h, and P_d. *J. Appl. Phys.*, vol. 38, No. 2, February 1967.
- Wang, F.E.: The Mechanical Properties as a Function of Temperature and Free Electron Concentration in Stoichiometric TiNi, TiCo, and TiFe Alloys. *Proc. First International Conf. on Fracture*, vol. 2, 1965, pp. 899-908.
- Wang, F.E., et al: Growth of TiNi Single Crystals by a Modified "Strain-Anneal" Technique. *J. Appl. Phys.*, vol. 35, No. 12, December 1964, p. 3620.